



MONASH University

Understanding the evolution of infectious
disease at the invasion front

Louise Solveig Nørgaard

MSc Biological Sciences

A thesis submitted for the degree of Doctor of Philosophy at

Monash University in 2019

School of Biological Sciences

Copyright notice

© The author 2019.

I certify that I have made all reasonable efforts to secure copyright permissions for third-party content included in this thesis and have not knowingly added copyright content to my work without the owner's permission.

Abstract

Epidemic outbreaks of infectious disease are of great concern to human health, agriculture and wildlife, and understanding the underlying mechanisms of the spatial spread of emerging pathogens is a major global challenge. Classic theory considers the spread of disease in homogeneous host populations, which, is a simplification of the conditions met in nature. Natural populations are instead characterised by changing population dynamics across a landscape. For example, in range expanding, invasive, or analogous metapopulations with high extinction rates, empty habitat patches are regularly colonized by dispersing individuals, generating a dynamic landscape of populations that vary in their time since initial colonization. Thus, understanding what happens when an infectious propagule encounters, infects and spreads through a landscape of dynamic host populations, is essential for understanding the evolution of infectious disease in natural populations.

The overall aim of my thesis is to explore how the conditions met in such patchy and range expanding host populations may impact on pathogen performance and alter the types of infection strategies that are likely to be favoured. In four experimental chapters, I study different aspects of this complex topic, using two different model-systems: the planktonic crustacean *Daphnia magna* and its gram-positive pathogen *Pasteuria ramosa*, and the ciliate *Paramecium caudatum* and its bacterial parasite *Holospora undulata*.

First, I uncovered that population dynamics arising during host colonization selected for different pathogen dispersal-colonization strategies; conditions of a host population that maximised initial pathogen invasion was not identical to the conditions that maximised transmission, nor the long-term maintenance in a host population. In a follow-up chapter, I linked changes in population density to the ability of both a host and pathogen to acquire and expend energy. Both chapters reinforce how patch quality for a pathogen operates at two different scales; within-host proliferation

was optimized at low population densities with high energy availability, but conversely minimal opportunities for secondary infections.

Next, I explored the importance of trade-offs between the damage caused to a host during infection, and the reduction in host dispersal that often follows, for pathogen evolution. Using the *Daphnia* system again, I showed how different type of hosts circulating in a population, in this case males and females, allow a pathogen to optimize transmission in one host sex and dispersal in the other. Finally, working with ciliates, I provide evidence that pathogens can evolve in response to dispersal selection imposed on its host population; pathogens at the invasion front evolved reduced negative impact on host dispersal, and this adaptation was associated with increased vertical transmission and reduced negative impact of infection.

Collectively, my work demonstrates that population dynamics arising during range expansion and patch colonization are important mediators of the evolution of infectious disease. I show how tension between conditions that favour within-host proliferation versus between-host secondary transmission might cause changes in the selective pressures experienced by a pathogen as it spreads through a landscape. I also uncover the importance of host dispersal and the ability of a pathogen to evolve in response to dynamics encountered in the host population.

Publications during enrolment

Nørgaard, L. S., Phillips, B., Hall, M. D., 2019. Infection in patchy populations: contrasting pathogen invasion success and dispersal at varying times since host colonization. *Evolution Letters* 3-5:555-566.

Nørgaard, L. S., Phillips, B., Hall, M. D., 2019. Can pathogens optimize both transmission and dispersal by exploiting sexual dimorphism in their hosts? *Biology Letters*.

<http://dx.doi.org/10.1098/rsbl.2019.0180>

Thesis including published works declaration

I hereby declare that this thesis contains no material which has been accepted for the award of any other degree or diploma at any university or equivalent institution and that, to the best of my knowledge and belief, this thesis contains no material previously published or written by another person, except where due reference is made in the text of the thesis.

This thesis includes two original papers published in peer reviewed journals and two unpublished papers intended for submission in peer reviewed journals. The core theme of the thesis is evolutionary biology. The ideas, development and writing up of all the papers in the thesis were the principal responsibility of myself, the student, working within the School of Biological Sciences under the supervision of Dr Matthew David Hall. I have renumbered sections of published papers in order to generate a consistent presentation within the thesis.

The inclusion of co-authors reflects the fact that the work came from active collaboration between researchers and acknowledges input into team-based research. In the case of chapters 2, 3, 4, and 5, my contribution to the work involved the following:

| Thesis Chapter | Publication Title | Status | Nature and % of student contribution | Co-author name(s) Nature and % of Co-author's contribution* | Co-authors, Monash student |
|-----------------------|---|---------------|--|---|-----------------------------------|
| 2 | Infection in patchy populations: contrasting pathogen invasion success and dispersal at varying times since host colonization | Published | 70%. Experimental design, data collection, data analysis, and writing of manuscript. | 20%. M.D. Hall: data analysis, edits to manuscript. 10% B.L. Phillips: invasion index and edits to manuscript. | No |
| 3 | Energetic constraints in range expanding and colonizing populations and their consequences for pathogen fitness | Not submitted | 75%. Experimental design, data collection, data analysis, and writing of manuscript. | 20%. M.D. Hall: data analysis, edits to manuscript. 5%. G. Ghedini & B. Philips: experimental design and edits to manuscript. | No |
| 4 | Can pathogens optimize both transmission and dispersal by exploiting sexual dimorphism in their hosts? | Published | 75%. Experimental design, data collection, data analysis, and writing of manuscript. | 20%. M.D. Hall: data analysis, edits to manuscript. 5% B.L. Phillips: edits to manuscript. | No |
| 5 | Pathogens on the move – high host-facilitated dispersal is associated with evolutionary changes in parasite life-history traits | Not submitted | 65%. Experimental design, data collection, data analysis, and writing of manuscript. | 15%. G. Zillio: data collection, edits to manuscript 10% O. Kaltz: data collection, edits to manuscript 8% M.D. Hall: data analysis and edits to manuscript. 1% C. Gougat: lab work 1% E. Fronhoffer: data analysis | No |

Acknowledgements

First, a big thanks to Matt Hall for supervising me throughout the last 3.5 years. It has been a very exciting journey with a steep learning curve; going from having a very limited knowledge about statistics and the use R-software, to actually drawing my own figures and running complicated mixed effect models with error structures that I never knew existed. Matt, I want to thank you for your support throughout my PhD. Your support started already at day one upon arrival, where you picked me up in the airport and invited me to stay at you and Neika's house for a few days, until I got settled in this new big city. From there, you have provided huge support to all of my initiatives. Importantly, my schedule has been slightly different, compared to other PhD students, and I am ever thankful that you have supported me in undertaking long trips to Europe for conferences, projects and never the least, periods of working from Danish Universities and from home. Your trust in that my initiatives will eventually turn into something exciting, has enabled me to gain full ownership of my PhD, and I am very thankful for this. No supervisor-student relationship is the identical, and I appreciate your way of interacting with me, even if communication has been sparse at times. Thank you also for being persistent on certain topics along the way (in particular when it comes to collaborative projects), which, in the long run, turned out to be for my own benefit!

Thanks also to my co-supervisor, Ben Phillips, for support, valuable feedback and good discussions on experimental data and new ways to interpret unexpected results. I would also like to thank all of my panel members, David Chapple, Jeremy Barr, Kathryn Hodgins and Tim Connallon, who has provided constructive feedback during my milestone seminars, as well as general support throughout the PhD journey.

The Hall lab has been invaluable during the long hours in the lab as well during discussions of research results and journal clubs. Stephen, thanks for being a good example on how to be a successful PhD student, and for giving me lots of advice on any aspect of the PhD-life and

academia. Toby, thanks for being my “partner in crime”. I am so happy that we started our PhD’s at the same time, and have been able to share so much time together at work as well as private, in the climbing gym, at bars in Melbourne, or on outdoor adventures in beautiful Australia. Our friendship and deep conversations about life has been invaluable throughout the last 3.5 years, and I wouldn’t have come this far without your support. Lindsey – no words can explain! Thanks for being the best lab manager ever! Thanks for being so positive at all times, for making the lab a pleasant place to work, and first and foremost, thanks for being my friend! Isobel, a special thanks to you for letting me move into your apartment for a short-term period, which turned into almost a year worth of “house-mating”. I have really enjoyed the time in St. Kilda, and I hope that I one day can return the favour, in case you ever need a place to stay (wherever in the world I will be positioned ☺). Thanks also to all volunteers and honours students in the Hall lab – you guys have made the lab a fun place to be. During my time at Monash, I have also met a bunch of cool fellow PhD-students who played a large part in making my PhD experience enjoyable. Among many cool people, a special thanks to Julie, Emily, Melissa, Sonia, Clem, Michael, Niki, Lotte, Quam, Beccaa, Cathy and Evatt.

Despite many hours in the lab and countless hours at the desk (which for me can be a serious challenge, given my energy level), I have also managed to prioritise a private life. I have somehow managed to get out and do what I love the most on many lovely weekend trips. Through my passion for climbing and mountain biking, I have made many invaluable friends for life, and had it not been for you guys, then I would never have made it through. A special thanks to my friend Russel, who have supported and helped me though long nights drilling experimental jars, cutting silicone tubing and thinking of smart ways to set up new experiments. Thanks also for allowing me to use your mums shed for building all of these crazy experimental setups, and for supporting me in work and in life.

A big thanks also to my family. Thank you for being open and supportive towards my decision about moving overseas, even when the distance is long. I am indeed out of a travelling family, and who knows where the wind will take us over the next couple of years, but I am looking forward to living closer to you all soon again. Thank you for supporting me in the completion of this PhD, even if the topic and findings does not always make sense, when I try to explain it 😊

Finally, a special thanks to Samuel Gervais. Thank you for making my life cheerful and for sticking with me despite terrible timing and lots of stress for both of us. You have seen the worst of me (and me of you), and we have still managed to get the best out of the situation. Thanks for stimulating positive thinking, progressivity and self-esteem during the hard times. Life isn't always easy, but you have taught me how to fight for myself and stay strong! Thanks for being my spirit bird.

Je t'aime!

Table of Contents

| | |
|---|-----------|
| Abstract | 3 |
| Publications during enrolment | 5 |
| Thesis including published works declaration | 5 |
| Acknowledgements | 7 |
| Chapter 1: General Introduction | 12 |
| Patchy habitats, metapopulations and the potential for evolutionary change | 14 |
| Patchy population alter the types of host-parasite interactions | 15 |
| Dispersal opportunities and coupled life-history trade-offs | 16 |
| Food resources, energy scope and the importance of patch quality | 18 |
| Other sources of host heterogeneity that can alter pathogen evolution | 20 |
| The need for controlled experimental systems | 21 |
| Thesis organisation | 23 |
| Chapter 2: Infection in patchy populations: contrasting pathogen invasion success and dispersal at varying times since host colonization | 24 |
| Abstract | 24 |
| Impact summary | 25 |
| Introduction | 26 |
| Materials and methods | 30 |
| Results | 36 |
| Discussion | 38 |
| Acknowledgements | 42 |
| Chapter 2 - Figures and tables | 43 |
| Chapter 2 - Supplementary material | 49 |
| Chapter 3: Energetic constraints in range expanding and colonizing populations and their consequences for pathogen fitness | 57 |
| Abstract | 57 |
| Introduction | 58 |
| Materials and methods | 61 |
| Results | 66 |
| Discussion | 70 |
| Acknowledgements | 73 |
| Chapter 3 - Figures and tables | 74 |
| Chapter 3 - Supplementary material | 79 |

| | |
|---|------------|
| Chapter 4: Can pathogens optimize both transmission and dispersal by exploiting sexual dimorphism in their host? | 84 |
| Abstract | 84 |
| Introduction | 84 |
| Materials and methods | 86 |
| Results | 88 |
| Discussion | 89 |
| Acknowledgements | 91 |
| Chapter 4 - Figures and tables | 92 |
| Chapter 4 - Supplementary material | 94 |
| Chapter 5: Pathogens on the move – high host-facilitated dispersal is associated with evolutionary changes in parasite life-history traits | 99 |
| Abstract | 99 |
| Introduction | 100 |
| Materials and methods | 104 |
| Results | 110 |
| Discussion | 114 |
| Acknowledgements | 117 |
| Chapter 5 - Figures & Tables | 118 |
| Chapter 5 - Supplementary material | 125 |
| Chapter 6: General discussion | 133 |
| The stepwise invasion process and the potential for diversifying selection | 133 |
| How energy scope and host life-history determine pathogen fitness | 134 |
| Sexual dimorphism as a lever for life-history optimization | 135 |
| Dispersal and correlated changes in parasite life-history | 136 |
| Conclusions | 138 |
| Future directions | 139 |
| Cited literature | 140 |

Chapter 1: General Introduction

Understanding epidemic spread and its devastating consequences for human health, agriculture and wildlife, is a major challenge to epidemiologists and evolutionary biologists (Anderson and May, 1981; Parratt, Numminen and Laine, 2016; Penczykowski, Laine and Koskella, 2016). At its simplest, a pathogen moving through a host population can be thought of as a traveling wave, and in spatially homogeneous populations, classic theory predicts the spread of highly exploitative (i.e., virulent) pathogens with high transmission potential (Anderson and May, 1981; Andre and Hochberg, 2005). Conditions met in nature, however, are not always that simple. Instead, most host populations are highly dynamic and are undergoing recurrent extinction and recolonization processes. As a result, accurate predictions for the rate at which a pathogen spreads through a landscape, or how it might evolve during an epidemic, depend on the complex interactions between the demographic configuration of the host population, the environment (Becker, Hall, et al. 2018; Becker, Snedden, et al. 2018), and the existence of any trade-offs between the damage a pathogen caused during infection, and the subset dispersal abilities of its host (Griette, Raoul and Gandon, 2015; Osnas, Hurtado and Dobson, 2015).

In this thesis, I explore how host population dynamics that arise during range expansion, invasion, or in analogous metapopulations, impact on the evolution of infectious disease (see Fig. 1). First, however, let us consider how successful pathogen invasion (Fig. 1, A) requires a pathogen to overcome multiple barriers (sensu, Blackburn et al. 2011; Hall, Bento, & Ebert, 2017) through a stepwise invasion process. To begin with, a pathogen must establish in the host population after an infected carrier or propagule arrives (stage 1). Next, the pathogen must proliferate inside the infected host (stage 2), followed by spreading the infection to neighbouring susceptible hosts (secondary infection) within the same population (stage 3). Lastly, the pathogen must also disperse to new patches (passively or, for many pathogens, via host movement), to infect host populations in

a patchy landscape, or keep pace with the rate of its host's range expansion (stage 4). As a consequence of such a step-wise invasion process, multiple opportunities may arise for host population dynamics to alter the types of pathogen transmission and virulence strategies that are favoured, and in turn, the spread of infectious disease. In this general introduction, I describe the different types of ecological or evolutionary processes that can influence a pathogen's invasion strategy.

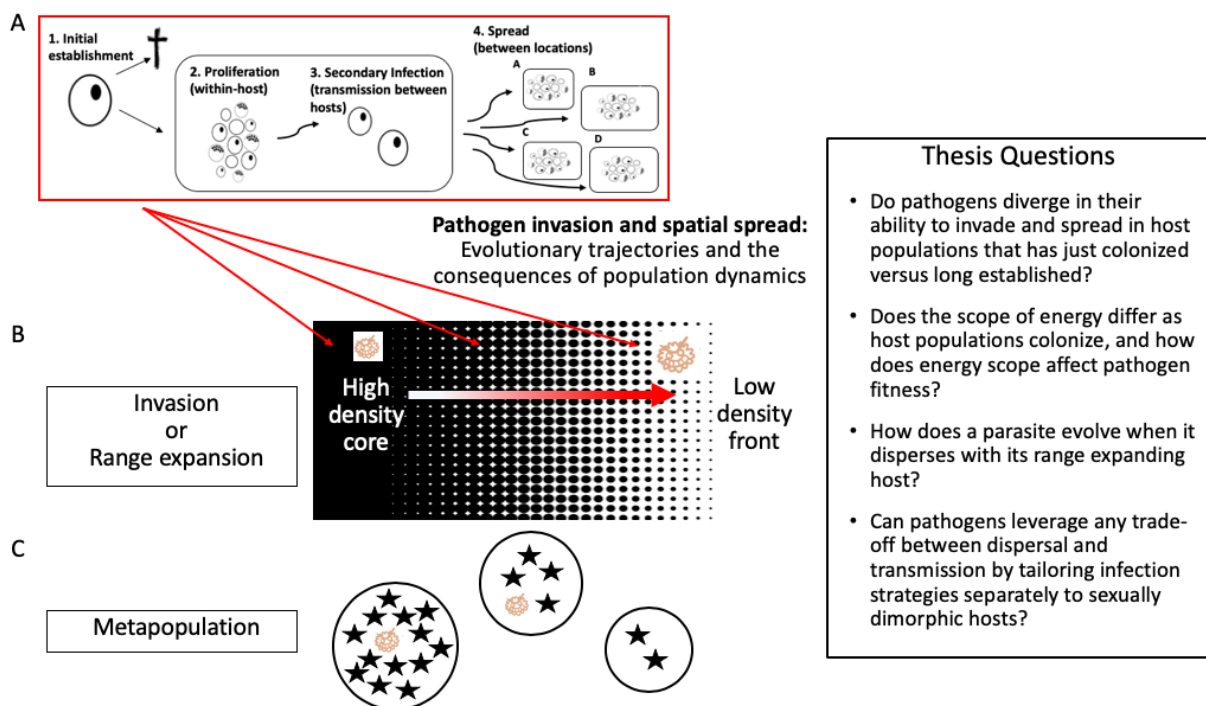


Figure 1: A schematic overview of my thesis. The four invasion steps that a pathogen must overcome to successfully establish and spread (A): 1. initial establishment by entering a susceptible host, 2. within-host proliferation, 3. secondary transmission to susceptible hosts in the same population, and 4. spatial spread between locations, to encounter and infect susceptible hosts in a new population. My thesis then centres on understanding how the encounter with host populations at different places along an invasion gradient (B, invasion or range expanding host population), or populations at various phases of patch colonization (C, metapopulation dynamics), alters the pathogen invasion strategies that are favoured. Finally, overall thesis questions are outlined in the black box to the right, and each question is addressed in each of the experimental chapters.

Patchy habitats, metapopulations and the potential for evolutionary change

As described by classic metapopulation theory (Hanski, 1991; Hanski and Gilpin, 1991), most populations are organised in a network of spatially interconnected habitat patches that are undergoing repeated extinction and recolonization processes. Here, the demographic conditions met in recently established host populations differ from conditions in long established populations at, or near their carrying capacity. Generally, populations undergo an exponential growth phase just after colonization, until eventually reaching the carrying capacity, potentially with some demographic overshoot in between (Gilpin and Ayala, 1973; Hanski and Gilpin, 1991; Drake and Griffen, 2009). Similar conditions arise in a host population spreading through a landscape, where the expansion front is growing exponentially (Giometto et al. 2014), and the core parts of the population are often density regulated (Sakai et al. 2001; Dwyer and Morris 2006; Phillips, 2009, 2015; Sullivan et al. 2017). Thus, conditions at the invasion front is characterised by low population density, high resource availability, high reproductive rates, and in turn, low conspecific competition (see Burton, Phillips, & Travis, 2010).

Arising from the recognition that repeated extinction and recolonization events generate a landscape of host populations that vary in their time since colonization, tension between colonization and competition has emerged as a key modifier of pathogen life history. Considering the step-wise pathogen invasion process as described above (see Fig. 1A), emerging literature suggests that a fundamental trade-off exist between pathogen performance in established host populations versus their capacity to disperse to, and establish in new patches (Boots, Hudson and Sasaki, 2004; Bradley and Altizer, 2005; Burton, Phillips and Travis, 2010; Fellous et al. 2012). Therefore, an invading pathogen genotype will rarely, if ever, be good at both, and it is possible that conditions that favor different pathogen establishment or competitor strategies arise as an organic part of the host colonization processes itself (Ebenhard 1991; Hanski and Gilpin 1991; Soubeyrand and Laine

2017). We may therefore expect that the process of range expansion, invasion or patch colonization, could generate a gradient of different selection pressures acting on pathogens across a landscape (or over time in case of a metapopulation colonization). In the following sections, I more explicitly consider a variety of different ways that selection on a pathogen might change as a consequence of patchy populations.

Patchy population alter the types of host-parasite interactions

A useful place to start when thinking of variation in the performance of a pathogen across a landscape, is to consider how spatial structure within a single population, or between populations in a metapopulation, can alter the way host and pathogens encounter each other. First, populations may vary in the density of susceptible hosts, thus providing different opportunities for secondary transmission. Next, connectivity between patches may vary greatly, and such differences causes changes in the likelihood of successful dispersal of both hosts and pathogens between habitat patches (see Parratt, Numminen and Laine, 2016; Penczykowski, Laine and Koskella, 2016). As a result, transmission of a pathogen between hosts can occur at both small spatial scales (local interactions) and large spatial scales (global interactions), with each having a specific influence on how a pathogen might evolve.

At the local scale, transmission occur between neighbouring susceptible individuals, and as a consequence, pathogen genotypes are likely to be more closely related, infected hosts tends to be clustered, and pathogens with high infectivity will therefore “self-shade” (Boots and Sasaki, 1999, 2000; Boots, Hudson and Sasaki, 2004). On the contrary, if populations become more mixed, as a consequence of long-distance (global) dispersal, a parasite will encounter more susceptible hosts, genetic structuring will be diminished, and quickly transmitting pathogens will have an advantage (see Ewald 1995).

Theory, as a consequence, predicts that local interactions in a spatially structured population, should select for reduced pathogen infectivity (Boots and Sasaki, 1999, 2000; Haraguchi and Sasaki, 2000) and virulence (Boots, Hudson and Sasaki, 2004; Kerr et al. 2006). Two different explanations for this prediction has been put forward; i) kin-selection, or ii) “self-shading”, where clustering of infected individuals reduce the transmission potential of highly exploitative pathogens (see for review on theoretical approach Lion and Gandon, 2015). Oppositely, when infection occur at a distance, theory predict that pathogens will be selected for more rapid transmission and higher virulence (see Boots, Hudson and Sasaki, 2004)

To test such predictions, one method is to manipulate the spatial structure in a host population, and observe how different levels of spatial structure impact on pathogen life-history evolution. One example of an experimental manipulation of local versus global interactions was achieved by increasing the viscosity of food media in populations of phycitid larvae moths, infected with a granulosis virus (Boots and Meador, 2007). Using this approach, local interactions was found to cause evolutionary loss of infectivity, but also showed how local interactions caused pathogen-driven changes in host population stability, indicating higher impact of infection with local interactions (see Boots et al. 2009). Similarly, restricted migration in a phage infecting *E.coli* favoured the evolution of pathogens with low infectivity and low virulence (Eshelman et al. 2010). Thus, empirical examples support the prediction that local interactions and constrained dispersal limits the evolution of pathogen infectivity and virulence (Boots and Sasaki, 1999; Haraguchi and Sasaki, 2000; Boots, Hudson and Sasaki, 2004).

Dispersal opportunities and coupled life-history trade-offs

The ability of hosts and pathogens to spread through a landscape also often differ, and such asymmetry in dispersal abilities are observed in many natural populations (see Hajek and Tobin, 2011; discussed in Penczykowski, Laine and Koskella, 2016). One example of such, is the spread of

a trematode parasite (*Microphallus sp.*) and its freshwater snail host. Here, parasite gene flow was much higher than that of the host, and helped to reintroduce genetic diversity within the local populations (Dybdahl and Lively, 1996). Asymmetry in dispersal abilities between a host and pathogen are predicted to lead to different levels of local adaptation for each. Gandon et al. (1996), for example, showed that pathogens should be more adapted to their local host population when their migration rate is higher than their hosts. This prediction was explained by a decrease in resistance with high host migration, since susceptible hosts are frequently introduced. Oppositely, with low migration, resistance increased; thus, in this model, when either host or parasite had low dispersal rates, an increase in dispersal by one of the two, reduced the others local adaptation. In most systems, however, infection often reduce (Fellous et al. 2011; Nørgaard, B. L. Phillips and Hall, 2019; Nørgaard, Ben L. Phillips and Hall, 2019), or alter host dispersal in one way or another (Thomas et al. 2002; Hawley et al. 2013; Wesolowska and Wesolowski, 2014).

During host invasion and range expansion processes, differences in dispersal abilities arise due to both adaptive processes, and the ongoing spatial sorting within a host population (Phillips, Brown and Shine, 2010; Perkins, Boettiger and Phillips, 2016). Such increased dispersal abilities have been demonstrated in a series of natural species (Cwynar and MacDonald, 1987; Hill, Thomas and Blakeley, 1999; Simmons and Thomas, 2004), including the classic example of the invasive cane toads in Australia (Phillips et al. 2006) Thus, individuals at the invasion front evolves higher dispersal rates, although recent theoretical work has reiterated that stochasticity in invasion processes can cause large variation (see Phillips, 2015). Since many pathogens spread to new habitats via host-facilitated dispersal, it is then plausible that pathogens infecting the front of an invading, or range expanding host population, must necessarily invest in strategies that have the least detrimental impact on host dispersal (Phillips et al. 2010), or even, in specific circumstances, facilitating greater host dispersal (see also Lion, Van Baalen and Wilson, 2006).

Studies on the spread of the bacterium *Mycoplasma gallisepticum* in house finches through in North America (Hawley et al. 2013) have, for example, led to the emergence of novel theory suggesting that the ability of a pathogen to spread via host-facilitated dispersal may trade-off with virulence and transmission (Osnas, Hurtado and Dobson, 2015). In this scenario, pathogens at the invasion front is expected to cause minimal interference with host dispersal (Lion, Van Baalen and Wilson, 2006), and maintain more prudent infection strategies, relative to parasites in the parasites infecting the core population. However, if pathogen virulence evolution is not driven by such trade-offs, the opposite predictions apply, and high dispersal (long-distance / global transmission) is predicted to select for increased virulence in space (Boots, Hudson and Sasaki, 2004; Berngruber et al. 2013; Griette, Raoul and Gandon, 2015), as observed in in the emergence of the virulent rabbit haemorrhagic disease virus (Moss et al. 2002; Boots, Hudson and Sasaki, 2004). Thus, theoretical predictions are rather contradictory, and rely on how dispersal is incorporated into disease predictions, and there is an increasing need for empirical studies to test how pathogens may evolve in response to host dispersal.

Food resources, energy scope and the importance of patch quality

Another important component linked to spatially distributed, and demographically variable host populations, is that different patches will vary in their quality. Such inequality in patch quality (in this case, experienced by a host) was first defined Pulliam (1988) as source-sink dynamics. This theory describes how a habitat patch of high quality (source) can sustain high population density (and growth rate), whereas a neighbouring habitat patch might be of low quality (sink), and would go extinct, if there were no incoming emigrants from the source population (Pulliam, 2016). In a host-pathogen context, such high-quality, or resource rich patches, both attract and support greater host and pathogen densities, which facilitate a constant supply of infected carriers across a landscape (e.g., Leach et al. 2016; Becker et al. 2018).

In terms of patch quality, another important consideration is the direct role of population density, which ultimately dictates the degree of resource competition experienced for the host, but also the number of susceptible hosts that a pathogen is likely to encounter. The amount of resources available for organismal maintenance (be that the host or pathogen) may therefore differ relative to the density of surrounding competitors in a patch, potentially giving rise to fundamental variation in the rate at which organisms consume, transform and expend energy (Buckley, Nufio and Kingsolver, 2014; Ghedini, White and Marshall, 2017). Across a density gradient, we might therefore expect to see differences in the amount of energy within a host, that is available for optimization of life-history traits such as growth, reproduction or fighting infection (Ghedini, White and Marshall, 2017). Such differences in resource availability has been shown to alter various components of host and pathogen fitness, potentially due to changes in the pool of resources available for the pathogen to exploit (Bedhomme et al. 2005; de Roode, Yates and Altizer, 2008), or changes in immune investment (Brown, Loosli and Schmid-Hempel, 2000; Seppala et al. 2008).

The difference between organismal energy intake and expenditure can be defined as discretionary energy, and an increase in discretionary energy could, for example dampen the proliferation and spread of a pathogen, if it allows a resource intensive immune response to either clear infection, or limit pathogen proliferation (Sheldon and Verhulst, 1996; Hite and Cressler, 2018). On the other hand, if the flow of energy translates directly into pathogen performance, then the spread of disease will be accelerated under conditions that increase energy availability (Hall, Knight, et al. 2009; Hall, Simonis, et al. 2009; Cressler et al. 2014; Civitello et al. 2015). Recent empirical work has established that individuals in low density conditions, such as at the invasion front, maintain more discretionary energy (Ghedini, White and Marshall, 2017). How such increase in discretionary energy, however, translates into pathogen performance remains unexplored, but will likely have large impact on the risk of epidemic outbreaks in range expanding and patchy host populations.

Other sources of host heterogeneity that can alter pathogen evolution

Aside from spatial and demographic variation in host populations, other sources of heterogeneity represent the different types of hosts that are circulating in a population. As such, hosts within a population can vary greatly in their size, age, dispersal behaviour, and their susceptibility to infection, which are all factors that can modify the performance of an invading pathogen. Several studies have confirmed that when host heterogeneity is large, a range of possible pathogen virulence strategies can be maintained (Regoes, Nowak and Bonhoeffer, 2000; Gandon, 2004; Osnas and Dobson, 2011). In addition, when hosts differ in the resources they provide to a pathogen, theory predicts that pathogen proliferation will be optimized in the more exploitable host (Hall, Knight, et al. 2009).

One widespread source of host heterogeneity that is applicable to many species, are differences between male and female hosts. In sexually dimorphic species, males and females are likely to differ in a series of life-history traits such as size, dispersal behaviour (Fairbairn, 1997; Li and Kokko, 2018), and in their prevalence and response to infection (Poulin, 1996; Schalk and Forbes, 1997; Zuk, 2009). Such fundamental differences between two host types is known to impact on host-pathogen coevolution in a variety of ways (see review Gipson and Hall, 2016). Furthermore, some studies have captured the interplay between key pathogen fitness components by linking one host sex to the spatial distribution of a pathogen (Streicker et al. 2016), and revealing how investment in dispersing life-stages (Soghigian and Livdahl, 2017) or modes of transmission (Fellous and Koella, 2009) depends on host sex. Those studies provide great evidence that the existence of two different host sexes are likely to provide a pathogen with different opportunities in terms of proliferation and spatial spread. However, the possibility that pathogens could simultaneously optimize both transmission and dispersal by tailoring infection strategies to different kinds of hosts, be that males and females, has gone largely unexplored.

The need for controlled experimental systems

The evolutionary impact of host population dynamics arising along an invasion gradient, or during patch colonization is challenging to evaluate, and particularly difficult to measure in nature.

Theoretical approaches, however, offers a strong tool to overcome some of this complexity, but although the current disconnects between theoretical predictions suggest that there is an increasing need for development of experimental systems, in which the influence of several demographic and epidemiological components can be isolated and assessed on an ecologically and evolutionary relevant scale. In this thesis, I develop such controlled laboratory systems, in which we can test different predictions about evolutionary disease dynamics.

To do so, I use two different experimental model systems in a series of chapters. In chapters 2, 3 and 4, I use the crustacean host *Daphnia magna* and its bacterial pathogen *Pasteuria ramosa*. *D. magna* is a facultative parthenogenetic crustacean inhabiting freshwater lakes and ponds throughout Eurasia and North America. *Daphnia* encounter *P. ramosa* through filter feeding, after which spores start to proliferate within the infected host and the first mature transmission spores appears about 18 days post infection, at which point infection is easily recognized due to a change in the coloration of the infected host (Ebert et al. 2016). *P. ramosa* is a strictly horizontally transmitted pathogen, and infection causes severe loss of fecundity, an increase in body size (pathogen-induced gigantism), and reduces survival of infected hosts (Hall and Ebert 2012; Ebert et al. 2016). The *Daphnia-Pasteuria* model system is a particularly good candidate for studying questions about pathogen performance and how this is affected by population demography because both host life-history and pathogen performance can be impacted by the density of conspecifics in a population (see Michel, Ebert and Hall, 2016), and reduced resource intake (and quality; Penczykowski et al. 2014), reduces both host fecundity and pathogen spore production (Pulkkinen and Ebert, 2004; Cressler et al. 2014).

In chapter 5, I use the ciliate host *Paramecium caudatum* and its bacterial parasite *Holospora undulata* to test the impact of dispersal selection on the host, for evolution of parasite life-history traits. *P. caudatum* is a filter-feeding freshwater protozoan ciliate, inhabiting still water bodies in the Northern Hemisphere (Wichterman, 1986). Upon filter-feeding, *P. caudatum* can get infected with the gram negative alpha-proteobacteria, *H. undulata*, which can be transmitted both horizontally (by s-shaped infectious forms, 15µm) upon host death (or during cell division), and vertically, when reproductive bacterial forms (5µm) segregate into daughter nuclei of a mitotically dividing host (Görtz and Dieckmann, 1980). Infection with *H. undulata* reduces host cell division and survival (Restif and Kaltz, 2006) and also host dispersal (Fellous et al. 2011). This system is highly suitable for experimental evolution experiments due to the short generation time of the host (up to 3 divisions a day) and the parasite (1-2 divisions a day), as well as ease of culturing. In addition, spatial spread of the infection is only possible via movement of infected carriers (Fellous et al. 2011), and host population dynamics has been shown to change transmission strategies of *H. undulata* (see Nidelet, Koella and Kaltz, 2009; Magalon et al. 2010).

In the context of my experimental chapters, I employ the terminology “pathogen” for infection of *D. magna* with the bacterial *P. ramosa*, whereas in the ciliate system, the bacterial *H. undulata* is referred to as a “parasite”. In the primary literature, however, those two terms are generally used interchangeably, and my choice of terminology is related to the nature and tradition within each of the two laboratories that I have been working in.

Thesis organisation

The overall aim of my thesis is to explore how host population dynamics and various demographic factors associated with metapopulation colonization and range expansion processes, impact on the evolution of infectious disease (see Fig. 1).

Shortly, in my first experimental chapter, I explore how the different stages of host colonization influences each step of the pathogen invasion process differently (Fig. 1A). I show that the transient dynamics of host population colonization ultimately provides the conditions required for diversifying selection to act on a pathogen species. Next, I explore how differences in energy scope at various densities, impact on pathogen fitness, and I found that both the host and pathogen benefited from more energy available in low density populations. In my fourth chapter, I explore and confirm the idea that that pathogens can mitigate the trade-off between transmission and dispersal by exploiting sexual dimorphism in their hosts. In my final experimental chapter, I take an experimental evolution approach using *P. caudata* and *H. undulata*, and show how dispersal selection on the host population cause correlated changes in parasite infection strategy.

This thesis is presented as a “thesis including published works” consisting of a general introduction (Chapter 1), two peer-reviewed and published papers (Chapters 2 & 4) and two manuscripts intended for publication in peer-reviewed journals (Chapters 3 & 5). Chapter 2 is published in *Evolution Letters* and Chapter 4 is published in *Biology Letters*.

I was responsible for the planning, research, laboratory work, data collection & analysis, and manuscript preparation for each presented chapter. However, the first-person plural is used in subsequent chapters to reflect the collaborative nature of my research.

Chapter 2: Infection in patchy populations: contrasting pathogen invasion success and dispersal at varying times since host colonization

Louise S. Nørgaard^{1,2}, Ben L. Phillips³ and Matthew, D. Hall¹

Manuscript is published in *Evolution Letters* 3-5: 555-566.

Abstract

Repeated extinction and recolonization events generate a landscape of host populations that vary in their time since colonization. Within this dynamic landscape, pathogens that excel at invading recently colonized host populations are not necessarily those that perform best in host populations at or near their carrying capacity, potentially giving rise to divergent selection for pathogen traits that mediate the invasion process. Rarely, however, has this contention been empirically tested. Using *Daphnia magna*, we explored how differences in the colonization history of a host population influence the invasion success of different genotypes of the pathogen *Pasteuria ramosa*. By partitioning the pathogen invasion process into a series of individual steps, we show that each pathogen optimizes invasion differently when encountering host populations that vary in their time since colonization. All pathogen genotypes were more likely to establish successfully in recently colonized host populations, but the production of transmission spores was typically maximized in either the subsequent growth or stationary phase of host colonization. Integrating across the first three pathogen invasion steps (initial establishment, proliferation, and secondary infection) revealed that overall pathogen invasion success (and its variance) was, nonetheless, highest in recently colonized host populations. However, only pathogens that were slow to kill their host were able to maximize host-facilitated dispersal. This suggests that only a subset of pathogen genotypes - the

less virulent and more dispersive - are more likely to encounter newly colonized host populations at the front of a range expansion, or in metapopulations with high extinction rates. Our results suggest a fundamental trade-off for a pathogen between dispersal and virulence, and evidence for higher invasion success in younger host populations, a finding with clear implications for pathogen evolution in spatiotemporally dynamic settings.

Keywords: competitor versus colonizer, diversifying selection, dose-density response, *Daphnia magna*, evolution of disease, epidemiology, *Pasteuria ramosa*, spatial spread

Impact summary

Infectious disease is a major threat to human and wildlife well-being, and it is well recognized that pathogens have the ability to evolve over time to persist in a host population. Host–pathogen theory has largely centred on the evolution of disease in stable and nondynamic host populations.

However, natural host populations are rarely static and rather characterized by changing population dynamics (and densities) across time and space. For example, in range expanding species, or analogous metapopulations with high extinction rates, empty habitat is regularly colonized by dispersing individuals. Thus, understanding how infectious disease evolves as it spreads through a patchy landscape, and what pathogen strategies may be favored at different times of the host colonization process, is essential for understanding the evolution of pathogens in nature.

Using the water flea *Daphnia magna* and its associated bacterial pathogen *Pasteuria ramosa*, we experimentally tested the idea that different pathogen strategies may be favored whenever pathogens encounter host populations that vary in their time since colonization. Our results show that pathogen genotypes optimized the invasion process in different ways, and an invasion strategy that is successful when invading newly colonized host populations is unlikely to be successful when encountering host populations undergoing the subsequent growth or stationary phases. In particular, the ability of a pathogen to disperse via its infected carrier determines whether a pathogen is likely to

coincide with newly colonized host populations. Our results suggest that prudent and highly dispersive pathogens are more likely to encounter (or keep pace with) newly colonized host populations at the range front of an expanding host population or in metapopulations. Our work demonstrates that pathogen invasion success and spatial spread is strongly linked to the host population dynamics encountered. This empirical work thus reiterates the importance of developing a better understanding of how host population dynamics influences the evolution of infectious disease in spatially explicit settings

Introduction

In 1951, GE Hutchinson coined the term “fugitive species” for species that are specialized colonizers (Hutchinson 1951). These species, he argued, while good at colonizing empty patches, are typically poor competitors. As such, they exist in a tenuous niche, constantly needing to colonize newly available space before they are outcompeted in their current location by later arriving, but competitively superior species (Calcagno et al. 2006). Although originally applied to the distribution of free-living species across a patchy landscape (Tilman 1994), tension between colonization and competition is emerging as a key modifier of pathogen life history as well. Studies have observed, for example, that the initial performance of a pathogen after invading a host population does not necessarily translate into long-term persistence (Fellous et al. 2012), that migratory animals can have a lower pathogen prevalence than their nonmigratory relatives (Bradley & Altizer 2005), and that pathogens can lag behind their hosts during periods of host range expansion (Boots, Hudson, and Sasaki 2004; Phillips et al. 2010; Fellous et al. 2011). Collectively, these examples imply a fundamental trade-off between pathogen performance in established host populations versus their capacity to disperse to, and establish in, new patches, such that an invading pathogen genotype will rarely, if ever, be good at both.

Conditions that favor different pathogen establishment or competitor strategies are routinely met in host metapopulations (Ebenhard 1991; Hanski & Gilpin 1991; Soubeyrand & Laine 2017). Here, stochastic extinction at the patch level generates vacant habitat available for recolonization by dispersing hosts, resulting in a landscape of populations at different colonization phases. Typically, populations undergo an exponential growth phase just after colonization, through to density-regulated dynamics in older populations at or near the carrying capacity, possibly with some demographic overshoot in between (Gilpin & Ayala 1973; Hanski & Gilpin 1991; Drake & Griffen 2009). A similar range of demographic scenarios exist in a host population spreading through space, where the expansion front is growing exponentially (Giometto et al. 2014), and the core parts of the population are often density regulated (Sakai et al. 2001; Dwyer & Morris 2006; Phillips 2009, 2015; Sullivan et al. 2017).

In general, opportunities for diversifying selection to act on a pathogen will occur organically as a consequence of the invasion process itself. Invasion, much like other complex processes such as infection (Hall et al. 2017) or zoonotic spillover (Plowright et al. 2017), requires a pathogen to overcome multiple barriers to successfully reproduce, transmit, and disperse (see Fig. 1; sensu Blackburn et al. 2011). For an outbreak of infectious disease to occur, a pathogen must first establish in the host population after an infected carrier or propagule arrives (stage 1). It must then proliferate inside the infected host (stage 2) and spread the infection to new susceptible hosts (secondary infection) within the same population (stage 3). Finally, the pathogen must also disperse to new patches (passively or, for many pathogens, via host movement) to infect new host populations in a patchy landscape, or keep pace with the rate of its host's range expansion (stage 4). Viewing this process through the lens of diversifying selection implies that the demographic conditions in any given host patch will define what is optimal for a given pathogen genotype at each stage of the invasion process, and in turn, the types of pathogen strategies that are likely to be favored in any given patch or time (e.g., Wei and Krone 2005).

Theory describing the types of pathogen strategies that are favored during the invasion process has traditionally focused on long-term changes in selection. Highly transmissible and virulent pathogens, for example, are expected to prevail at the start of the invasion (i.e., epidemic phase), whereas more prudent exploitation strategies are favored once a pathogen is maintained stably in the host population (i.e., endemic phase) (Lenski & May 1994; Day & Proulx 2004; Day & Gandon 2007; Berngruber et al. 2013). These predictions, however, centre only on one part of a pathogen's invasion process (i.e., stages 2 and 3, Fig. 1) and the long-term evolutionary dynamics of pathogens in isolated and demographically stable host populations. Instead, trade-offs between the damage a pathogen causes its host versus its capacity to disperse into new patches (steps 2 and 3 vs. 4, Fig. 1) have emerged as the defining characteristic of how a pathogen might evolve when host populations vary in time and space (Griette et al. 2015; Osnas et al. 2015). When trade-offs between dispersal and virulence occur, theory predicts that evolution will favor more prudent host exploitation strategies at the expanding range edge (Osnas et al. 2015). In the absence of such a trade-off, highly virulent pathogen strategies are expected to prevail at the range edge (Griette et al. 2015).

Accurate predictions for the rate at which a pathogen spreads through space, or how it might evolve during an invasion, thus depend on both the demography of a host patch and the occurrence of any trade-offs between exploitation and dispersal. Yet, few studies have directly estimated whether different pathogen genotypes diverge along such a colonizer-competitor continuum. Here, we used the water flea *Daphnia magna* and its bacterial pathogen, *Pasteuria ramosa* (Ebert et al. 2016), to explore the sensitivity of each step of a pathogen's invasion (i.e., Fig. 1) to changes in the demography of the host population. *Daphnia* are an excellent candidate for exploring the effects of population dynamics, as habitat patches are commonly recolonized in response to seasonal changes, leading to large fluctuations in population density and disease prevalence over time (e.g., Bieger and Ebert 2009; Altermatt and Ebert 2010). The fitness of *P. ramosa* is also tied to the demography

of its host as transmission depends on both virulence (i.e., host mortality) and the production of transmission spores (see Hall and Mideo 2018), both of which respond to changes in host density (Ebert et al. 2000; Michel et al. 2016). However, little is known about how infection alters host movement and subsequent spatial spread of disease.

With this system, we experimentally invaded multiple pathogen genotypes into host populations at different colonization phases, and evaluated whether pathogen genotypes varied along the competition-colonization axis that is integral to recent models of pathogen invasion (Griette et al. 2015; Osnas et al. 2015). First, we demonstrated that host populations possess three clear (and repeatable) population growth phases following initial colonization (rapid growth after initial colonization, overshoot, and stationary phase). Next, in a series of experiments, we showed how each step of a pathogen's invasion (i.e., Fig. 1; initial establishment, proliferation, secondary infection) is highly sensitive to the colonization phase of the host population experienced and differs between pathogen genotypes. Finally, using a simple epidemiological model, we integrated each component of a pathogen's invasion into a single metric of invasion success at each host colonization phase, and compared this with their ability to disperse. Our invasion metric and dispersal measures supported the prediction that diversifying selection may arise as a natural consequence of host population colonization. Here, pathogens will either be good at invading established host populations or good at dispersing via movement of infected carriers. With this in mind, we discuss how changes in host colonization dynamics can provide the conditions that should favor different colonization or competitor strategies in patchy landscapes, and the implications this has for the evolution of pathogen virulence.

Materials and methods

The study system

Daphnia magna Straus is a filter-feeding cladoceran that reproduces via cyclic parthenogenesis (matures at approximately 10 days old, Ebert 2005). It is found in freshwater brackish lakes and ponds throughout Eurasia and North America and populations experiences large fluctuations in density throughout a year (Ebert 2005; Altermatt & Ebert 2010). A common pathogen of *Daphnia* is the endospore forming, Gram-positive bacteria, *Pasteuria ramosa* Metchnikoff, 1888. *Daphnia* encounter *P. ramosa* through filter feeding, after which spores start to proliferate and the first mature transmission spores appears about 18 days post infection (DPI), at which point infection is easily recognized due to a change in the coloration of the infected host (Ebert et al. 2016).

Transmission is exclusively horizontal, and symptoms of disease includes castration, gigantism, and reduced lifespan (Hall & Ebert 2012; Ebert et al. 2016). The host used in this study originated from Hungary (HU-HO-2), and the five novel *P. ramosa* genotypes originated from Russia (C1), Finland (C14), Germany (C19), UK (C20), and Belgium (C24), representing a wide geographical and ecological distribution (Luijckx et al. 2011). These five pathogen genotypes vary considerably in virulence (i.e., the reduction of host lifespan) and production of transmission spores (Clerc et al. 2015; Hall & Mideo 2018).

Overview of experimental design and conditions

This study consists of five sections: (1) first, we characterized the dynamics of host colonization within a multi-patch system by tracking changes in population size over time within each patch; (2) we then measured how the first two steps of pathogen invasion for multiple pathogen genotypes (establishment and proliferation, Fig. 1), varied with host colonization phase; (3) we estimated how infection rates at different host densities relate to the number of transmission spores potentially released from an infected carrier; (4) we measured the impact of infection on host dispersal; and

finally, (5) we integrated the above pathogen traits (except for dispersal) into a single metric of pathogen invasion success. Unless stated otherwise, all experiments were maintained following standard protocols and growing conditions as outlined in the Suppl. material (section A).

Section 1: Characterizing host colonization dynamics

To determine the repeatability of host colonization, we first created four replicates of three interconnected experimental patches built from 500-mL containers filled with 400 mL artificial media (see Erm et al. 2019). On day 1, five 3-day old juveniles and one adult *Daphnia* were introduced into the first patch, and the subsequent population sizes at each patch were counted weekly thereafter. Different age-classes were incorporated to recreate more natural populations with overlapping generations. Populations were fed 50 million green algae (*Scenedesmus* sp.) cells three times a week and 50% of the media was renewed fortnightly. After 70 days, when all patches were inhabited, the experiment was terminated. From these results, we defined three repeatable characteristics of the colonization process: rapid growth after initial colonization, overshooting the carrying capacity from day 20, and stationary phase from day 40 onwards (see Results section, Fig. 2, and Suppl. material, section B).

Section 2: Characterizing pathogen establishment and within-host proliferation

We then tested how conditions in host populations undergoing these different phases of colonization (rapid growth, overshoot, and stationary), influenced the ability of a pathogen to successfully establish in a given host population and proliferate within their infected host (steps 1 and 2, Fig. 1). A total of 240 experimental populations were established using 500-mL glass jars. Each population was fed three times a week and had 50% of their media renewed fortnightly. Populations were allowed to colonize for either 40, 20, or 0 days prior to introducing six 10-day-old *Daphnia*, infected with one of the five pathogen genotypes. Each pathogen genotype and host colonization phase were replicated 16 times ([3 host colonization phases × 5 pathogen genotypes

× 16 replicates = 240 experimental populations] × 6 individuals introduced per population = 1440 infected individuals). Deaths of the infected *Daphnia* introduced to experimental populations were monitored daily and cadavers were frozen individually in vials filled with 500 µL RO (removing the chance for secondary infections to arise by horizontal transmission). After 20 days (at which point all surviving *Daphnia* will have produced mature transmission spores, Clerc et al. 2015), all surviving *Daphnia* (infected and uninfected) were collected, checked for infection under a dissecting microscope, and frozen individually as described above. Spore loads of infected animals were later quantified using an Accuri C6 flow cytometer (BD Biosciences, San Jose, California) following standard procedures as outlined in Gipson and Hall (2018). This procedure allowed us to estimate (1) the probability that the introduced infected *Daphnia* survive long enough for the pathogen to produce mature transmission spores within an infected host (E_{dg} , based on the proportion of recovered infected hosts that contained mature spores, where dg denote demographic phase and pathogen genotype); and, (2) pathogen transmission potential (L_{dg} , calculated as mean spore count within each host colonization phase and pathogen genotype).

Section 3: Characterizing the potential for secondary infections

Following successful establishment and within-host proliferation, the number of secondary infections immediately gained from the release of spores from a single cadaver depends on the number of infective spores released and the density of hosts in a given patch (stage 3, Fig. 1). We tested the influence of spore dose and host density on infection rates in a fully factorial setup using five environmentally relevant densities of *D. magna* (20, 80, 160, 240, or 320 individuals L⁻¹; $n = 20, 12, 8, 6,$ and 4) and three different doses of the five *P. ramosa* genotypes (50 000, 150 000, and 450 000 spores; i.e., low, medium, and high).

To establish the density treatments, the number of individuals required to create the densities (1, 4, 8, 12, and 16 individuals) were raised from birth in 50 mL ADaM. At seven days old, the host density

treatments were exposed to one of the three pathogen spore doses for 24 hours. After the exposure period, animals were transferred to jars with fresh media, at a standard density of four individuals per jar (within same density and pathogen combination) to maintain identical rearing conditions (and food availability) for all treatments. Experimental jars were then checked daily for deaths, and infection status was determined at 25 DPI based on the presence of mature spores. Due to mortality, we obtained infection status for 3857 out of 4020 individuals. Finally, assuming a density-dependent transmission model, we use these data (proportion of individuals infected at each host density and pathogen spore dose) to estimate the transmission coefficient for each pathogen genotype for use in our index of pathogen invasion success (β_g ; see Suppl. material, section F).

Section 4: Experimental measures of pathogen dispersal

To measure dispersal behavior of infected *Daphnia* and the consequent spread of *P. ramosa*, we introduced a single infected host (or uninfected control) into individual interconnected three-patch systems, built from 50-mL falcon tubes connected by 10 cm of food-graded silicon tubing. Dispersal was only allowed in forward direction and when reaching the third patch, two additional patches (with fresh ADaM) were provided. Dispersal and survival were tracked daily, and at death, *Daphnia* were frozen individually in vials filled with 500 μ L RO and stored at -20°C for later spore counts (as described above). Each infection treatment was replicated 20 times (5 pathogen genotypes + control \times 20 replicates = 120 experimental replicates). We then estimated the rate at which individuals move through space (patches traveled per day), as well as the total dispersal distance (sum of patches traveled in a lifetime) for hosts infected with each pathogen genotype and uninfected controls.

Section 5: an index of pathogen invasion success

Finally, we integrated each step of the pathogen invasion process (step 1, 2 and 3, Fig. 1) into an index of invasion success, allowing us to contrast the within-patch exploitation versus between-

patch dispersal capacity of each pathogen genotype (step 4, Fig. 1). Our measure of invasion success for each pathogen genotype (w_{dg} , detailed below) captures the likelihood of generating new secondary infections within a population of susceptible hosts at a standard density (arbitrarily, $S = 1$). By standardizing host density, w_{dg} focuses on relative fitness of pathogen genotypes, and diverges from the basic reproduction number of an infection (R_0 , Anderson & May 1981; Heffernan et al. 2005), which is often used to assess the rate at which a pathogen will invade a population. Our metric incorporates the uncertainty of a pathogen being able to establish in a patch after the initial introduction (step 1, Fig. 1). It also focuses purely on a pathogen's capacity to initiate an outbreak in a given population (i.e., the first secondary infection) rather than longer term persistence (which depends on host carrying capacity, birth rates, and death rates, as has previously been incorporated into estimates of R_0 for infections in *Daphnia* by the fungal pathogen *Metschnikowia bicuspid*; Civitello et al. 2013; Dallas et al. 2018).

To estimate w_{dg} , we first calculated the number of spores expected to be produced by each pathogen genotype in the three host colonization phases (P_{dg} , colonization phase d and genotype g), using data from Section 2. P_{dg} results from multiplying the probability that an infected carrier establishes within a given patch (E_{dg} , see Section 2) by the subsequent mean number of mature transmission spores (L_{dg} , see Section 2) that an infected individual would produce. We next used P_{dg} to develop our measure of pathogen invasion success (w_{dg}) under the mass-action assumption that the number of new infections would be $I_{dg} = \beta_g P_{dg} S$ (where S is an arbitrary host density and β is a transmission coefficient; see Suppl. material; section F). Here, β_g is our independent estimate of transmission for each pathogen genotype, and is obtained from the data in Section 3, where $\beta_{gijk} = \frac{I_{gijk}}{P_{ik}S_{jk}}$ is the per replicate measure of β , where I_{gijk} is the response variable (number of infected individuals), and P_{ik} and S_{jk} are the factor levels for pathogen dose and host density, respectively (k indexes the replicate within factor levels). We average this measure across i, j, k , to generate a

genotype-level estimate of β_g , and use bootstrapping to capture uncertainty in this estimate. We then estimate the number of new infections at a standard density ($S = 1$) to provide a standardized metric of pathogen invasion success, $w^{dg} = \hat{\beta}_g * P^{dg}$, for each combination of pathogen genotype and host colonization phase. We used the bootstrap distributions for β and P such that uncertainty propagated through to our estimate of w (see Suppl. material, section F).

Statistical analysis

All statistical analyses were performed in R (version 3.4.1; R Development Team, available at www.r-project.org). In Section 1, we analyzed the host colonization data using a generalized additive model with days modeled as a thin plate spline (see Suppl. material). In Section 2, we used a linear and generalized linear mixed-effect model, respectively, to analyze spore loads and the probability of establishment (using a binomial error structure). In each case, we used a two-factor analysis of variance (Type III) with colonization phase (growth, overshoot, and stationary phase), pathogen genotype, and their interaction as fixed effects, and experimental jar as a random effect, as implemented via the lme4 package (Bates et al. 2015). In Section 3, we modeled the probability of infection using a generalized linear mixed-effect model with a binomial error structure, as part of a two-factor analysis of covariance (Type III) with pathogen genotype and spore dose (low, medium, and high) as fixed effects, host density as an interacting covariate, and experimental jar as a random effect. In Section 4, we analyzed dispersal behavior of infected hosts and uninfected controls in two different ways. First, as the total number of patches traveled (square root transformed before analysis) via an analysis of variance with infection treatment as a fixed effect. Second, we analyzed dispersal rate (accumulated patches traveled over time), as estimated via a linear mixed-effects model with accumulated patches as response, infection treatment as fixed effect, time (in days) as an interacting covariate, and individual identity as random effect.

Results

Experimental *Daphnia* populations undergoing colonization in patchy habitats displayed characteristic colonization trajectories that were repeatable in space (Fig. 2). Three broad transitions were evident: (1) a period of rapid population growth following the initial colonization; (2) an overshoot phase whereby a maximum population density is reached (with a brief decline as carrying capacity has been exceeded); and finally, (3) a stationary phase where relatively stable population sizes at or around the carrying capacity is maintained (around 350 individuals litre⁻¹, reflecting naturally observable population sizes; Kvam and Kleiven 1995). Importantly, colonization in the second and third patches followed the same demographic transitions, but with a time lag of ~14 days. The demonstrated repeatability of colonization dynamics then allowed us to test how differences in colonization history may alter pathogen invasion success (Fig. 2 and Suppl. material, section B).

Pathogen establishment and within-host proliferation under different host colonization phases

The ability of a pathogen to establish in a new patch (by surviving long enough to produce mature spores) and its subsequent transmission potential (spore production in hosts that successfully established) was highest when confronted with host populations undergoing rapid growth (Fig. 3). The exact responses, however, depended on a pathogen's genotype as evidenced by a significant genotype by host colonization phase interaction for both traits (probability of establishment: d.f. = 8, $\chi^2 = 31.853$, $P < 0.001$; spore load in established infections: d.f. = 8, $\chi^2 = 20.310$, $P < 0.001$; see Suppl. material, section C). Pathogen C1 and C14, for example, maximized both traits when introduced to populations undergoing rapid growth, but less so as the population exceeded or reached carrying capacity. In contrast, the responses of pathogen C19 and C20 were trait specific; the probability of establishment was highest in host populations undergoing rapid growth, but production of transmission spores peaked instead in host populations at stationary phase.

Opportunities for secondary infections and subsequent dispersal into new patches

We next conducted an experiment to estimate the ability of a pathogen to secondarily infect susceptible hosts at different densities (steps 3, Fig. 1). We found a decreasing probability of infection with increasing host density (Fig. 4), but this trend was modified both by pathogen genotype (d.f. = 4, $\chi^2 = 15.959$, $P < 0.003$) and a dose-by-density interaction (d.f. = 2, $\chi^2 = 6.522$, $P = 0.038$). This decline in infection rate was strongest at low spore dose; increasing the number of hosts in a fixed volume presumably dilutes the inoculation that each host effectively receives, to a point where infection is no longer completely assured (infection rates are known to increase in a dose-dependent manner; sensu Ben-Ami, Regoes, and Ebert 2008). Thus, at higher spore doses, this dilution effect is reduced.

Finally, a pathogen must disperse to invade new susceptible host populations (step 4, Fig. 1). Here, infection reduced the dispersal capacity of a host (Fig. 5), with significant variability both in the total distance covered among parasite genotypes and their uninfected counterparts (d.f. = 5, 111, F -value = 35.662, $P < 0.001$), and in the rate at which animals moved through space (slope by infection treatment interaction: d.f. = 5, $\chi^2 = 445.114$, $P < 0.001$). Across all infection treatments, the total distance covered ($r = 0.816$, d.f. = 112, 95% CI = 0.743–0.869, $P < 0.001$) and dispersal rate ($r = 0.304$, d.f. = 112, 95% CI = 0.127–0.462, $P < 0.001$) was positively correlated with the lifespan of an individual, albeit only weakly in the case of dispersal rate. More virulent pathogens (i.e., shorter host lifespan; Gipson and Hall 2018), therefore, appear to curtail the movement of the host on which their dispersal depends.

Contrasting integrative pathogen invasion success with dispersal capacity

Integrating within-population invasion steps (steps 1–3, Fig. 1) into a single metric of invasion success highlights the tension that a pathogen faces between within-population exploitation and between-population redistribution. Overall, pathogen invasion success was highest when

establishing in populations undergoing rapid growth and reduced as the host population colonization progressed (see Fig. 6A). However, the response of each pathogen genotype to the different host population colonization phases varied. For example, pathogen C14, C20, and C1 invaded recently colonized populations with high, indistinguishable success rates (95% CI), whereas pathogen C1 had much higher invasion success than the other pathogens in host populations at overshoot or carrying capacity, and pathogen C24 had low invasion success in all host colonization phases (Fig. 6A).

Comparing the invasion success of each pathogen genotype with their dispersal rate and total distance covered suggested that complex (rather than simple colonizer-competitor) relationships exist between within-population performance and dispersal (Fig. 6B, C). For example, when using total distance as our dispersal metric, the genotype with the highest invasion success in a recently colonized host population also had the highest capacity to disperse (C14), whereas the genotype with the highest invasion success in populations at carrying capacity traveled the least (C1; Fig. 6B). Our results are less clear when contrasting dispersal rate; here, pathogen C24 is the most virulent and least successful invader, but has the highest dispersal rate during the short lifespan of their hosts.

Discussion

Spatiotemporal variation in host demography is commonly observed in metapopulations and during range expansions (Hanski & Gilpin 1991; Phillips et al. 2010b). The resulting distribution of host demographic phases enables pathogens to potentially diversify along a colonizer-competitor axis (Wei & Krone 2005; de Roode et al. 2008; Magalon et al. 2010), such that pathogens that excel at establishing in newly colonized host populations are likely to be less fit in host populations at overshoot or carrying capacity. If such a diversification and trade-off exist, it has important implications for emerging theory on the evolution of virulence during invasions (Griette et al. 2015;

Lion & Gandon 2015; Osnas et al. 2015), but it has rarely (if ever) been demonstrated empirically (but see Phillips et al. 2010c, 2012; Mondet et al. 2014). By experimentally introducing pathogens into experimental host populations undergoing different phases of colonization, we show that the conditions required for diversifying selection for a pathogen is indeed embedded within the demography of the host population.

Across each stage of the pathogen invasion process (e.g., Fig. 1), we observed significant variation among genotypes and a change in the rank order for invasion traits at each host colonization phase. All pathogens, for example, were more readily able to establish in recently colonized host populations, but the decline in the probability of establishment as host populations aged was felt more greatly by some genotypes (C1 vs. C20, Fig. 3A). Also, pathogen C19 and C20 produced more transmission spores when establishing in host populations at overshoot or carrying capacity, whereas all other pathogens had lower spore production in those populations (Fig. 3B). There were likewise significant differences among genotypes in their capacity to generate new secondary infections under different host densities (Fig. 4), as well as their ability to disperse into new patches (Fig. 5). Taken together, we observe highly complex reaction norms for each pathogen in response to host demography, suggesting that not all pathogens are adopting the same invasion and dispersal strategies.

Our integrated metric of invasion success for each pathogen genotype highlights the evolutionary importance of a host population's colonization history for disease outcomes (Fig. 6A). Here, pathogen invasion success was highest in recently colonized host populations, and declined with the subsequent demographic transitions of the host population. This decline in invasion success, however, was not felt equally among all pathogen genotypes. As host populations transitioned toward the stationary phase, not only did the average invasion success decline, but so too did the differences among genotypes. Together, these observations suggest that newly colonized host populations are the most evolutionarily liable for the pathogen, allowing for higher invasion success

and greater adaptive potential (i.e., more genetic variability; Connallon & Hall 2018), in concert with a host population that is free from density-dependent regulation and is rapidly expanding (e.g., Giometto et al. 2014; Fronhofer et al. 2017).

The higher pathogen invasion success in recently colonized populations contrasts with studies of other *Daphnia* and pathogen species, where the likelihood of an infectious outbreak (as estimated by R_0) was maximized in either intermediate (Civitello et al. 2013) or high-density populations (Dallas et al. 2018). Dallas et al. (2018), for example, demonstrated that secondary infections and epidemic size increase with host density. This result mirrors theory on the role of patch quality in host metapopulations. Here, high-quality or resource rich patches both attract and support greater host and pathogen densities, facilitating a constant supply of infected carriers across a landscape (e.g., Leach et al. 2016; Becker et al. 2018). In contrast, Civitello et al. (2013) found that pathogens are more likely to invade populations of intermediate density, as foraging interference limits transmission at higher host densities. Our study (and invasion metric) instead highlights the sensitivity of an invading infected carrier to the demography of the host population encountered and the dependence of any response on the pathogen genotype involved. From a pathogen's perspective, therefore, the quality of a patch is not just shaped by host density. It is also affected by the colonization history of the host population, the changes in demography that ensue, and the pathogen's capacity to invade and exploit these different colonization phases. Thus, the conditions of a host population that maximize the initial pathogen invasion may not necessarily be the same that maximize transmission, or the long-term maintenance in a host population.

The above results, in isolation, suggest that the optimal investment for a pathogen in traits associated with the invasion process would be those that maximize performance in newly colonized host populations. Within a single location, however, such prime conditions are very transient (i.e., Giometto et al. 2014). To be able to routinely exploit newly colonized host populations, a pathogen inevitably requires a high dispersal capacity (Phillips et al. 2010; Hajek and Tobin 2011, sensu

Bonte and Dahirel 2016). Here, not all pathogen genotypes showed this capacity. Pathogen C14 most closely matched our profile of a “fugitive genotype”; it was most successful at invading newly colonized host populations and better able to disperse. In contrast, pathogen C1 maintained its competitive advantage at all stages of host colonization, but was also unlikely to take advantage of any greater success in newly colonized patches due to its low dispersal (Fig. 5). Thus, rather than a simple divergence in pathogen invasion strategies along a single colonizer-competitor axis, we instead identify a variety of relationships between pathogen invasion success and dispersal, suggesting that the tension between colonization and competition might be optimized in various ways.

Emerging theories on the short-term evolution of virulence during a spatially spreading epidemic centre on whether a trade-off between virulence and dispersal occurs (see Griette et al. 2015; Osnas et al. 2015). In our study, infection always reduced dispersal distance (Fig. 5), but this reduction was highly variable among genotypes (e.g., C1 vs. C14), and correlated with lifespan of the host. Thus, pathogen genotypes that allow for high host-facilitated spread are likely to be less virulent, because infection typically acts to reduce host lifespan (Gipson & Hall 2018). Our results support the subset of spatiotemporal models predicting that the need for dispersal will constrain the evolution of virulence (see Osnas, Hurtado, and Dobson 2015 and discussion in Altizer, Bartel, and Han 2011). In our system, then, we would expect evolution to favor less virulent pathogens at the edge of a range expanding host population (Osnas et al. 2015), and in analogous metapopulations.

Our results suggest a number of predictions for infectious disease evolution that are likely testable in the field (see also Hall and Mideo 2018). In nature, *Daphnia* populations experience large fluctuations in population size due to rapid responses to environmental conditions (i.e., winter thaw Carvalho & Crisp 1987), or the colonization of new rock pools founded by individuals in a metapopulation setting (Pajunen & Pajunen 2003; Haag et al. 2006). We suggest that both recently colonized patches and the outer edge of a diffusing population are more likely to be founded by the

more dispersive, uninfected *Daphnia*. Our results also suggest that the pathogen genotypes that arrive first in a new population are likely to have relatively low virulence, but eventually, these fugitive genotypes will be out-competed by the later arriving, but competitively superior pathogen genotypes.

In summary, our work demonstrates the potential for diversifying selection to operate within a single pathogen species across a gradient of host colonization. Although we might expect this diversifying selection to generate a clear spectrum of pathogen genotypes along a colonizer-competitor gradient, our results indicate that a complex array of pathogen strategies are possible, depending on the demographic conditions of their host population. Given the inevitable variation in host demographic stages in the real world (driven by invasion front or metapopulation dynamics), these selection differences could maintain a diversity of pathogen invasion strategies across space and time. Whether pathogens in these spatiotemporally dynamic situations evolve to become more or less virulent will depend on the trade-off between pathogen virulence and dispersal, and our work reiterates that this trade-off may often be a real fundamental constraint on virulence evolution.

Acknowledgements

We thank the Hall group for helpful input and valuable discussions. This work was supported by an Australian Research Council grant (DP160101730) to BLP and MDH. The authors have no conflict of interest.

Chapter 2 - Figures and tables

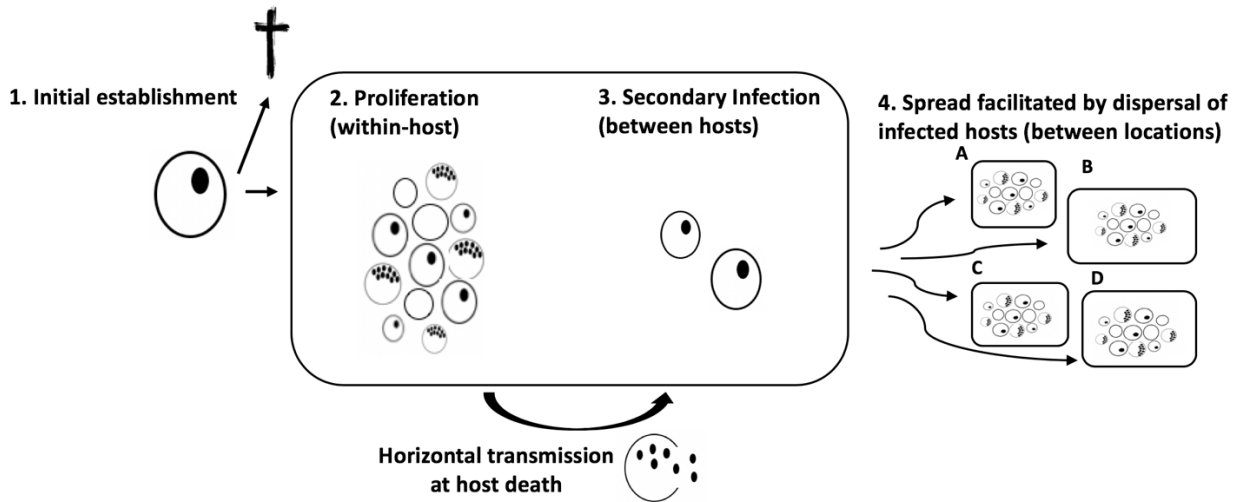


Figure 1: The four steps that a pathogen faces to successfully establish and spread in host populations. 1) a pathogen must successfully establish in a new susceptible host (circle) after an infected carrier or propagule enters a host population; 2) proliferation and production of mature transmission spores (black filled dots) within infected host; 3) generate secondary infections (after host death) in new susceptible hosts within the same population; and finally, 4) spread between populations in order to infect new host populations in a patchy landscape, or keep pace with the rate of its range expanding hosts. Host growth trajectories and population density influences each pathogen invasion step, and will define what is optimal for a pathogen at each stage of its invasion process.

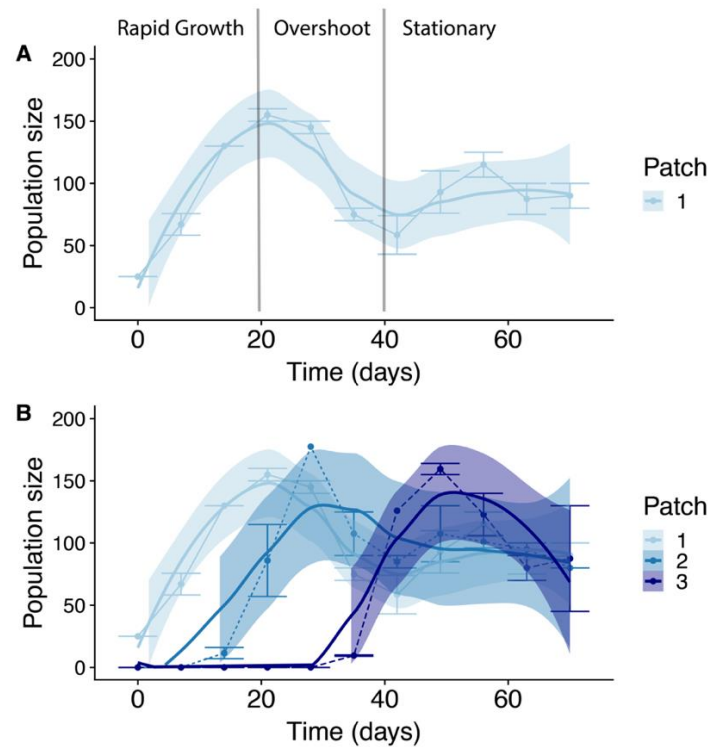


Figure 2: Repeated colonization events of *Daphnia* populations (female & juveniles) in interconnected experimental patches. A) a population undergoing different colonization phases in a single habitat patch, defined as i) a period of rapid population growth following initial establishment, ii) a short period of population overshoot, and iii) density regulated carrying capacity or stationary phase. In our interconnected habitats, dispersers move from an established patch to a new one, after a time-lag of approximately 14 days, and the characteristic colonization phases are then repeated in time and space (B). Coloured filled lines represent fitted GAM predictions of population size for each interconnected patch, and shaded area depicts 95% confidence intervals. Thin dotted lines represent raw data and corresponding error bars represent standard errors. Written annotations and arrows in A visualize the population colonization phases (i – iii) for patch 1.

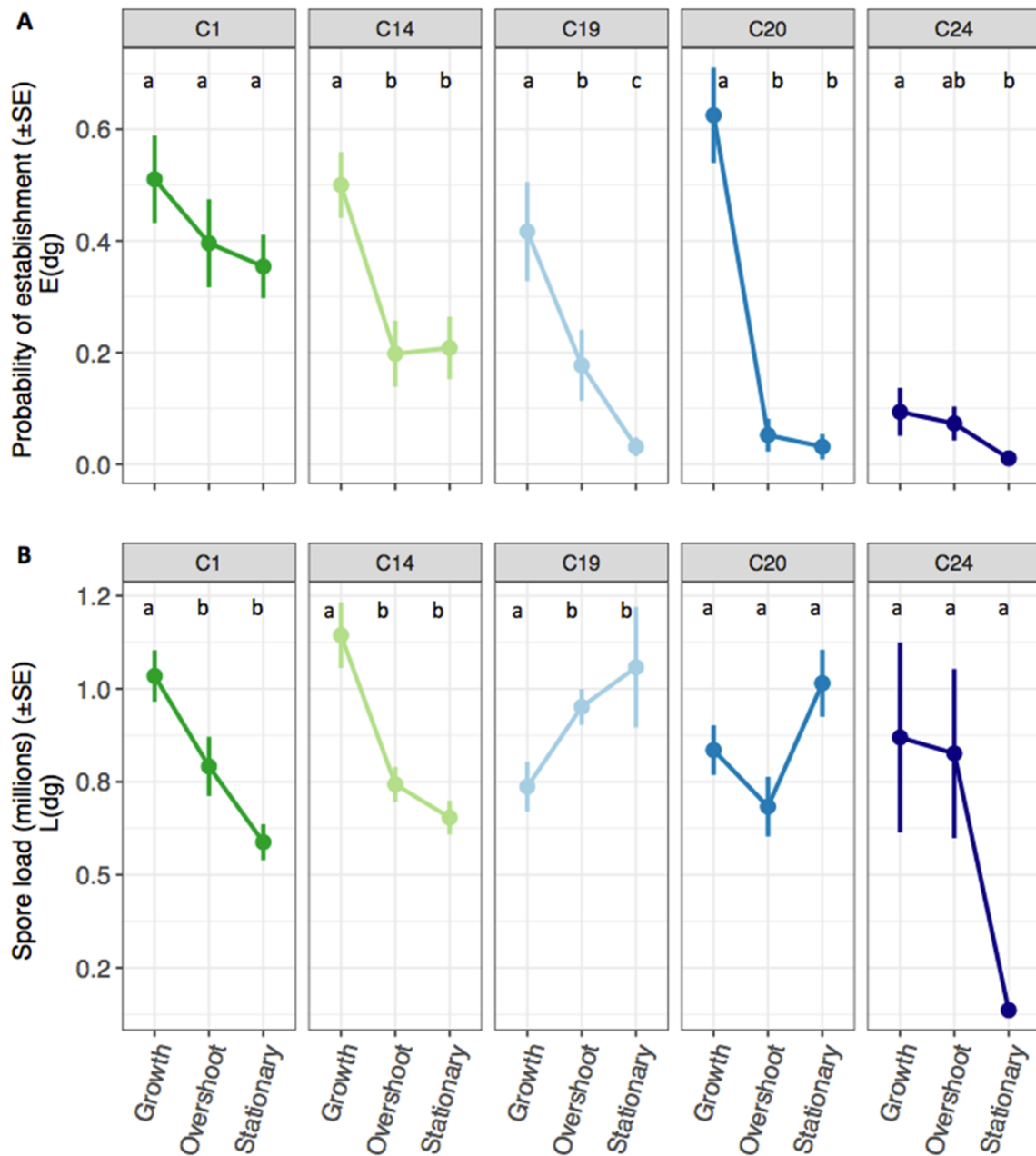


Figure 3: The influence of host colonization phase (rapid growth, overshoot and stationary) on pathogen performance during the first two stages of the invasion process. A) the probability that a pathogen successfully establishes and produces mature transmission spores (\pm SE). B) pathogen spore load (transmission potential) in millions (\pm SE) at host death or experimental termination. Letters refer to Tukey post-hoc significance test between host colonization phases within each pathogen genotype.

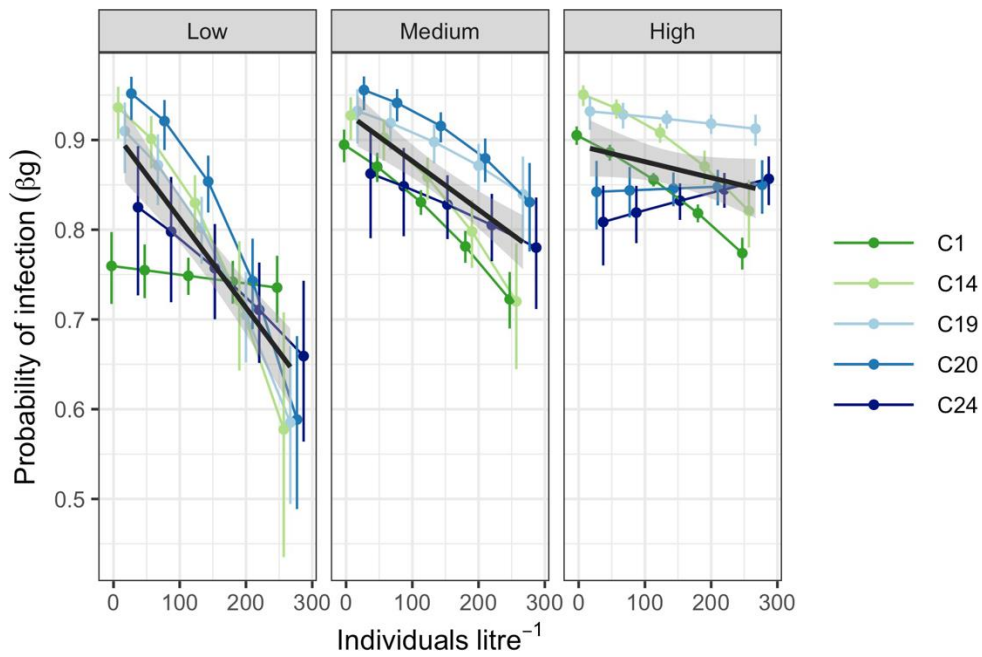


Figure 4: The influence of host density on the probability of infection (as per step 3, Fig. 1). Shown is the probability of infection at different population densities, exposed to three doses (low, medium and high) of *P. ramosa* spores. In colour are the predicted values with associated confidence intervals based on a fitted generalised mixed-effect model, for each pathogen genotype, and the black line with grey shading depicts the overall trends (\pm 95% CI) across all pathogen genotypes.

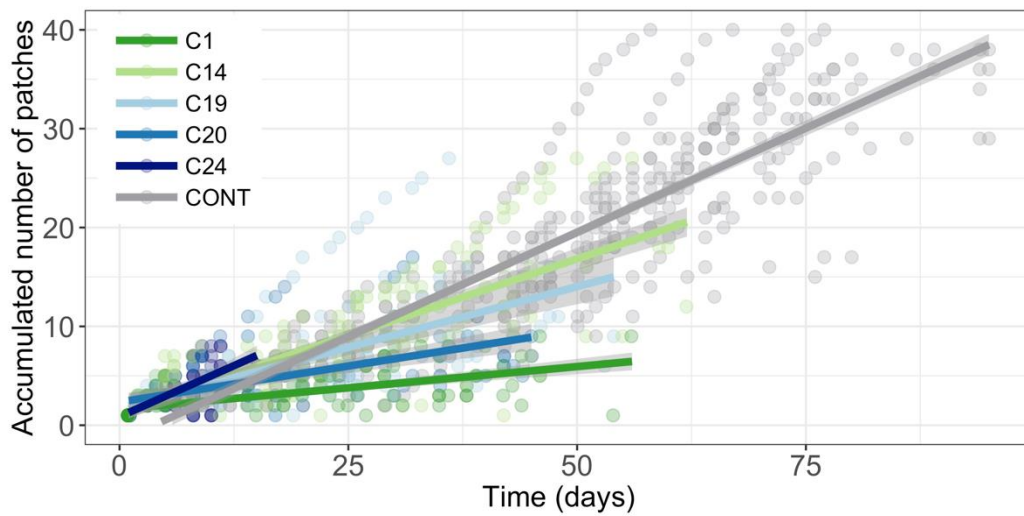


Figure 5: Host facilitated dispersal of pathogen genotypes and uninfected hosts. Shown is the accumulated number of patches travelled over time (days) in interconnected patchy habitats. Differences in length of the curves indicates the average lifespan of infected animals (pathogen induced reduction in lifespan) and uninfected controls. Dots represent individual replicate dispersal. Grey shaded area represents 95% confidence interval associated with model predictions.

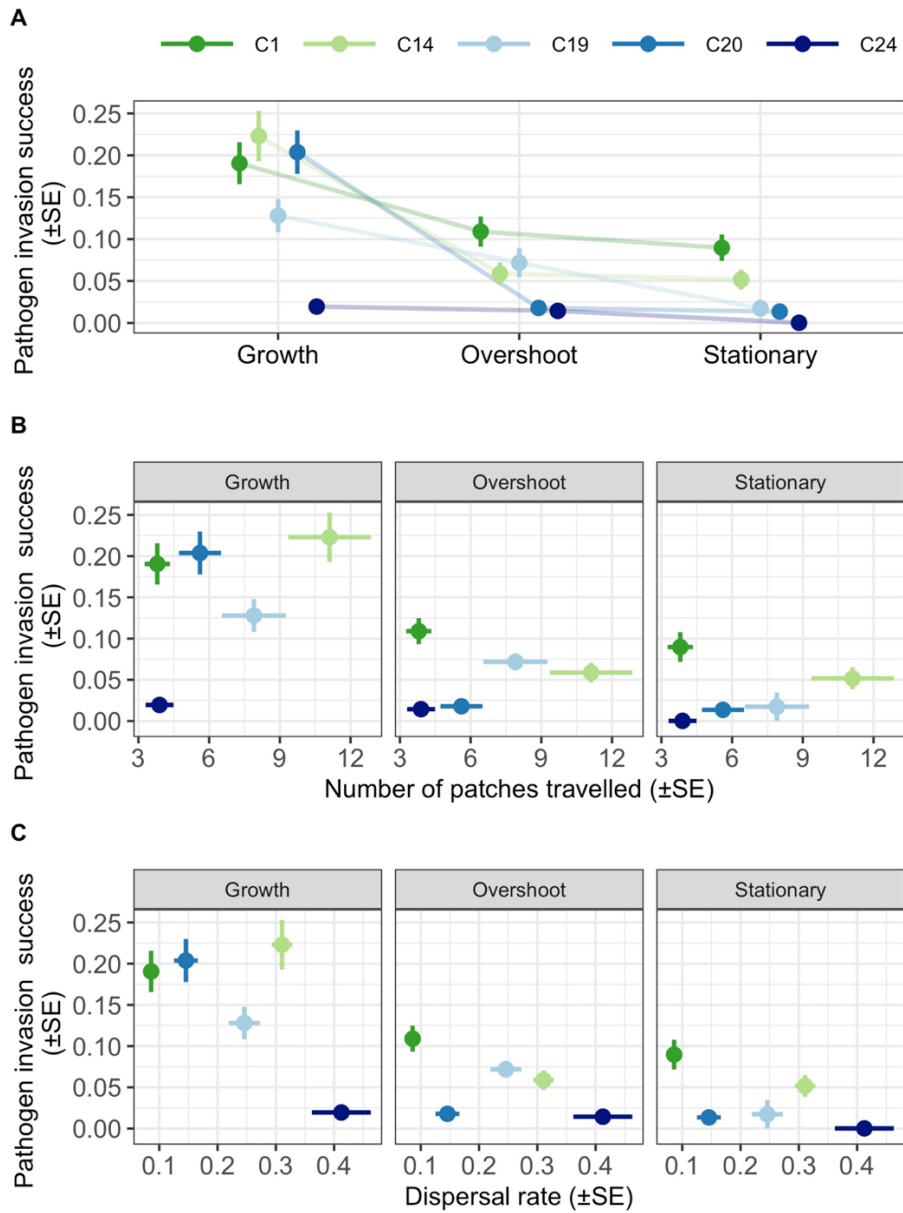


Figure 6: Estimates of integrative pathogen invasion success versus the dispersal capacity of each pathogen genotype. Shown are: A) pathogen invasion success (\pm SE) when invading host populations undergoing rapid growth, overshoot and stationary phase; B) the relationship between pathogen invasion success and total distance covered when contrasted with each host colonization phase; and C) the relationship between pathogen invasion success and dispersal speed of infected hosts, as estimated by the slope of the accumulate number of patches travelled versus time in days.

Chapter 2 - Supplementary material

Section A: Standard experimental conditions

To prepare experimental animals, *Daphnia* females were isolated from stock cultures and reared under standard conditions (60-mL jars filled with 50 mL artificial *Daphnia* medium (ADaM, Klüttgen et al. 1994; modified by Ebert et al. 1998) for three asexual generations. Animals were fed daily with green algae *Scenedesmus sp.* following standard feeding procedures, gradually increased from 0.5 to 5 million cells, to accommodate the developing animal's needs. All animals were maintained in a controlled temperature room under standard conditions (20°C, 16L:8D light cycle). Individuals were transferred to fresh ADaM twice a week and trays were rearranged daily to minimise any positional effects. Infected animals for use in subsequent invasion experiments were generated by exposing *Daphnia* housed individually in 60-mL jars (filled with 20 ml ADaM) to 20,000 spores at ages 3 and 4 days (i.e., 40,000 spores in total).

Kluttgen, B., Dulmer, U., Engels, M., Ratte, H., Klüttgen, B., Dülmer, U., et al. (1994). ADaM, an artificial freshwater for the culture of zooplankton. *Water Res.* 28:743–746.

Ebert, D., Zschokke-Rohringer, C.D. & Carius, H.J. (1998). Within–and between–population variation for resistance of *Daphnia magna* to the bacterial endoparasite *Pasteuria ramosa*. *Proc. R. Soc. B.* 265:2127–2134.

Section B: Characterising host colonization dynamics

To test for the repeatability of the colonization process in experimental populations, we used a generalised additive model to predict how changes in total population size vary with the time since the first colonizing disperser arrives in a given patch (modelled as a thin plate spline), and independently the patch number of an interconnected three-patch system (via the *mgcv* package (Woods 2006)). We found a significant effect of time since colonization on population size (d.f. = 6.725, $F = 29.63$, $p < 0.001$) and no difference in average population size with patch (d.f. = 2, $F = 1.012$, $p = 0.370$). We then compared this model to one where the change in population size with time was allowed to vary by patch. We found that allowing the trends to vary by patch did not significantly improve the fit of the model (d.f. = 3.703, $F = 1.783$, $p = 0.151$) thus confirming the repeatability of colonization phases across patches (Fig. S.1).

Three characteristic colonization phases were evident from the changes in population size since the first colonizing disperser arrives, as discussed in the results (rapid growth = 0 to 20 days, overshoot = 20 to 40 days, and carrying capacity = 40 days onwards). To confirm that the population dynamics at each phase were indeed different, we regressed total population size against time for each phase category individually. We found that during the rapid growth phase, populations size increased with time since colonization (slope = 8.18, SE = 1.623, $p < 0.001$), but were readily reduced (reached a peak and then reduced) during the overshoot phase (negative slope = -3.012, SE = 0.992, $p = 0.008$), and remained stable during the stationary phase (slope = 0.435, SE = 0.573, $p = 0.461$). Thus, in our analyses, we chose to partition host colonization dynamics into three broad phases; rapid growth, overshoot, and carrying capacity.

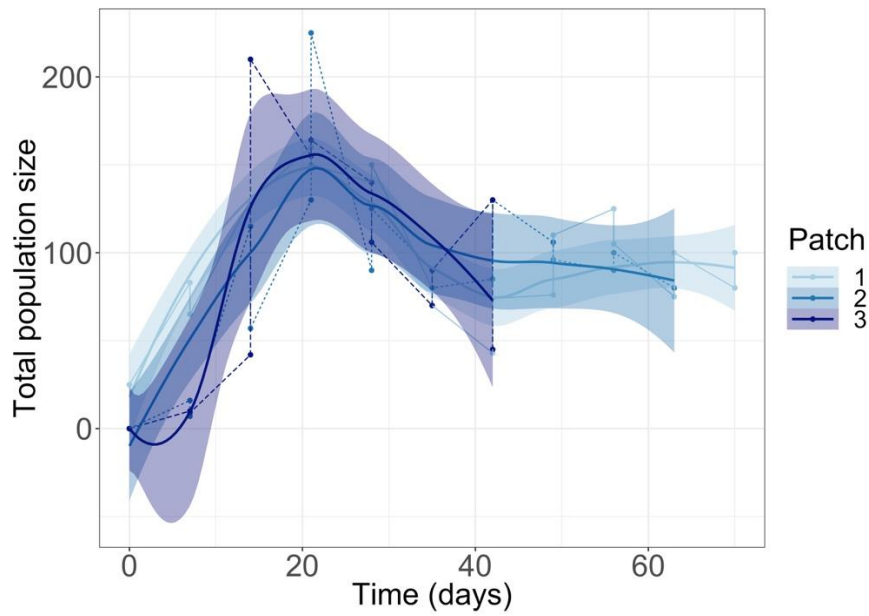


Figure S.1. Total host population size over time (days) since first colonizing disperser arrives in a given patch (patch 1, 2 and 3 in different blue nuances). Dots represent raw measures and lines represent a fitted generalised additive model with days modelled as a thin plate spline.

Woods, S. N. (2006). *Generalised Additive Models – An Introduction with R*. CRC/Chapman & Hall, New York.

Section C: Pathogen establishment and within-host proliferation

Table S.1. ANOVA results. Effect of population colonization phase and pathogen genotype (Gp) on: A) pathogen establishment, and B) spore load in infected individuals that are establishing in a given host population. This data, and the measures of proportion of individuals that become infected at a given host density and pathogen spore dose, is used to calculate the transmission coefficient in the integrated metric of pathogen invasion success. (* $p < 0.05$, ** $p < 0.01$, *** $p < 0.001$).

| A) Probability of establishment | χ^2 | d.f. | P-value | Sign. code |
|--|----------|-------------|----------------|-------------------|
| Colonization phase | 59.853 | 2 | <0.001 | *** |
| Gp | 55.889 | 4 | <0.001 | *** |
| Colonization phase x Gp | 31.853 | 8 | <0.001 | *** |
| B) Spore load | | | | |
| Colonization phase | 16.761 | 2 | <0.001 | *** |
| Gp | 37.693 | 4 | <0.001 | *** |
| Colonization phase x Gp | 20.310 | 8 | <0.01 | ** |

Section D: The potential for secondary infections

Table S.2. ANOVA results predicting the probability of infection using a generalised mixed-effect model using spore dose (low, medium and high) and pathogen genotype as fixed effects, population density (individual per litre) as a continuous covariate and experimental jar as a random effect.

| Effect | d.f. | χ^2 | Pr ($>\chi^2$) | Sign. code |
|---------------------|-------------|----------------------------|-------------------------------------|-------------------|
| Dose | 2 | 1.128 | 0.569 | |
| Pathogen (Gp) | 4 | 15.959 | 0.003 | ** |
| Density | 1 | 37.121 | >0.001 | *** |
| Dose x Gp | 8 | 11.238 | 0.189 | |
| Dose x Density | 2 | 6.522 | 0.038 | * |
| Gp x Density | 4 | 8.118 | 0.087 | . |
| Dose x Gp x Density | 8 | 9.216 | 0.324 | |

Section E: Experimental measures of pathogen dispersal

Table S.3. ANOVA results for the full model predicting square root transformed total number of patches dispersed using infection treatment (pathogen genotypes and uninfected control, Trt) as fixed effect.

| Total patches | d.f. | F-value | Pr (>F) | Sign. code |
|---------------------------|-------------|----------------|-------------------|-------------------|
| Infection treatment (Trt) | 5 | 35.662 | <0.001 | *** |
| Residuals | 111 | | | |

Table S.4. ANCOVA results from a linear mixed effect model with accumulated number of patches as a continuous response variable and time (in days) as a continuous covariate, and infection treatment (pathogen genotypes and uninfected control) as fixed effects and individual id as random effect.

| Dispersal rate | d.f. | χ^2 | P-value | Sign. code |
|---------------------------|-------------|----------------------------|----------------|-------------------|
| Infection treatment (Trt) | 5 | 35.779 | <0.001 | *** |
| Day number | 1 | 218.044 | <0.001 | *** |
| Day number x Trt | 5 | 445.114 | <0.001 | *** |

Section F: An index of pathogen invasion success

The aim of this model is to estimate pathogen invasion success at the three identified characteristic host population growth phases: rapid growth, overshoot and stationary phase (Fig. 2). By integrating our empirical measures of pathogen life-history traits (sensu Fig. 1) into a simple SI framework that is robust to the density of hosts that a pathogen encounters, we can investigate how pathogen invasion success varies depending on the time since colonization of the host population.

First, we were interested in modelling the probability that an infected individual or infective propagule invades a healthy host population and survives long enough to become infective (produces mature spores) and thus generate new secondary infections. Here, we let E be the probability that an introduced individual survives long enough to become infective, and L the number of infective spores that an infected individual produce, given that it survives long enough for mature spores to be produced. We can then estimate the number of spores likely introduced into the population for each of our five experimentally tested pathogen genotypes, with accompanying levels of uncertainty, calculated by 1000 bootstrap iteration as integrated via the boot function in R:

$$\hat{P}_{dg} = L_{dg}E_{dg} \qquad \text{Equation S.1}$$

Here, d and g denote host population colonization phase and pathogen genotype, respectively. P_{dg} can be estimated in our case from the data of establishment and proliferation generated in section 2 of the main methods.

Next, the number of new infections produced by release of a given number of spores in the environment depends on the density of susceptible hosts (S), the number of spores introduced (P), and the transmission coefficient, β . Thus, in any given host population, variation in pathogen infection is driven entirely by variation in β and P .

$$I_{dg} = \beta_g P_{dg} S \qquad \text{Equation S.2}$$

From this, and the data from section 3 – on number of new infections (I) for each genotype across a range of spore loads (P) and host densities (S), we can now estimate β_g and accompanying uncertainty levels by bootstrapping the mean:

$$\hat{\beta}_g = \frac{1}{n} \sum_{ijk} \frac{I_{gk}}{P_{ik}S_{jk}} \quad \text{Equation S.3}$$

where i and j represent treatment levels for spore load and host density respectively, k represents replicates within treatment levels, and n is the total number of replicates in the experiment.

Finally, for the purpose of calculating a standardized metric of pathogen invasion success, w_{dg} , we set $S = 1$, thus capturing how different colonization phases influence the relative capacity of a pathogen genotype to initially invade such a patch, irrespective of the variability in host numbers within each population. Then our pathogen invasion success metric for each pathogen genotype and host population colonization phase is:

$$w_{dg} = \beta_g P_{dg} \quad \text{Equation S.4}$$

Finally, we contrasted pathogen invasion success at each host population colonization phase with our experimental measures of host facilitated dispersal, to look for evidence of diversifying selection and trade-off dynamics among the different pathogen genotypes.

Chapter 3: Energetic constraints in range expanding and colonizing populations and their consequences for pathogen fitness

Louise Solveig Nørgaard¹, Giulia Ghedini¹, Ben Phillips² & Matthew D. Hall¹

¹School of Biological Sciences and Centre for Geometric Biology, Monash University, Melbourne 3800, Australia

²Department of Biosciences, University of Melbourne, Parkville, VIC, Australia

Manuscript is prepared for submission to Ecology

Abstract

The spread of infectious disease through a host population is determined by the ability of a pathogen to proliferate within and spread between susceptible hosts. Processes that limit the performance of a pathogen thus occur at two possible scales: one being the availability of energy within a host, the other being the pool of susceptible host in a given patch. These two processes are intimately linked. By modifying how readily hosts are able to compete for, and expend resources, a shift in host density may contribute to immediate differences in the flow of energy in a host-pathogen system, both in term of the energy available for a host to grow, reproduce and to fight infection, as well as the energy available for a pathogen to exploit. In this study, we use the host *Daphnia magna* to explore the relationship between energy intake and expenditure at various population densities. Then, by infecting hosts with the bacterial pathogen *Pasteuria ramosa*, we explored whether infection changes the scaling relationship between energy intake and expenditure across density, and how energy scope translates into pathogen fitness. Our work demonstrates that feeding rate decline at a faster rate with density than does metabolic rate, leaving more discretionary

energy available for both hosts and their dependent pathogens at low population density. This energetic advantage appears to translate positively into both host and pathogen fitness, as estimated via growth and proliferation respectively, counter to the expectation that a host might use an excess of discretionary energy to mount a more robust immune response. Our results show how the flow of energy in a population, as mediated by changes in resource competition and population density, affect pathogen performance through both correlated changes in host life-history such as growth, as well as a direct connection between energy scope and a pathogen's transmission potential.

Introduction

As a pathogen spreads through a host population it inevitably experiences substantial differences in the density of its target host. Such differences in the density of target hosts can arise as an organic part of spatial processes such as range expansion, invasion, or patch colonization, whereby newly colonized areas are characterised by low population density. From the perspective of a pathogen, these differences in host density alter the supply of susceptible hosts available for secondary infection, on which the further spread of an epidemic depends (Anderson & May 1981; Schmidt-Hempel 2011). However, the leading edge of a range expanding host population (Phillips 2009), or a newly colonized host patch (Hanski & Gilpin 1991; Drake & Griffen 2009), coincides not only with low population density, but also high resource availability, and in turn, low conspecific competition between hosts (see Burton, Phillips and Travis, 2010). Thus, by modifying how readily hosts are able to compete for and expend resources, a shift in host density may contribute to immediate differences in the flow of energy in a host-pathogen system, both in terms of the energy available for a host to grow, reproduce and fight infection, as well as the energy available for within-host pathogen exploitation.

An understanding of the energy available for optimization of both host and pathogen life-history traits ultimately begins by exploring the difference between rates of energy assimilated (energy

intake through feeding) and rates of energy expended on respiration – the magnitude of which describes the scope for energy production or overall “discretionary energy” (Buckley et al. 2014; Ghedini et al. 2017). While the effect of energy acquisition (as estimated by food consumption, Jenkins et al. 1999) and expenditure (metabolic rate estimated by oxygen consumption, DeLong and Hanson, 2009; DeLong, Hanley and Vasseur, 2014; Yashchenko et al. 2016; Malerba, White and Marshall, 2017) are known to scale with population density, recent work by Ghedini et al. (2017) has reiterated how both acquisition and expenditure can covary with population density in a number of complex ways (Ghedini et al. 2017). Across a density gradient, as typified by the transition from either the core to the front of an expanding host population, or from well-established to newly colonized host patches, more or less discretionary energy may be available at low population densities, depending on the relative strengths at which per capita feeding and metabolic rates change with the number of hosts competing for resources (see Fig. 1, modified from Ghedini et al. 2017).

The rate at which a host consume, transform and expend energy may therefore provide an opportunity to link the ecological processes at play during a pathogens invasion into new host patches, to the resulting spread and severity of infectious disease. While different pathogen invasion and transmission strategies (such as competition and colonization abilities) can be favoured in various environments within a metapopulation (Tilman 1994; Calcagno et al. 2006), such predictions are often highly specific to the host population dynamics encountered, or pathogen genotypes involved (see Nørgaard, Phillips, and Hall 2019a). Instead, estimates of energy flow in a host-pathogen system offer a mechanistic view of how population and community level processes can influence pathogen performance occurring within a single host, in a way that is more readily generalisable to any host and pathogen system. An increase in discretionary energy, for example, might dampen the proliferation and spread of a pathogen if it allows a resource intensive immune response to either clear infection, or limit pathogen proliferation (Sheldon & Verhulst 1996; Hite &

Cressler 2018). Conversely, if the flow of energy translates directly into pathogen performance, then the spread of disease will be accelerated under conditions that increase energy availability (Hall et al. 2009a, b; Cressler et al. 2014; Civitello et al. 2015).

In this study, we explore how rates of energy intake and expenditure co-varies across a gradient of population densities, and how such patterns of co-dependency impact on pathogen fitness. We explored these questions using the crustacean *Daphnia magna* and its gram-positive bacterial pathogen, *Pasteuria ramosa*. *Daphnia* is a suitable candidate for density manipulation experiments since natural populations undergo frequent extinction and recolonization processes (Ebert 2005; Altermatt & Ebert 2010), experiences large fluctuations in resource availability, and responds to conspecific density by reducing growth, feeding, and reproductive rates (Burns 2000; Lürling et al. 2003). In this system, filter-feeding, growth, fecundity (Burns 2000; Lürling et al. 2003), and metabolic rate (DeLong et al 2014) all scales negatively with population density. The performance of *P. ramosa* has been linked to the body size of an infected carrier (see Pulkkinen and Ebert, 2004), to the sex of its host (Gipson & Hall 2018; Hall & Mideo 2018; Nørgaard et al. 2019a), and the colonization history of a given host population (Nørgaard et al. 2019b), all of which are intricately linked through fluctuations in resource availability and population dynamics. Both host and pathogen performance, therefore, will be influenced by the outcome of resource competition and the scaling relationship between energy intake and expenditure at various population densities. Whether, and how discretionary energy varies across a gradient of host densities (Fig. 1), and whether higher amount of discretionary energy, increase or decrease pathogen performance, will have critical impact on the spread of infectious disease. Following the approach utilised by Ghedini et al. (2016), we here measured rates of energy intake and expenditure across a gradient of environmentally relevant host densities, in uninfected and infected hosts. Using this approach, we were able to identify how energy scope changes across a density gradient, and how such density-mediated responses caused correlated changes in individual body size (growth). Next, by measuring

pathogen spore production in infected hosts, as a proxy for pathogen transmission potential (see Clerc, Ebert and Hall, 2015; Hall and Mideo, 2018), we explored whether estimates of discretionary energy can predict pathogen fitness, or whether density-mediated changes in host life-history likewise impacts on the performance of an invading pathogen. Collectively, we observed noticeable differences in energy scope across density, and we here present novel evidence for how energy scope and density-mediated changes in host life-history traits jointly impact on pathogen fitness, all of which favours the transmission potential of the pathogen at low population densities.

Materials and methods

The study system

Daphnia magna Straus is a filter-feeding cladoceran, found in freshwater and brackish ponds and lakes throughout Eurasia and North America. *D. magna* reproduces via cyclical parthenogenesis and is naturally infected by a range of pathogens, including the endospore forming, gram-positive bacteria, *Pasteuria ramosa* Metchnikoff, 1888. In this system, both host life-history and pathogen performance can be impacted by host density (see Michel, Ebert and Hall, 2016), and reduced resource intake (and quality; Penczykowski et al. 2014), for example, reduces both host fecundity and pathogen spore production (Pulkkinen & Ebert 2004; Cressler et al. 2014). *P. ramosa* is a strictly horizontally transmitted pathogen, and infection causes severe loss of fecundity, an increase in body size (pathogen induced gigantism), and reduces survival of infected hosts (Ebert et al. 2016). In this study, we use host genotype HUHO-2 originating from Hungary, and two novel *P. ramosa* genotypes originating from Russia (C1) and Germany (C19).

Experimental design and infection procedure

Prior to the experiment, female *Daphnia* were collected from stock cultures and maintained under standard conditions for three asexual generations (reared in 60-mL jars filled with 50 mL artificial *Daphnia* media (ADaM, Kluttgen et al. 1994; modified by Ebert et al 1989). Animals were fed

daily with green algae *Scenedesmus sp.* and feeding regimes were gradually increased from 0.5 million cells per animal at birth to 5 million cells per day as an adult, to accommodate the developing animal's needs (see Michel, Ebert and Hall, 2016). All animals were maintained in a temperature-controlled room under standard laboratory conditions (20°C, 16L:8D light cycle) and individuals were transferred to fresh artificial media twice a week.

Experimental animals were collected from the standardized mothers and raised with three individuals per jar from birth in 60-mL jars filled with 20 mL media. At age three days old, each animal was then randomly allocated to either the pathogen genotype C1, C19 or the unexposed control treatment groups, and on day three and four days old, each individual received either 20,000 spores (40,000 in total) or an equivalent volume of placebo-solution (crushed uninfected individuals). At seven days old, animals were randomly (within exposure treatments) pooled into different population densities of either 20 (one individual jar⁻¹), 60 (three individuals jar⁻¹), 120 (six individuals jar⁻¹), 180 (nine individuals jar⁻¹), 240 (12 individuals jar⁻¹) and 300 (16 individuals jar⁻¹) individual per litre. Animals remained at the manipulated densities until the measurement of metabolic rate and algae intakes could begin, as detailed below. The experiment was divided into three experimental blocks, each containing four replicates of all density and exposure combinations (3 infection treatments x 6 densities x 3 blocks x 4 replicates = 216 experimental populations of varying densities).

Estimating energy expenditure via measurements of metabolic rates

Oxygen consumption rates (VO₂) were obtained by using a fluorescence-based respirometry system, and this measure was used as a proxy for a population's metabolic rate (see White 2011 and Guillia et al. 2017). Oxygen consumption was measured at 21 days post infection, since, at this point, infections are well established in the infected hosts (pathogens produce mature spores, see Ebert et al. 2016). All animals from a given density manipulation were first rinsed in sterilised

media, and then loaded into 20-mL glass vials with oxygen sensor spots in the bottom (all animals from each density treatment into one vial). Prior to measurements, oxygen sensor spots were calibrated using air-saturated sterile media (100% air saturation) and media containing 2% sodium sulphite (0% air saturation).

To measure oxygen consumption rates, we used four 24-channel PreSens oxygen readers (SDR SensorDish, Precision Sensing GmbH, Germany), each loaded with 9 experimental populations and 2 blank vials containing media only, equally distributed among the density and exposure combinations. Measurements took place in a dark, temperature-controlled room at 20° C for 2.5 hours with oxygen consumption measurements taken once every second minute. Animals were left to acclimate for 20 minutes before the recording process began and were also starved for 14 hours prior to oxygen consumption measurements to allow for accurate testing of both metabolic and feeding rates on the same day (see below).

The rate of oxygen consumption ($\dot{V}O_2$, units) was calculated following Alton et al. (2007) from the change in oxygen saturation over time ($\% h^{-1}$) as $\dot{V}O_2 = -1 \times [(m_a - m_c)/100] \times V \times \beta O_2$, where m_a is the rate of change in oxygen saturation for an experimental treatment, m_c is the per run average rate of change for the blank controls, βO_2 is the oxygen capacitance of air-saturated water at 20° C (6.40, Cameron 1986), and V is the water volume of the vials (0.020 L). The parameters m_a and m_c were estimated using the *LoLinR* package in R (Olito et al. 2017), which uses local linear regressions to objectively estimate the monotonic rates from oxygen consumption data. $\dot{V}O_2$ estimates ($mL O_2 h^{-1}$) were then converted to metabolic rate (Joules h^{-1}) using the calorific conversion factor of 20.08 J $mL^{-1} O_2$ (Lighton 2008) and metabolic rate per individual was obtained by dividing the measured metabolic rate per jar (Joules h^{-1}) by the number of individuals in a given density treatment (J $h^{-1} individual^{-1}$).

Estimating energy intake via feeding rates

After oxygen consumption measurements, all populations of experimental animals were transferred into 60 mL glass jars filled with 20 mL fresh autoclaved media. We then measured feeding rates by adding 40 million *Scenedesmus* algae cells to each population and gently rotated the cultures to homogenise algae in the water column. *Daphnia* were then allowed to feed for 1.5 hrs ($T_{1.5}$), after which all jars were again gently homogenised and sampled for subsequent algae counts. We also sampled control jars (with no animals) at the start of the energy intake assay to use as a representative of the starting algae concentration (T_0). Algae concentrations were measured using Accuri BD flow cytometer (BD Biosciences, San Jose, CA, USA) with custom gates based on fluorescence (FL3) and side scatter (SSA) to isolate algae cells from animal debris, and otherwise following similar protocols as outlined below, for the characterisation of spore load (see below). Energy intake was calculated from estimates of algae consumption (difference between algae concentration at start and the end of feeding trials; i.e., T_0 - $T_{1.5}$) by converting the known carbon content of algae ($2.85 * 10^{-8}$ mg C cell⁻¹) to calories, where 1 mg C approximates 11.4 calories (Platt & Irwin 1973). To avoid overestimation of energy intake, we assumed a 70% assimilation efficiency in *Daphnia* following (Nielsen & Olsen 1989). However, altered assimilation efficiencies will not change the slope at which feeding rate changes with population density. Following feeding rate measurements, we measured body size of each individual using a dissecting microscope and converted to dry weight (mg) as per Yashchenko et al. (2016) (i.e., $0.00535 * (\text{body size}^{2.72})$). Infected animals were then frozen individually in 500 μ L RO for later spore counts.

Estimating pathogen transmission potential

To estimate pathogen transmission potential, frozen infected animals were thawed and their spore loads were measured using an Accuri C6 flow cytometer (BD Biosciences, San Jose, California). Samples were prepared by thawing an infected animal, crushing it with a pestle, and samples were

then homogenised on a 24-well multiplate shaker (Biosan, Riga) at 1200 rpm for 20 minutes. 10 µL of homogenised *Daphnia* sample were then diluted into 190 µL of 5 mM EDTA, mixed and loaded into one well of a round-bottomed PPE 96-well plate for analysis using flow cytometry. To identify mature spores, we used custom gates based on fluorescence (FL3) to distinguish algae cells from pathogen spores, and side scatter (SSA) to separate mature spores from pre-spores and animal debris. Finally, spore load was measured twice per infected individual and then averaged.

Statistical analyses and energy calculations

All statistical analyses were performed in R (ver. 3.3.3; R Development Core Team, available at www.r-project.org). From our experimental approach we obtained direct estimates of feeding rates, metabolic rates, host dry weight and pathogen spore loads. To subsequently estimate discretionary energy, we subtracted model predicted metabolic rates from model predicted feeding rates, and modelled this trait using the non-linear power curve as described below. We likewise estimated mass-specific rates of feeding, metabolism and discretionary energy by dividing by the average dry weight per jar. Prior to analysis, we removed 29 feeding rate measurements, which revealed a negative or zero feeding rate or were lost due to handling errors, giving a total of 186 measures of feeding rate across all population density and exposure treatments. Similarly, for metabolic rate measurements, we lost 5 measures due to handling errors, and removed extreme outliers in low population densities leading to a total of 209 measures of metabolic rate.

For each trait, we modelled the change in the mean trait values for each experimental jar with increasing population density as a power curve ($\text{jar mean} = a \times \text{density}^b$) via the packages *drc* (Ritz et al. 2015) and *aomisc* (available at github.com/OnofriAndreaPG/aomisc). Infection treatment (uninfected, pathogen C1 and C19, except for spore loads where only pathogen C1 and C19 were included as levels) was included as fixed-effect factor. We first used the *mselect()* function of *drc* to compare the fit of a power curve model versus quadratic and linear models, and in all cases the non-

linear model proved to be a better fit (see Suppl. material, Table S.1 for results from model comparison). Next, to test for differences between infection treatments in the scaling relationship between population density and our traits of interest, we compared the fit of a model (based on partial-F tests) where each treatment shared a common set of values for the conversion factor (the constant a) and the scaling exponent (b), to one where these values could vary by treatment (akin to allowing an interaction between treatment and both a and b).

Lastly, we explored how any change in spore load produced by a pathogen is related to dry weight and discretionary energy of an infected carrier. First, we \log_{10} transformed and standardized the two predictor variables (mean 0, standard deviation 1), to obtain comparable parameter estimates. We fit a series of multivariate analysis of covariance models, using log-transformed spores as our response variable and pathogen genotype as an additional fixed effect factor. These models estimate the partial effects of increasing discretionary energy on the changes in spore load, after controlling for the effect of a host's dry weight (and vice-versa). To test whether the relationship between our covariates and spore loads was the same for each genotype, we compared the fit of this model (using partial-F tests) to one that additionally included the interactions between pathogen genotype and both dry weight and discretionary energy. The results were visualized for each trait (dry weight and discretionary energy) using the partial residuals obtained via the *visreg* package (Breheny & Burchett 2017).

Results

Part 1: The scaling relationship between energy intake and expenditure versus density

Using a non-linear modelling approach, we found negative density-dependence of feeding and metabolic rates for both infected and uninfected *Daphnia* (Fig. 2A and B, Table 1), which in all cases was a significant improvement in fit over a linear or quadratic model (see Suppl. material Table S.1). For feeding rates, we observed that the relationship between per capita intake and

population density did not differ significantly between any of the exposure treatments ($F_{4, 158} = 1.806$, $p = 0.132$), although C1 appears to have a lower feeding rate at lower densities, and a lower conversion factor and scaling exponent as a result (Table 1). In contrast for metabolic rates, the scaling relationship between per capita intake and population density varied with exposure treatments ($F_{4, 172} = 8.796$, $p < 0.001$). This was driven by a difference between uninfected and infected animals (either C1 or C19 infected) only, as the trends for the pathogen genotypes themselves did not significantly differ ($F_{2, 112} = 0.381$, $p = 0.684$). Overall, uninfected animals had lower metabolic rates at all densities, as capture by a lower conversion factor in general (Table 1). For all treatments, feeding rates were higher at low population density, and declined at a faster rate (~6-fold difference in feeding rate between 20 and 300 individuals L^{-1}) than metabolic rates, as evidenced by the higher conversion factors (e.g. 0.376 to 0.540 versus 0.062 to 0.071) and higher scaling exponents (-0.056 to -0.083 versus -0.009 to -0.010) for each trait and exposure combination (Fig. 2B, Table 1). The rapid decline in feeding rate and gradual decline in metabolic rate across density gave rise to an energetic advantage in terms of increased discretionary energy at low population densities (Fig. 2B), and an overall decline of discretionary energy with density (Fig. 2C). The rate of decline, however, differed between the exposure treatments. Animals infected with pathogen C1 had less discretionary energy available at most population densities due to both a lower conversion factor and scaling exponent (Table 1), and this scaling relationship was significantly different to both the uninfected animals ($F_{2, 32} = 6.629$, $p = 0.004$) and animals infected with genotype C19 ($F_{2, 32} = 6.823$, $p = 0.003$). There was no significant difference in the scaling relationship between density and discretionary energy between uninfected animals and hosts infected with pathogen C19 ($F_{2, 32} = 0.044$, $p = 0.957$).

Part 2: Density effects on host and pathogen growth

We found that the growth of both host (change in dry weight) and pathogen (production of transmission spores) scaled non-linearly with population density (see Suppl. material, Table S.1).

Hosts at low density were larger (higher dry weight), and dry weight declined with increasing density (Fig. 3A). Infection by both pathogen genotypes increased the size of their hosts relative to uninfected hosts in a similar fashion, leading to differences in the decline in dry weight with population density between the treatments ($F_{4, 180} = 9.11$, $p < 0.001$), but not between the two pathogens ($F_{2, 117} = 0.223$, $p = 0.801$). As a result, all exposure treatments showed similar scaling exponents between dry weight and density (e.g., -0.022 to -0.025, Fig. 3A, Table 1), with infected animals having higher conversion factors in general (0.224 versus 0.206, Table 1).

Both pathogen genotypes produced more spores when infecting low density hosts (~2.5-fold difference in spores produced in hosts at 20 and 300 individuals L^{-1}). However, pathogen C19 typically produced more spores in all densities (Fig. 3B), leading to significant difference between the genotypes in the rates of change in spores loads with increasing population density ($F_{2, 117} = 12.059$, $p < 0.001$), and a higher conversion factor and scaling exponent for C19 overall (Table 1). Importantly, even when correcting for the size of infected hosts (i.e., dry weight), we still observed a negative density-dependence in mass-specific spore load (Fig. 3C, see also Suppl. material, Table S.1). As such, both pathogens were thus able to more efficiently convert resources from hosts in low density, although pathogen C19 maintained higher mass-specific spore production overall, associated with a higher conversion factor and lower scaling exponent ($F_{2, 117} = 14.841$, $p < 0.001$). Similar results were also found when correcting feeding rate, metabolic rate and discretionary energy for average body size, indicating that for all traits, host and pathogens are performing at a level greater than expected based on their mass alone (see Suppl. material Fig. S.1, Table S.2 and S.3).

Part 3: Energy scope and consequences for pathogen fitness

Finally, we explored how the joint effect of host growth and discretionary energy impacted on pathogen fitness. In this system, pathogen spore production and host growth are tightly correlated. As part of the infection process, *P. ramosa* acts to castrate the host (Ebert et al. 2004; Clerc et al. 2015) and by limiting reproductive opportunities, at least temporarily (Hall et al. 2019), the excess resources are predicted to flow into host growth (i.e., gigantism) and pathogen proliferation (Clerc et al. 2015). In turn, host starvation both reduces host body size and pathogen spore production (Pulkkinen & Ebert 2004). For this study, therefore, whether the improved pathogen transmission potential in low density hosts is a consequence of the pathogen having more discretionary energy to exploit, or simply because hosts with more discretionary energy are larger, and thereby provides more room for growth, requires additional exploration.

Using a multiple regression approach, we found that the availability of discretionary energy predicted an increase in pathogen spore loads even after simultaneously controlling for host size (and vice versa, Fig. 4). On average, pathogen genotype C19 had a higher spore load for a given discretionary energy or dry weight (pathogen genotype main effect: $F_{1, 117} = 15.292$, $p < 0.001$), with the slopes for both traits otherwise consistent across each genotype (pathogen by trait interactions: $F_{2, 115} = 0.410$ $p = 0.665$). The effect of host dry weight on spore production, however, was higher than the effect of discretionary energy (standardized weight: $\beta = 0.206 \pm \text{SE } 0.023$, $p < 0.001$; standardized discretionary energy: $\beta = 0.099 \pm \text{SE } 0.024$, $P < 0.001$). Both host growth and discretionary energy, therefore, appear to independently influence pathogen transmission potential, with the effect heavily weighted towards density and energy-mediated changes in host body size.

Discussion

The occurrence and spread of infectious disease depend on a balance between a pathogen's within-host (Schmid-Hempel 2009; Hall et al. 2017) and between-host performance (Anderson & May 1991; Grenfell & Harwood 1997), ultimately generating two contrasting levels of selection where a pathogen most successful at proliferation is not always the one that generate the most new infections (see Nowak and May, 1994; Coombs, Gilchrist and Ball, 2007; Mideo, Alizon and Day, 2008). An important component impacting on such balance is density-mediated differences in energy availability (Anderson & May 1991; Cressler et al. 2014; Civitello et al. 2015). Indeed, whether the amount of energy available differ across a density gradient, and whether the availability of high energy translates into increased pathogen performance (see S. R. Hall et al. 2007; Seppala et al. 2008; Civitello et al. 2015; Dieter Ebert, Zschokke-Rohringer, and Carius 2000; Dieter Ebert et al. 2004; Bedhomme et al. 2005), or results in a stronger immune response in the host (Lochmiller and Deerenberg 2000; reviewed in Sheldon and Verhulst 1996), will have major impact on disease outcomes. While previous work has shown that pathogen fitness is highly influenced by within-host resource availability (Mideo et al. 2008; Penczykowski et al. 2014) and quality (Hall et al. 2009a), this study unravels how density-dependent differences in energy scope and density-mediated changes in host life-history jointly impact on pathogen fitness.

By estimating rates of feeding and metabolism at various densities, we found that uninfected hosts at low density maintained higher amounts of discretionary energy (Fig. 2), achieved by a greater non-linear increase in energy gained from feeding rates at low population density, relative to energy expended on metabolism. Of the possible predictions for the scaling relationship between energy intake (feeding rate) and expenditure (metabolic rate) at different population densities, our results thus follow the scenario where feeding rate decline faster than metabolic rate, leaving less discretionary energy at high density (Fig. 1C). This support previous findings by Ghedini et al.

(2017), whereby decreasing discretionary energy across a density gradient was identified in colonies of the sessile colonial bryozoan, *Bugula neritina*. In their study, the decline in individual body size with increasing population density could be predicted by estimates of energy intake and expenditure, with colonies reducing their energy use and expenditure per gram of mass in the presence of an increasing number of competitors. We find similar patterns in that per gram of mass, average feeding rates, metabolic rates and discretionary energy all decrease with population density (Fig. S.1).

Importantly, infection by any of the two pathogens, that vary in their proliferation and exploitation strategies (Clerc et al. 2015; Hall & Mideo 2018), did not fundamentally alter the scaling relationship between density and discretionary energy, as, even for infected animals, feeding rates continued to decline faster than metabolic rates (Fig. 2B). Instead, infection induced an increase in metabolic rate at all densities (Fig. 2A), leading to more subtle differences in the rate at which overall discretionary energy declines with population density (Fig. 2C). Both pathogens also produced more spores in low density hosts (Fig. 3B). Even when we corrected for the size of infected hosts at various densities, we observed that both pathogens produced more transmission propagules per gram of host mass at lower population densities (Fig. 3C). Such findings immediately rule out the possibility that increased discretionary energy in a host facilitates development of a stronger immune-response that could be used to curtail the proliferation of the pathogen, although the general assumption is that immune investment is costly and trades off with other energy demanding processes such as growth and reproduction (see review in Lochmiller and Deerenberg, 2000). Rather, our results suggest that higher amount of discretionary energy in hosts at low density are associated with an increase in both host and pathogen growth.

Our results show how the flow of energy in a population, as mediated by changes in resource competition and population density, affect pathogen performance though both correlated changes in host life-history such as growth, as well as a direct connection between energy scope and a

pathogen's transmission potential (Fig. 4). Both pathogens, however, appear to be benefiting most by increased energy indirectly, through the increase in host mass at low density. These findings reinforce that patch quality for an invading pathogen occurs at two scale (see Cressler et al. 2014). Within host proliferation of the pathogen will be accelerated when resources are locally abundant, or competition between hosts for resources are low (see Hall, Bento and Ebert, 2017; Cressler et al. 2014; Civitello et al. 2015). Conversely, between host dynamics are likely to be maximised in high density populations, where the encounter rate with susceptible hosts are higher (Anderson & May 1981), although natural disease outcomes still hinges on whether resource-trait links (such as fecundity and size) catalyse or inhibit disease spread (Civitello et al. 2015). Importantly, however, in the *Daphnia* system, filter-feeding could cause a dilution effect, ultimately reducing disease spread in highly dense populations (see Civitello et al. 2013; Strauss et al. 2015).

In summary, metabolic rates and energy scope is a common currency that provides a link between processes that shape community dynamics, such as feeding, competition or even facilitation (Civitello et al. 2015), and the growth and performance of a host or pathogen. With an increasing number of range expanding (Epstein 2000), invasive (Dunn & Hatcher 2015), or colonizing host populations (Thomas 2000), the anticipation of density-mediated differences in energy scope, and how this impact on the spread of infectious disease, becomes increasingly important. While we have shown that both a host and pathogen benefit from increased discretionary energy in low density, and that for the pathogen, the indirect benefit from increased host size was even stronger, a range of possible outcomes still exist (see Fig. 1). Whether other host and pathogen systems is underlined different density-dependent energy relationship still needs to be explored, and could provide yet other unique disease dynamics in spatiotemporally dynamic host populations. Lastly, understanding the complexity of higher-level interactions on energy budget in various population densities might be essential for predicting how individual and population-level energy flow impacts on the evolution, spread and severity of infectious disease.

Acknowledgements

We thank Dustin Marshall and members of the Hall lab group for valuable discussion, and Amanda Petterson and Stephen Gipson for advice on using oxygen consumption equipment.

Chapter 3 - Figures and tables

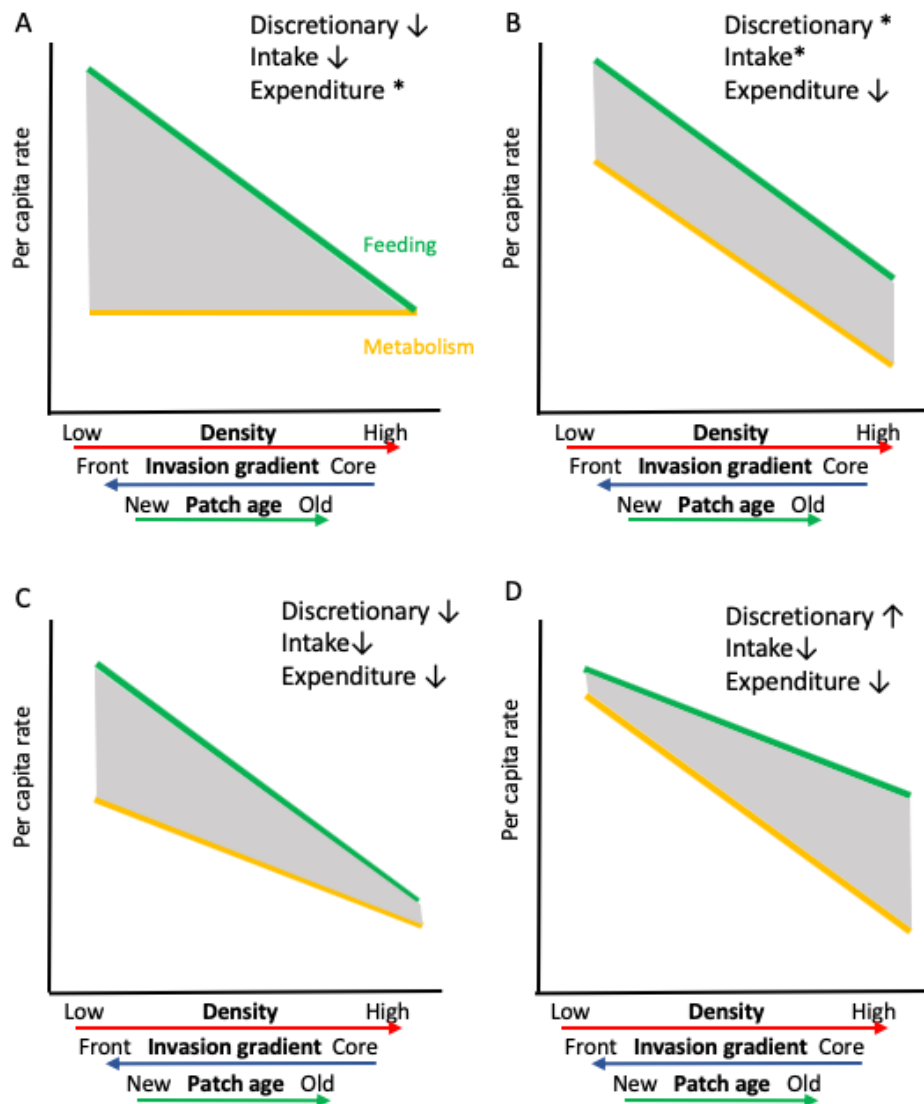


Figure 1. Predictions for the scaling relationship between energy intake (feeding rate – green line) and energy expenditure (metabolic rate – orange line) at different population densities, or analogously, along a gradient of range expansion, or patch age since initial colonization, and how this influence discretionary energy (grey shaded area). A) with increasing population density, feeding rate decline, but metabolic rate is stable, causing a net reduction in discretionary energy. B) both feeding and metabolic rate decline with density, leaving a constant amount of discretionary energy. C) feeding rate decline faster than metabolic rate, leaving less discretionary energy at high density. D) metabolic rate decline faster than feeding, leaving more discretionary at high density. Figure is modified from Ghedini et al. (2017).

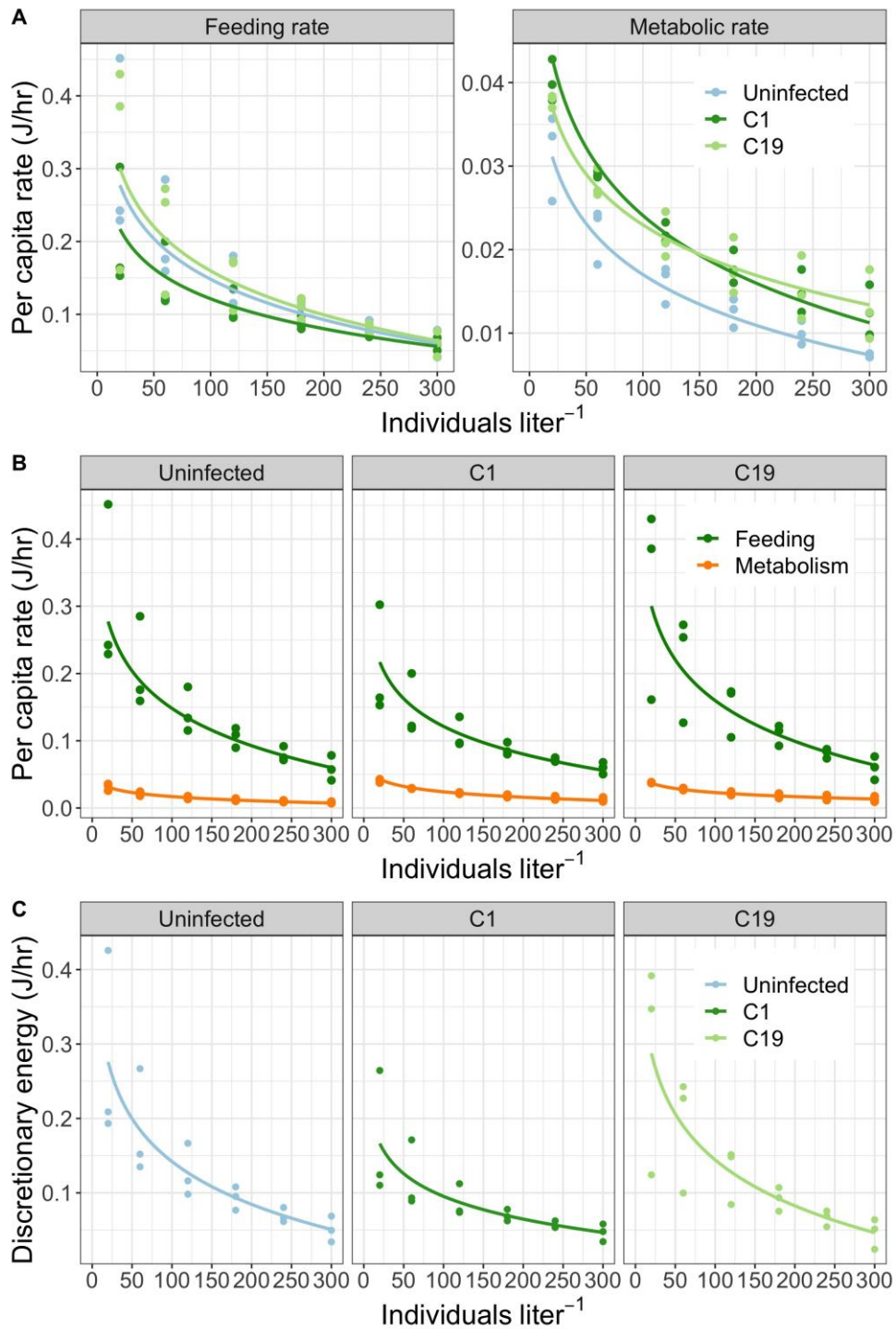


Figure 2. The relationship between population density and A) feeding (left panel) and metabolic (right panel) rates (J/hr) for all exposure treatments visualized separately, B) co-dependency of feeding (green) and metabolic (orange) rates (J/hr), and C) discretionary energy (J/hr) across population densities, calculated as the difference between predicted feeding and metabolic rates. Lines represents the best fitting power curve, and points are median predicted values for each experimental block.

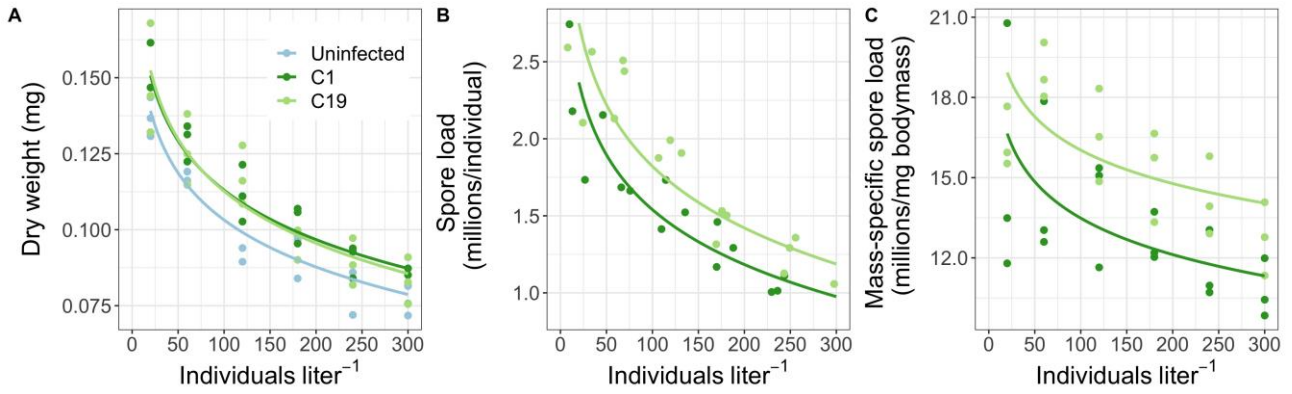


Figure 3. The relationship between population density and A) dry weight of hosts (all exposure treatments), B) spore load in infected carriers (million spores/individual), and C) mass-specific spore load (millions/mg dry weight). Fitted lines represent the best fitting power curve for each trait, and points are mean values for each experimental block. Colours are uninfected (blue), and pathogen genotypes C1 (dark green) and C19 (light green).

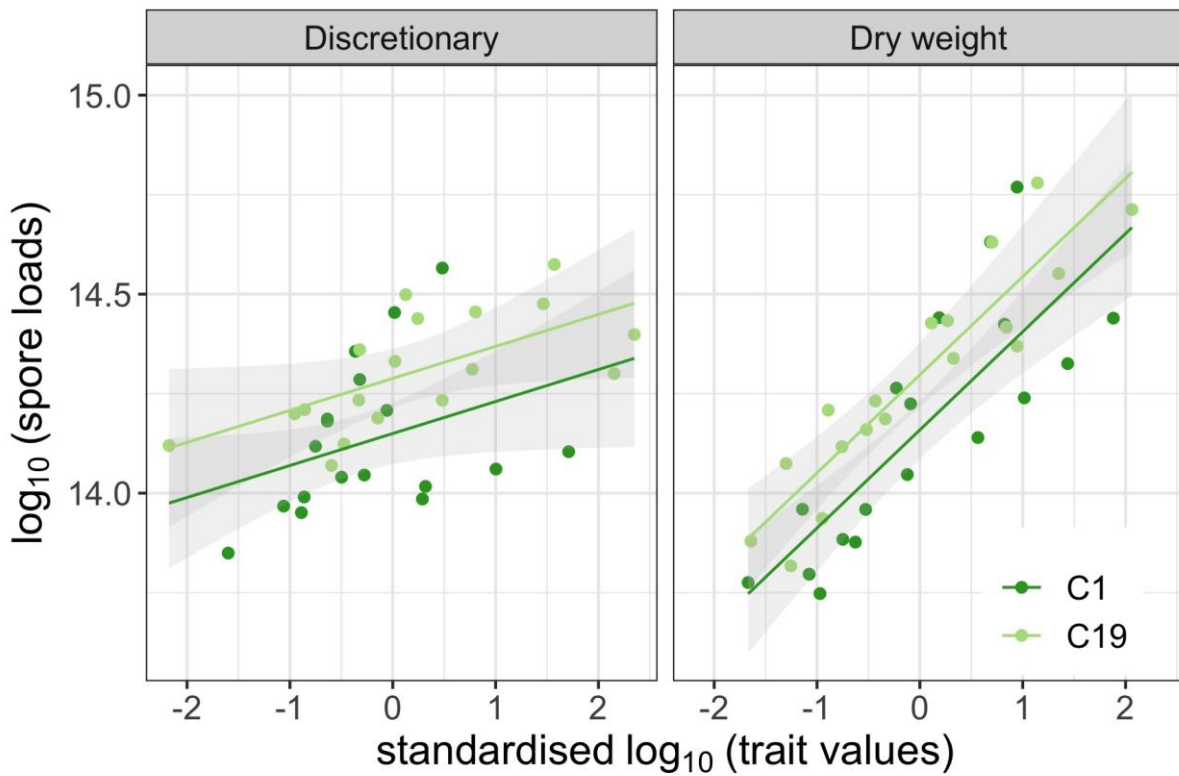


Figure 4. The predicted partial effects of discretionary energy and dry weight on spore loads in infected animals. Estimates of discretionary energy is obtained by subtracting predicted metabolic rates from predicted feeding rates. Shown are the partial residuals and predicted fit (and 95% confidence intervals) for the analysis of covariance for each trait-pathogen combination.

Table 1. Parameter estimates for all measured traits (for each exposure treatment) using the power curve, whereby parameter a refers to the conversion factor constant and parameter b the scaling exponent.

| Trait | Treatment | Param. | Estimate | Std. Error | p-value |
|---|------------------|---------------|-----------------|-------------------|----------------|
| Feeding rate | Uninfected | a | 0.473 | 0.059 | < 0.001 |
| | | b | -0.071 | 0.012 | < 0.001 |
| | C1 | a | 0.376 | 0.054 | < 0.001 |
| | | b | -0.056 | 0.011 | < 0.001 |
| | C19 | a | 0.540 | 0.061 | < 0.001 |
| | | b | -0.083 | 0.012 | < 0.001 |
| Metabolic rate | Uninfected | a | 0.062 | 0.004 | < 0.001 |
| | | b | -0.009 | 0.001 | < 0.001 |
| | C1 | a | 0.071 | 0.005 | < 0.001 |
| | | b | -0.010 | 0.001 | < 0.001 |
| | C19 | a | 0.065 | 0.005 | < 0.001 |
| | | b | -0.009 | 0.001 | < 0.001 |
| Discretionary | Uninfected | a | 0.525 | 0.067 | < 0.001 |
| | | b | -0.083 | 0.014 | < 0.001 |
| | C1 | a | 0.298 | 0.043 | < 0.001 |
| | | b | -0.044 | 0.009 | < 0.001 |
| | C19 | a | 0.555 | 0.073 | < 0.001 |
| | | b | -0.089 | 0.015 | < 0.001 |
| Dry weight | Uninfected | a | 0.206 | 0.007 | < 0.001 |
| | | b | -0.022 | 0.001 | < 0.001 |
| | C1 | a | 0.221 | 0.008 | < 0.001 |
| | | b | -0.023 | 0.002 | < 0.001 |
| | C19 | a | 0.226 | 0.008 | < 0.001 |
| | | b | -0.025 | 0.002 | < 0.001 |
| Spores (millions) | C1 | a | 3.905 | 0.25 | < 0.001 |
| | | b | -0.514 | 0.05 | < 0.001 |
| | C19 | a | 4.48 | 0.231 | < 0.001 |
| | | b | -0.577 | 0.047 | < 0.001 |
| Mass-spec. spores (millions/mg dry weight) | C1 | a | 22.54 | 2.194 | < 0.001 |
| | | b | -1.966 | 0.439 | < 0.001 |
| | C19 | a | 24.339 | 2.027 | < 0.001 |
| | | b | -1.804 | 0.41 | < 0.001 |

Chapter 3 - Supplementary material

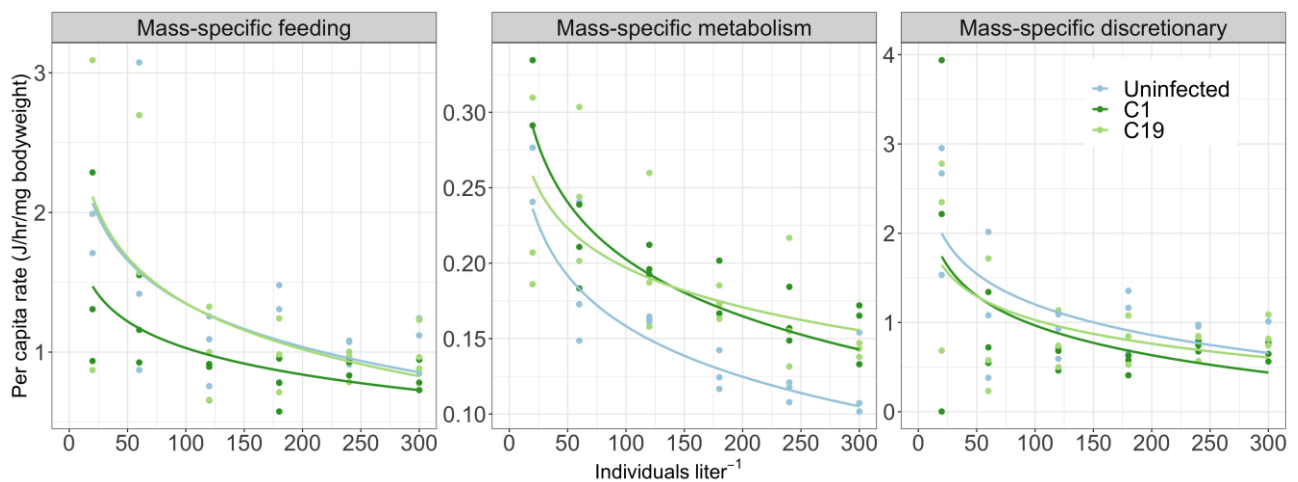


Figure S.1. The relationship between population density and mass-specific feeding rate (left), mass-specific metabolic rate (middle) and mass-specific discretionary energy (right) for all exposure treatments (uninfected, pathogen C1 and pathogen C19). Lines represent the best fitting power curve, and points are mean raw values for each experimental block.

Table S.1. Model comparison between a power curve, quadratic and linear regression on all measured host (feeding rate, metabolic rate, discretionary and mass corrected metabolic rate) and parasite traits (spores).

For each treatment, the best fitting model is evaluated by Δ AIC and AIC.

| Trait | Treatment | Model | ΔAIC | AIC weight |
|---------------------------------|------------------|--------------|-------------------------------|-------------------|
| Feeding | Uninfected | a | 0 | 0.55 |
| | | Quad | 0.442 | 0.441 |
| | | Lin | 8.24 | 0.009 |
| | C1 | a | 0 | 0.628 |
| | | Quad | 1.108 | 0.361 |
| | | Lin | 8.057 | 0.011 |
| | C19 | Quad | 0 | 0.831 |
| | | a | 3.199 | 0.168 |
| | | Lin | 14.007 | 0.001 |
| Metabolism | Uninfected | a | 0 | 0.907 |
| | | Quad | 4.552 | 0.093 |
| | | Lin | 22.113 | 0 |
| | C1 | a | 0 | 0.991 |
| | | Quad | 9.558 | 0.008 |
| | | Lin | 17.312 | 0 |
| | C19 | Quad | 0 | 0.632 |
| | | Lin | 1.878 | 0.247 |
| | | a | 3.3 | 0.121 |
| Discretionary | Uninfected | a | 0 | 0.735 |
| | | Quad | 2.831 | 0.179 |
| | | Lin | 4.293 | 0.086 |
| | C1 | a | 0 | 0.665 |
| | | Quad | 2.558 | 0.185 |
| | | Lin | 2.971 | 0.15 |
| | C19 | a | 0 | 0.727 |
| | | Quad | 2.791 | 0.18 |
| | | Lin | 4.101 | 0.093 |
| Mass-corrected discretionary | Uninfected | a | 0 | 0.467 |
| | | Lin | 0.565 | 0.352 |
| | | Quad | 1.894 | 0.181 |
| | C1 | a | 0 | 0.543 |
| | | Lin | 1.342 | 0.277 |
| | | Quad | 2.21 | 0.18 |
| | C19 | a | 0 | 0.54 |
| | | Lin | 1.314 | 0.28 |
| | | Quad | 2.195 | 0.18 |

Table S.1. continued.

| Trait | Treatment | Model | ΔAIC | AIC weight |
|-----------------------|------------------|--------------|-------------------------------|-------------------|
| Mass | Uninfected | a | 0 | 0.882 |
| | | Quad | 4.019 | 0.118 |
| | | Lin | 20.413 | 0 |
| | C1 | Quad | 0 | 0.906 |
| | | Lin | 5.262 | 0.065 |
| | | a | 6.883 | 0.029 |
| | C19 | Quad | 0 | 0.789 |
| | | a | 2.798 | 0.195 |
| | | Lin | 7.822 | 0.016 |
| Spores | Infected | a | 0 | 0.661 |
| | | Quad | 1.666 | 0.287 |
| | | Lin | 5.084 | 0.052 |
| Mass-corrected spores | Infected | a | 0 | 0.998 |
| | | Lin | 13.083 | 0.001 |
| | | Quad | 14.887 | 0.001 |

Table S.2. Model comparison between a power curve, quadratic and linear regression on mass-specific feeding rate, mass-specific metabolic rate and mass-specific discretionary energy. For each treatment, the best fitting model is evaluated by Δ AIC and AIC weight, and ranked with the top model first.

| Trait | Treatment | Model | ΔAIC | AIC weight |
|-----------------------------|------------------|--------------|-------------------------------|-------------------|
| Mass-specific feeding | Uninfected | a | 0 | 0.526 |
| | | Quad | 1.103 | 0.303 |
| | | Lin | 2.251 | 0.171 |
| | C1 | a | 0 | 0.511 |
| | | Quad | 0.553 | 0.387 |
| | | Lin | 3.227 | 0.102 |
| | C19 | Quad | 0 | 0.751 |
| | | a | 2.314 | 0.236 |
| | | Lin | 8.14 | 0.013 |
| Mass-specific metabolism | Uninfected | a | 0 | 0.752 |
| | | Quad | 2.307 | 0.237 |
| | | Lin | 8.394 | 0.011 |
| | C1 | a | 0 | 0.892 |
| | | Quad | 4.985 | 0.074 |
| | | Lin | 6.514 | 0.034 |
| | C19 | Lin | 0 | 0.604 |
| | | Quad | 1.748 | 0.252 |
| | | a | 2.871 | 0.144 |
| Mass-specific discretionary | Uninfected | a | 0 | 0.682 |
| | | Quad | 2.146 | 0.233 |
| | | Lin | 4.159 | 0.085 |
| | C1 | a | 0 | 0.578 |
| | | Quad | 0.828 | 0.382 |
| | | Lin | 5.343 | 0.04 |
| | C19 | a | 0 | 0.573 |
| | | Quad | 1.004 | 0.347 |
| | | Lin | 3.951 | 0.08 |

Table S.3. Parameter estimates for mass-specific feeding rate, mass-specific metabolic rate and mass-specific discretionary energy using the non-linear power curve, whereby parameter a refers to the conversion factor constant and parameter b the scaling exponent.

| Trait | Treatment | Param. | Estimate | Std. Error | p-value |
|-----------------------------|------------------|---------------|-----------------|-------------------|----------------|
| Mass-specific feeding | Uninfected | a | 2.903 | 0.552 | < 0.001 |
| | | b | -0.338 | 0.11 | 0.003 |
| | C1 | a | 2.118 | 0.457 | < 0.001 |
| | | b | -0.24 | 0.09 | 0.010 |
| | C19 | a | 3.337 | 0.529 | < 0.001 |
| | | b | -0.436 | 0.104 | < 0.001 |
| Mass-specific metabolism | Uninfected | a | 0.415 | 0.041 | < 0.001 |
| | | b | -0.054 | 0.008 | < 0.001 |
| | C1 | a | 0.422 | 0.041 | < 0.001 |
| | | b | -0.047 | 0.008 | < 0.001 |
| | C19 | a | 0.382 | 0.043 | < 0.001 |
| | | b | -0.04 | 0.009 | < 0.001 |
| Mass-specific discretionary | Uninfected | a | 3.248 | 0.693 | < 0.001 |
| | | b | -0.437 | 0.142 | 0.003 |
| | C1 | a | 3.21 | 0.796 | < 0.001 |
| | | b | -0.486 | 0.158 | 0.003 |
| | C19 | a | 2.481 | 0.589 | < 0.001 |
| | | b | -0.318 | 0.119 | 0.010 |

Chapter 4: Can pathogens optimize both transmission and dispersal by exploiting sexual dimorphism in their host?

Nørgaard, L. S., Phillips, B., Hall, M. D.

Manuscript is published in *Biology Letters*, <http://dx.doi.org/10.1098/rsbl.2019.0180>.

Abstract

Pathogens often rely on their host for dispersal. Yet, maximizing fitness via replication can cause damage to the host and an associated reduction in host movement, incurring a trade-off between transmission and dispersal. Here, we test the idea that pathogens might mitigate this trade-off between reproductive fitness and dispersal by taking advantage of sexual dimorphism in their host, tailoring responses separately to males and females. Using experimental populations of *Daphnia magna* and its bacterial pathogen *Pasteuria ramosa* as a test-case, we find evidence that this pathogen can use male hosts as a dispersal vector, and the larger females as high-quality resource patches for optimized production of transmission spores. As sexual dimorphism in dispersal and body size is widespread across the animal kingdom, this differential exploitation of the sexes by a pathogen might be an unappreciated phenomenon, possibly evolved in various systems.

Introduction

Many pathogens rely on their host for dispersal, yet maximizing the transmission benefits of within-host replication is often at odds with the need to disperse and encounter new hosts, since sick hosts are generally unlikely to move large distances (Binning et al. 2017). Such a trade-off places limits on the evolution of pathogens in spatially explicit settings, as a pathogen's long-term fitness is highly dependent on their ability to disperse once the local pool of susceptible hosts has been exhausted (Gandon 2002; Gandon & Michalakis 2002). Thus, for non-vectored pathogens, host movement, and how this is altered by infection (Moore 2002), is essential for understanding

any constraints on the epidemiology and evolution of infectious disease across space (Osnas & Dobson 2011; Daversa et al. 2017). If infection reduces host dispersal, for example, selection is expected to favour more prudent host exploitation strategies at the front of an expanding host population (Osnas & Dobson 2011).

Predictions for pathogen evolution in a patchy landscape often centre on a pathogen's dispersal ability relative to that of a generic host (Lion et al. 2006; Becker et al. 2018b), implying that there is one optimal dispersal strategy. In nature, however, hosts commonly vary in their dispersal capacity and provided resources, with one common source of host heterogeneity being sexual dimorphism. Each sex often differs in size, dispersal (Fairbairn 1997; Li & Kokko 2018) and in the prevalence and severity of disease (Poulin 1996; Schalk & Forbes 1997; Sheridan et al. 2000). Studies have captured the interplay between these key fitness components by linking one sex to the spatial distribution of a pathogen (Streicker et al. 2016) and revealing how investment in dispersing life-stages (Soghigian & Livdahl 2017) or modes of transmission (Fellous & Koella 2009) depends on host sex. Based on these findings, it is clear that sexual dimorphism influences both the evolution of a trade-off between within host replication and virulence (Duneau & Ebert 2012; Cousineau & Alizon 2014; Gipson & Hall 2016; Hall & Mideo 2018) and the potential redistribution of pathogens (Lion et al. 2006; Streicker et al. 2016). Yet, it remains to be tested if a pathogen can optimize both transmission and dispersal simultaneously by tailoring their infection strategies separately to males and females.

Here, we propose the idea that pathogens may be able to mitigate the trade-off between dispersal and within-host replication by taking advantage of sexual dimorphism of their host. In particular, we suggest that sexual dimorphism in host dispersal and size will play a crucial role in mitigating any trade-offs for a pathogen. For example, where there is strong sexual dimorphism in size - often a proxy for the resources that a host provides to a pathogen - we might expect pathogens to maximize production of transmission propagules in the larger host. Likewise, with sexual

dimorphism in dispersal, pathogens may maximize dispersal via the more dispersive sex. Where these two situations align, such that the sex providing the fewer resources is also the more dispersive, we would expect to see particularly strong opportunities for pathogens to exploit host sexual dimorphism.

In this study, we test this idea by using *Daphnia magna* and its pathogen *Pasteuria ramosa*. *Daphnia* are freshwater crustaceans, reproducing via cyclical parthenogenesis (females can produce genetically identical male and female offspring). Transmission of *P. ramosa* occurs exclusively horizontally, and infection is facilitated by filter-feeding, after which the pathogen sterilizes and kills its host (Gipson & Hall 2018). Males are smaller and have a shorter lifespan than females (Winsor & Innes 2002; Thompson et al. 2017) and display behavioural differences in mate-finding (Ebert et al. 2016). Males are also more resistant to infection, constrain the production of transmission spores and suffer from less pathogen-induced reduction in lifespan relative to females (Winsor & Innes 2002; Thompson et al. 2017; Hall & Mideo 2018). With this system, we then explored how host sex and infection interact to shape host dispersal behaviour in two different contexts: (i) the probability of dispersal from a crowded habitat and (ii) the rate and magnitude of any potential dispersal events. Overall, our experimental data suggest that pathogens are able to utilize male hosts as a vector for dispersal, and the female host as a high-quality patch for optimized spore production.

Materials and methods

We performed two experiments to investigate host sex and infection differences in (i) probability of dispersal from a crowded habitat (two-patch microcosms), and (ii) movement capacity of individuals (unlimited continuous microcosms). The host genotype used for these experiments originated from Hungary (HUHO-2), and the two *P. ramosa* genotypes originated from Russia (C1) and Germany (C19) and have previously been shown to vary in transmission and virulence

strategies (Clerc et al. 2015; Hall & Mideo 2018). For both experiments, animals were prepared by collecting female *Daphnia* from stock cultures and rearing following standard conditions (28°C, 16L:8D). Males were generated via hormone treatment (Winsor and Innes 2002, see electronic Suppl. material). To produce infected individuals, each animal was exposed to 20,000 spores of one of the two pathogen genotypes (C1 or C19) or an equivalent placebo-solution (i.e. unexposed and uninfected controls) at age 3 and 4 days (40,000 spores individual).

Experiment 1: The probability of dispersal from a crowded habitat

Two-patch microcosms were built by interconnecting two 950-ml containers with PVC-piping (15 mm diameter) and a closing valve between patches. We have previously shown that high density conditions in a local patch directly induce *Daphnia* dispersal (Erm et al. 2019) and that info-chemicals contained in ‘crowded’ water influence *Daphnia* life-history (Michel et al. 2016). To stimulate dispersal, we simulated a high-density environment in the first patch using crowded-conditioned water (electronic Suppl. material) and introduced 20 infected individuals (by pathogen C1 only) and 20 unexposed controls (i.e., uninfected) of each sex (2 sexes x 2 treatments (infected and uninfected) x 20 individuals x 15 replicates = 1200).

After a 24 h acclimatization period, we opened the valves and allowed for dispersal to the second patch, containing fresh *Daphnia* media. Six days later, we quantified the number of animals of each sex and treatment (infected or uninfected) in patch two. With this population-level approach, we cannot completely rule out differences in mortality between males and females (nor uninfected or infected animals) contributing to the observed results, but our approach does allow us to focus on the biologically meaningful aspect for this study: the probability of dispersal to a new patch.

Experiment 2: The rate and magnitude of individual dispersal

To assay the movement capacity of individual *Daphnia*, we used continuous microcosms built from 50 ml falcon-tubes interconnected by 10 cm silicon tubing (internal diameter 8 mm and outer

diameter 12 mm). For both host sexes, infected (pathogen C1 and C19) and uninfected animals were introduced individually into the first patch of a continuous microcosm system at 20 days post infection. Each treatment was replicated 20 times (2 sexes x 3 treatments [2 pathogens + controls] x 20 replicates = 120 animals) and checked daily for mortality and dispersal (back-dispersal was prevented by closing the tube after any dispersal event). At death, individual *Daphnia* were frozen in 500 ml RO for later spore count, using an Accuri C6 flow cytometer (BD Bio-sciences, San Jose, CA, USA) following standard procedures (Thompson et al. 2017).

Statistical analyses

All data analyses were performed in R (ver. 3.3.3; R Development Core Team). For Experiment 1, we analysed the probability of dispersal using a generalized linear model with a binomial distribution and logit-link function, with infection treatment (C1, C19 and uninfected), host sex and their interaction as fixed effects. For Experiment 2, we analysed dispersal rate by fitting a linear mixed model using an accumulated number of patches as the response variable, time as a covariate, host sex, infection treatment and their interaction as fixed effects. We used a two-factor analysis of variance to analyse total distance covered and spore loads (both response values square root transformed before analysis), with pathogen treatment (both pathogen genotypes, including uninfected when analysing total distance), host sex and their interactions as fixed effects.

Results

The probability of dispersal from a crowded habitat

The probability of dispersal from a crowded patch to a neighbouring patch depended on an interaction between host sex and infection status (d.f. = 1, $\chi^2 = 16.22$, $p < 0.001$, see Suppl. material Table S.1). In general, males appeared less likely to disperse from crowded conditions than females (Fig. 1), but the impact of infection reversed dispersal behaviour within each sex. Infected females were three-times less likely to disperse than uninfected females (d.f. = 1, $\chi^2 = 28.80$, $p < 0.001$). By

contrast, infection in males substantially increased their probability of dispersal from a crowded patch (d.f. = 1, $\chi^2 = 6.91$, $p = 0.009$).

The rate and magnitude of individual dispersal

Both the rate of dispersal (patches travelled per time, Fig. 2A) and total patches travelled by an individual (Fig. 2B) were affected by an interaction between host sex and infection treatment (dispersal rate: $\chi^2 = 666.5$, $p < 0.001$; total distance: $F_{2,93} = 13.49$, $p < 0.001$, see Suppl. material). For uninfected animals, dispersal rate was only marginally higher in males compared to females (slopes: male = 0.73 vs. female = 0.56, $p < 0.001$), and with no difference in the total number of patches travelled ($p = 0.612$). When infected with each pathogen, however, females moved substantially slower than males (Fig. 2A) and travelled fewer patches (Fig. 2B). Finally, the number of spores that a pathogen would release at host death in the final patch was four times higher in females, albeit influenced by pathogen genotype ($F_{1,35} = 14.962$, $p = 0.001$; see Suppl. material for details on size-corrected spore loads).

Discussion

Sexual dimorphism manifests across a range of taxonomic groups, with sex differences in body size and dispersal being among the most commonly observed (Fairbairn 1997; Li & Kokko 2018). The ubiquity of sexual dimorphism may present pathogens with an opportunity to specialize the tasks of optimizing fitness and dispersal to different host sexes. Such specialization potentially allows pathogens to mitigate the trade-off between within-host replication and dispersal, such that one sex can be exploited for dispersal, and the other for maximizing transmission. Despite the ubiquity of host sexual dimorphism, the possibility that pathogens might tailor exploitation strategies has gone largely unexplored in the literature (but see Fairbairn 1997; Ebert et al. 2016; Hall & Mideo 2018). Here, we explored this possibility using *D. magna* and its bacterial pathogen *P. ramosa*.

In line with our hypothesis, pathogens produced up to four times more spores in female hosts (Fig. 2C), but in doing so caused a substantial reduction in host dispersal. Infected females were less likely to leave crowded conditions and suffered a severe reduction in both dispersal rate (Fig. 2A) and total distance (Fig. 2B). For a pathogen, this should maximize the chance for secondary infections, as the release of a large number of transmission spores from a dying female is likely to coincide with a high-density population of (non-dispersing) animals. By contrast, while males allow for the production of fewer spores, infection increased the likelihood of dispersal (Fig. 1), and infected males showed dispersal rates and total distances comparable to uninfected males.

The differences we observe in dispersal behaviour between infected males and females appear to be a direct result of how the host sexes interact with the pathogen, and not an inherent property of each sex. Uninfected males and females, for example, had very similar rates and magnitudes of individual dispersal (Fig. 2A, B) and females were more likely to disperse from crowded habitats (Fig. 1). However, both patterns disappear once each sex is infected. The reduced dispersal of uninfected males from high-density conditions may be caused by the presence of females in these populations, since males might invest more energy in mating relative to dispersal (high-density conditions are one of the triggers for sexual reproduction in *Daphnia* (Duneau et al. 2012; Ebert et al. 2016). In this situation, the increase in dispersal probability in infected males could be a direct pathogen-induced manipulation (as observed in other species Moore 2002; Roulin et al. 2013), or an indirect outcome of the partial sterilization (Thomas et al. 2005).

Other studies have investigated how host sex may impact on the spatial spread of disease. The spread of vampire bat rabies between genetically isolated host populations, for example, is facilitated by dispersing male bats alone (Streicker et al. 2016). Mixed dispersal strategies for each sex also arise when microsporidia infect *Aedes* mosquitoes and invest a larger proportion of dispersing life-stages in females relative to males (Soghigian and Livdal 2017, see also Fellous and Koella 2009). However, by tracking pathogen proliferation and dispersal simultaneously, we here

connected these two observations and show how pathogen can leverage the sex of its host to maximize the transmission benefits of within-host replication, but also achieve dispersal within and between host patches.

In summary, motivated by isolated examples linking sex-differences to the mode of pathogen transmission and spread of disease (Fellous & Koella 2009; Streicker et al. 2016; Soghigian & Livdahl 2017), our test-case formally explored how sex-differences would alleviate the impact of pathogens on the movement of sick hosts. Whatever the proximate mechanisms, our results are consistent with the prediction that *Pasteuria* favours the production of spores in females, and host-assisted dispersal in males. This suggests that the sexes offer a mixed dispersal strategy, and a form of bet hedging for the pathogen (see Fellous and Koella 2009; Soghigian and Livdal 2017).

However, the degree to which our prediction holds in other systems will be sensitive to the direction of sexual dimorphism and the relative density of the two host sexes. Theory on pathogen evolution to sexually dimorphic hosts is currently limited to the evolution of virulence and proliferation (Cousineau & Alizon 2014; Hall & Mideo 2018), and does not account for dispersal in a spatial setting. Our work shows that pathogens can exploit this variation in their environment, and suggests that pathogen strategies tailored to sexual dimorphism might be widespread and have important implications for disease dynamics.

Acknowledgements

We thank the Hall group for valuable discussions.

Chapter 4 - Figures and tables

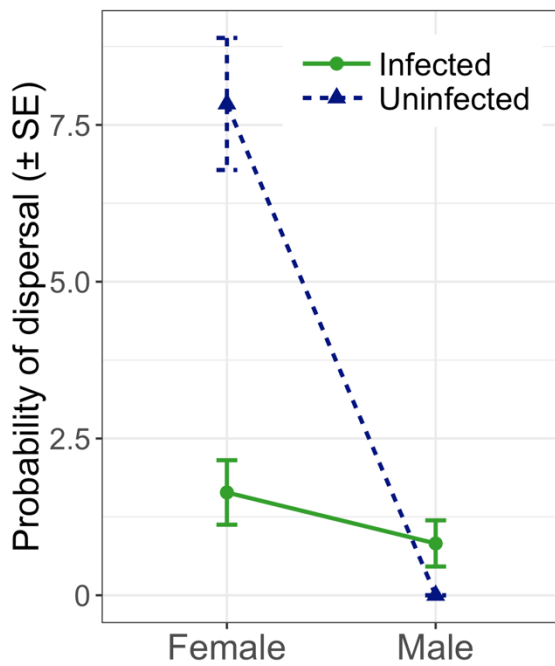


Figure 1. Probability of dispersal (mean \pm SE) from a crowded habitat to a neighbouring unhabituated habitat for infected (solid, green line and circles) and uninfected (dashed, blue line and triangles) male and female *Daphnia*.

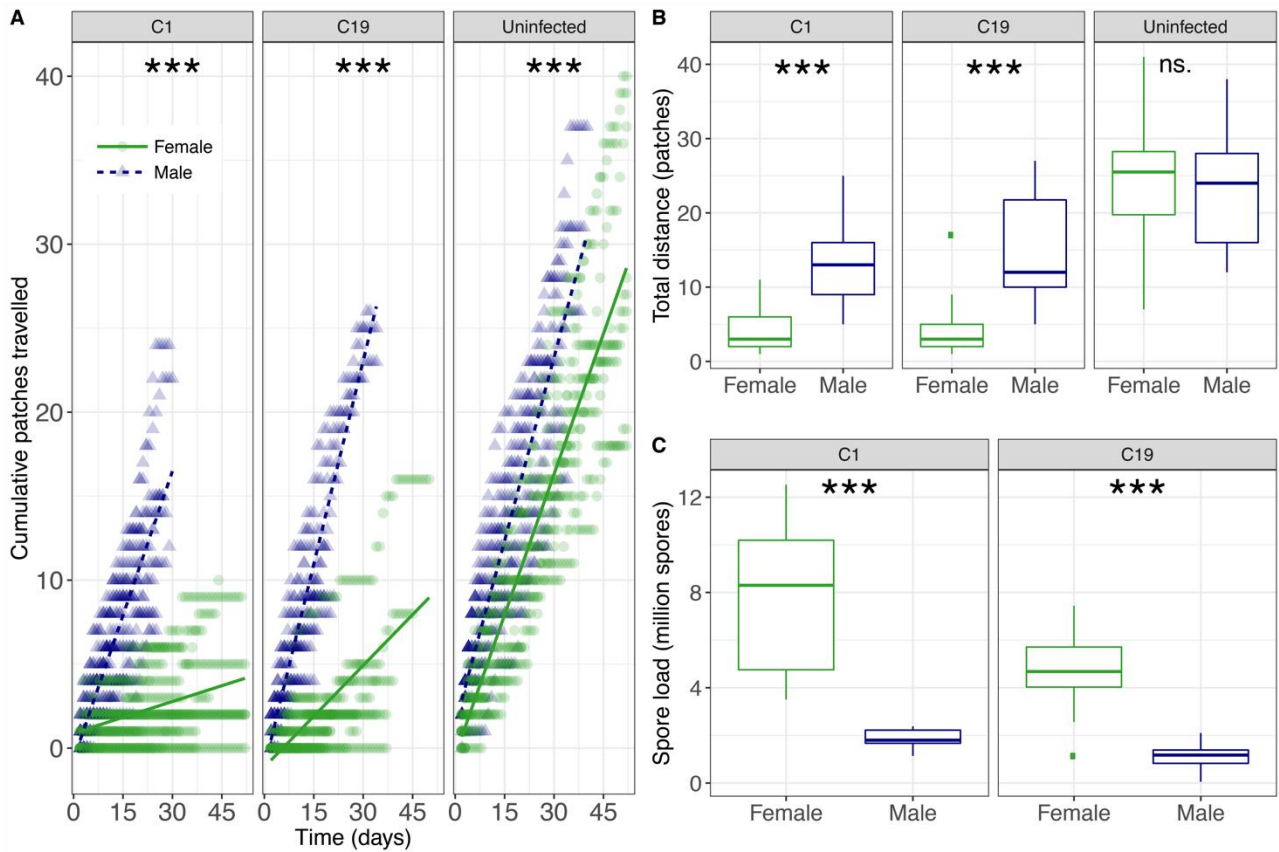


Figure 2. Individual dispersal in interconnected microcosms. A) the accumulated number of patches moved over time for male (blue triangles and dashed line) and female (green circles and solid line) *Daphnia*, infected with pathogen C1, C19 and uninfected. Coloured dots represent individual replicates and solid lines a fitted linear model. B) total distance (number of patches). C) pathogen spore load (millions) at death. Posthoc tests for differences between males and females in slope (A) or traits (B, C) are indicated at the top of each panel (ns $p > 0.05$, * $p < 0.05$, ** $p < 0.01$, *** $p < 0.001$).

Chapter 4 - Supplementary material

Production of male and female *Daphnia*

Naturally, female *Daphnia* can shift to producing male and female offspring given certain environmental conditions (Ebert 2005). However, in the laboratory, we can induce the production of males and females by exposing mothers to a small amount of juvenoid hormone, methyl farnesoate (Echelon Biosciences, product number S-0153). Specifically, experimental mothers were prepared by collecting juvenile female *Daphnia magna* from stock cultures and cultured individually in 60 mL jars filled with 50 mL artificial *Daphnia* medium (ADaM, Klüttgen et al. 1994; modified by Ebert et al. 1998) for three generations, to minimize maternal effects. *Daphnia* were transferred into fresh ADaM twice a week, maintained under standard conditions (20°C, 16L: 8D) and fed up to 5 million *Scenedesmus* algal cells daily; steadily increased to accommodate growing needs of the animal. Trays were rearranged every three days to minimise any positional effects.

To produce experimental male and females, the experimental mother generation were exposed to 300 µg L⁻¹ methyl farnesoate hormone, after producing their first clutch, and then transferred into fresh hormone-treated media every two days. Subsequent clutches were collected, and the sex of all offspring determined and used as experimental animals. *Daphnia* sex were determined by the presence of a “modified first leg” as per Ebert 2005, since sexual dimorphism in body size is minimal in juveniles (Ebert 2005). Finally, this method can be used to reliably produce male and female *Daphnia* while having no detectable impact on lifespan, fecundity, infection rates or spore loads (Thompson et al. 2017).

Manipulation of host density signals

In a variety of zooplankton, including *Daphnia magna*, info-chemicals and metabolic waste released from conspecifics, influence life-history investment in a variety of traits. Furthermore, presence of info-chemicals as a cue of stress, has been used in a variety of studies, exposing individuals to “stress conditioned water” (Folt & Goldman 1981; Gosler & Ratte 1994; Burns 2000; Lüring et al. 2003; Michel et al. 2016). In this experiment, we exploit release of info-chemicals to simulate cues related to high density in a two-patch experimental microcosm system. Conditioned water was produced by incubating healthy *Daphnia* in 500 mL glass jars (~250 adult *Daphnia* L⁻¹). After five days of incubation, we collected the conditioned water by using a coarse-meshed plankton net (mesh size 0.1 mm) to remove *Daphnia*, and then pumping the conditioned water through a 0.45 µm filter to remove debris and algae cells, following (Michel et al. 2016).

Supplementary tables

Table S.1. Probability of dispersal from a crowded habitat to an empty neighbouring habitat. Results show the analysis of variance from a generalized linear model using infection status (yes or no), host sex (male or female), and their interaction as fixed effects.

| Source | χ^2 | d.f. | P-value | Sign. code |
|------------------------|----------------------------|-------------|----------------|-------------------|
| Sex | 68.621 | 1 | <0.001 | *** |
| Infection status | 28.802 | 1 | <0.001 | *** |
| Sex x Infection status | 16.219 | 1 | <0.001 | *** |

Table S.2. ANCOVA results from a fitted linear mixed effect model using accumulated number of patches as a continuous response variable and time (in days) as a covariate, and host sex, infection treatment (uninfected control, pathogen C19 and C1) and their interaction, as fixed effects, and individual id as random effect.

| Source | χ^2 | d.f. | P-value | Sign. code |
|---------------------------|----------------------------|-------------|----------------|-------------------|
| Sex | 0.285 | 1 | 0.594 | |
| Infection treatment (Trt) | 4.437 | 2 | 0.109 | |
| Day number | 13251.183 | 1 | <0.001 | *** |
| Day number x Sex | 2507.064 | 1 | <0.001 | *** |
| Day number x Trt | 1464.637 | 2 | <0.001 | *** |
| Sex x Trt | 9.724 | 2 | 0.008 | ** |
| Day number x Sex x Trt | 666.494 | 2 | <0.001 | *** |

Table S.3. ANOVA results for model predicting square root transformed total number of patches travelled, using host sex and infection treatment (uninfected control, pathogen C19, and C1) as fixed effects.

| Source | d.f. | F | P-value | Sign. code |
|---------------------------|-------------|----------|----------------|-------------------|
| Sex | 1,93 | 37.820 | <0.001 | *** |
| Infection treatment (Trt) | 2,93 | 70.349 | <0.001 | *** |
| Sex x Trt | 2,93 | 13.489 | <0.001 | *** |

Table S.4. ANOVA results of two factor analysis of variance with square transformed pathogen spore load as response and using host sex and pathogen genotype (Gp, pathogen C1 or C19) as fixed effects.

| Source | d.f. | F | P-value | Sign. code |
|------------------------|-------------|----------|----------------|-------------------|
| Sex | 1, 64 | 106.717 | <0.001 | *** |
| Pathogen genotype (Gp) | 1, 64 | 13.923 | <0.001 | *** |
| Gp x Sex | 1, 64 | 1.425 | 0.237 | |

Size corrected spore load in male and female hosts

When accounting for standard body sizes obtained from the literature (male = 2 mm and female = 5 mm, Benzie, J. A. H. 2005), we find evidence that pathogens were able to produce more transmission spores in female hosts, compared to male hosts. This suggest that the pathogens are better at utilising female resources, or, that females provide a higher quality resource patch, for pathogen proliferation.

Table S.5. ANOVA results of two factor analysis of variance using relative pathogen spore production in male and female hosts, corrected for standard body sizes. Relative spore load is predicted using host sex, pathogen genotype (C1 and C19) and their interaction as fixed effects.

| Source | d.f. | F-value | P-value | Sign. code |
|-------------------------|------|---------|---------|------------|
| Sex | 1,64 | 23.0245 | <0.001 | *** |
| Pathogen genotype | 1,64 | 22.182 | <0.001 | *** |
| Sex x Pathogen genotype | 1,64 | 1.417 | 0.238 | |

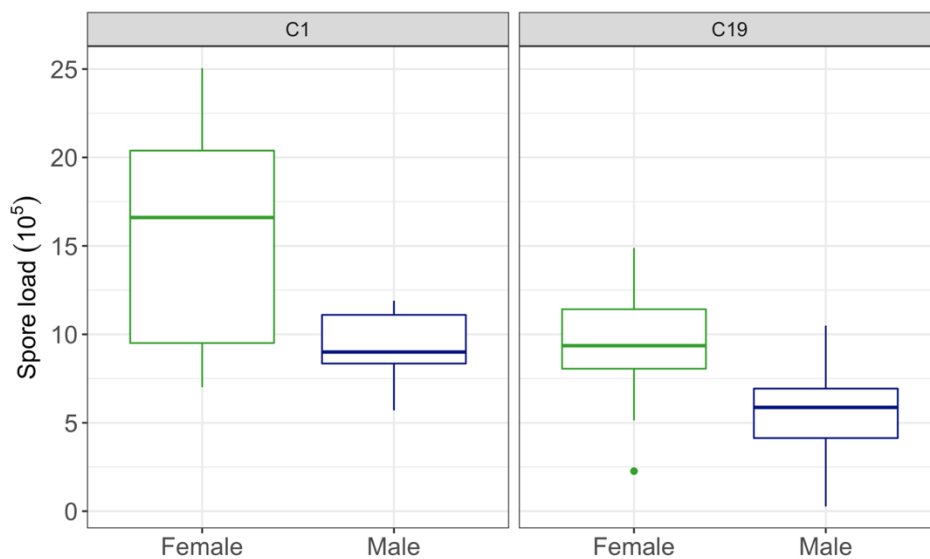


Figure S.1. Relative pathogen spore production corrected by standard body size (left: pathogen C1, right: pathogen C19) of males (blue) and females (green).

Chapter 5: Pathogens on the move – high host-facilitated dispersal is associated with evolutionary changes in parasite life-history traits

Louise Solveig Nørgaard^{1*}, Matthew D. Hall¹, Emanuel A. Fronhofer², Claire Gougat-Barbera², Oliver Kaltz^{2#} & Giacomo Zilio^{2#}

¹School of Biological Sciences and Centre for Geometric Biology, Monash University, Melbourne 3800, Australia

²ISEM, University of Montpellier, France

Target journal is still to be determined.

Abstract

Understanding the occurrence and spatial spread of infectious disease is a major challenge to epidemiologist and evolutionary biologist. In homogeneous populations, classic theory predicts the spread of highly exploitative parasites at the front of a spreading epidemic, but conditions met in nature are exceedingly more complex. Rather, most populations are highly dynamic or patchy, such as metapopulations, or in range expanding and invasive species. Furthermore, many parasites spread to new habitats via host-facilitated dispersal, and the evolution of such parasites may depend on what strategies that optimize transmission in response to changes in host demography, and correlated changes in strategies that optimize dispersal needs. Emerging theory suggest that a trade-off between host-facilitated dispersal and transmission may exist, but such predictions are yet to be tested empirically. In this study, we imposed directional selection for high and low dispersal in interconnected microcosm populations, such that populations of the freshwater host *Paramecium caudatum* and its bacterial parasite *Holospora undulata* represent the front and core of a range

expansion (and consequently, an epidemic). We tested whether dispersal selection on the host population caused correlated changes in parasite life-history traits, and predict that adaptations that facilitate higher host dispersal may come at the cost of reduced virulence and changes in transmission strategy towards more vertical (less virulent) transmission. Our results were broadly consistent with predictions and confirmed the idea that different segments of an epidemic wave can be under divergent selection pressures, shaping parasite infection life cycle, virulence and host dispersal facilitation. Such findings have important implications, not only for virulence evolution on a spatial scale, but also for our understanding of the role of parasites in the spatial spread of host species during range expansions, biological invasions, or in fragmented habitats with strong extinction-recolonization dynamics.

Introduction

Epidemic outbreaks of infectious disease are of great concern to human health, agriculture and wildlife conservation, and understanding the ecological and evolutionary drivers of their spread represents a major challenge to epidemiologists and evolutionary biologists (Parratt, Numminen and Laine, 2016; Penczykowski, Laine and Koskella, 2016). In spatially homogeneous populations, theory often predicts the spread of highly exploitative (i.e., virulent) parasites with a high transmission potential (Andre and Hochberg, 2005). Outbreaks of disease in the wild, however, generally occur in highly dynamic or patchy host populations, such as in metapopulations or in range expanding and invasive species. Since many parasites spread to new habitats via host-mediated dispersal, the evolution of such pathogens will now depend not only on the strategies that maximise transmission in response to changes in host demography (see discussion in Penczykowski, Laine and Koskella, 2016; Nørgaard, Phillips and Hall, 2019), but also on a correlated response to the spatial sorting of hosts with different dispersal capacities across a landscape (see Calcagno et al. 2006; Perkins et al. 2013). However, how the increased mobility of a

host during range expansion processes (Phillips, Brown and Shine, 2010) translates into the emergence and spread of infectious disease, remains rather unequivocal due to the high complexity of ecological and evolutionary dynamics at play (see Torchin et al. 2003; Perkins et al. 2008; Dunn and Hatcher, 2015).

By exploring the many different levels of virulence in nature, Ewald (1995) suggested that parasite transmission and virulence may evolve in response to changes in the opportunity for dispersal provided by a particular vector, as exemplified by the recurrent emergence of highly virulent cholera strains during periods with high water supply and low purification. Other studies have also established that moving parasites are likely to evolve 'invasion syndromes', with characteristic transmission strategies and dispersal behaviours, such as increased size of transmission propagules, and allowing for higher host-facilitated dispersal (Kelehear, Brown and Shine, 2012; Berngruber et al. 2013; Phillips and Puschendorf, 2013). Empirical support for such predictions have subsequently emerged, and show the emergence of highly virulent honey bee viruses (Mondet et al. 2014) and rabbit haemorrhagic disease virus (Moss et al. 2002; Boots, Hudson and Sasaki, 2004) at the front of a progressing epidemic. Yet, not all host-parasite systems necessarily show this pattern. For instance, the spread of the bacterium *Mycoplasma gallisepticum* in North American house finches was associated with decreased virulence in the newly invaded areas (Hawley et al. 2013). Likewise, in monarch butterflies, hosts that sustain long or frequent migrations is infected with less virulent pathogens (de Roode, Yates and Altizer, 2008).

Emerging theory has identified a trade-off between host exploitation and dispersal as key to determining whether the severity of an infectious disease outbreak will increase or decrease during an epidemic. Assuming a classic virulence-transmission trade-off (May and Anderson, 1983; Bull, 1994; Gandon et al. 2001) and local feedbacks between epidemiology and selection, one body of theory predicts that highly virulent parasites will evolve in connected landscapes (Boots, Hudson and Sasaki, 2004; Kamo and Boots, 2006; Kamo, Sasaki and Boots, 2007), or at the front of an

advancing epidemic (Griette, Raoul and Gandon, 2015), where host exploitation and transmission is not limited by local depletion of susceptible hosts (“self-shading”). In contrast, models that more explicitly consider the impact a pathogen has on its hosts dispersal, lead to a different prediction. If parasites travel with their infected hosts, exploitation of host resources may reduce dispersal, and thereby introducing a novel dispersal-virulence trade-off (Osnas, Hurtado and Dobson, 2015). In this scenario, selection at the moving edge favours more prudent and dispersal-friendly parasites that constantly escape the more virulent and transmissible parasites present at the core of the epidemic (Osnas, Hurtado and Dobson, 2015, see also colonization-dispersal trade-off; Calcagno et al. 2006).

With a growing number of range expanding (Epstein 2000), invasive (Dunn and Hatcher, 2015), or colonizing host populations (Thomas 2000), the spread and impact of infectious disease across a landscape ultimately depends on the types of 'invasion syndromes' that are favoured at the front and core of an expanding host population (see Dunn and Hatcher, 2015). While examples of natural epidemics provide evidence, sometimes conflicting, for how disease may evolve during an epidemic, controlled empirical studies that isolate the factor leading to any evolutionary change, remains rare. Most experimentally controlled approaches either manipulate demographic conditions mimicking the front and core of an expanding epidemic (Nørgaard, B. L. Phillips and Hall, 2019), or test how connectivity (and therefore local vs. global interactions) impact on disease evolution (Boots and Sasaki, 1999; Boots and Meador, 2007). While such approaches are highly valuable for our current understanding of epidemic spread and disease evolution, less evidence exists for how selection acting on host dispersal itself can drive correlated responses in the evolution of parasite exploitation strategies.

Studying the evolution of disease in experimental microcosm (meta)populations provide a powerful tool to test such hypotheses under controlled conditions for a large number of generations (Brockhurst and Koskella, 2013). Experimental microcosm systems, for example, has provided

valuable evidence for increased dispersal rate during invasion in a host population (Fronhofer and Altermatt, 2015) and independently shifts in pathogen transmission strategies in response to host population growth dynamics (Magalon et al. 2010). Here, we used such an experimental evolution approach to test the prediction that parasites may evolve characteristic “invasion syndromes”, represented by changes in transmission strategy, virulence and dispersal abilities, in response to dispersal selection imposed on the host population itself. In interconnected two-patch microcosm systems using the ciliate *Paramecium caudatum* and its bacterial parasite *Holospora undulata*, we established a simplified range expansion scenario, with a front population that were allowed to disperse into new microcosms and a core population remaining in place (and losing emigrants). Importantly, parasite dispersal was only possible together with infected hosts since horizontal transmission stages are immobile. After 55 cycles of dispersal selection, we isolated evolved front and core parasites, and tested for correlated evolutionary adaptations in the parasite in response to dispersal selection imposed on the host.

Previous work in this system has established that infection reduces host dispersal (Fellous et al. 2011), that virulence is related to the production of transmission stages (Restif and Kaltz, 2006) and both traits readily evolve in response to variation in demographic and ecological factors (Nidelet, Koella and Kaltz, 2009; Magalon et al. 2010). With our experimental setup, we allowed the parasite to evolve in response to dispersal selection on the host, and because parasite persistence in the front populations depended entirely on host dispersal, we predicted front parasites to evolve to minimise their impact on host dispersal, or to even increase dispersal of their infected hosts (Lion et al. 2006). Following Osnas et al. (2015), this could be achieved by reducing virulence or alternatively, shifting transmission strategies towards more vertical transmission. In contrast, with dispersal being selected against in core populations, core parasites were expected to be under selection primarily to maintain their capacity to transmit to new hosts.

Materials and methods

Study system

Paramecium caudatum is a filter-feeding freshwater protozoan ciliate, inhabiting still water bodies in the Northern Hemisphere (Wichterman, 1986). It has a germline micronucleus and a somatic macronucleus. Our cultures are maintained asexually on a lettuce medium with the food bacterium *Serratia marcescens* at 23 °C, allowing 1-2 population doublings per day (Nidelet and Kaltz, 2007). The gram negative alpha-proteobacterium, *Holospora undulata* infects the micronucleus of *P. caudatum*, and can be transmitted both horizontally (by s-shaped infectious forms, 15µm) upon host death (or during cell division), and vertically, when reproductive bacterial forms (5µm) segregate into daughter nuclei of a mitotically dividing host (Görtz and Dieckmann, 1980).

Infections arise via uptake of infectious forms which then escape the digestive vacuole and mediate their own transfer to the micronucleus. Within 24 hours, the invading infectious forms differentiate into reproductive forms and multiply inside the hosts micronucleus. Seven to 10 days later, a fraction of the reproductive forms differentiate back into infectious forms (Nidelet and Kaltz, 2007; Fels, Vignon and Kaltz, 2008). Infectious hosts (i.e., containing s-shaped transmission stages) can be easily identified under a contrast phase microscope (1000x magnification). Infection with *H. undulata* reduces host cell division and survival (Restif and Kaltz, 2006) and also host dispersal (Fellous et al. 2011).

Long-term experimental selection

In the long-term experiment, infected cultures experienced repeated episodes of directional selection for either high or low dispersal (see Fig. 1), as measured by the propensity of a host to swim from one microcosm to another via connection tubing. These opposing treatments mimic the selection experienced by a host at the front of an expanding population, and at the established core (see Fronhofer and Altermatt 2015).

Origin of host and parasite. The experiment was seeded from an uninfected *P. caudatum* strain ("63D") that had been under "core selection" (see below) for three years and showed characteristically low dispersal propensity (O.K., unpublished data). The 63D mass culture was infected with an inoculum of *H. undulata* prepared from stock cultures established from a single isolate of *H. undulata* brought into the lab in 2001. From the infected 63D mass culture, we established five experimental lines for each dispersal selection treatment (5 "core selection" + 5 "front selection" = 10 lines in total). All experimental lines were maintained in 50 mL falcon tubes in 20 mL lettuce medium at 23 °C, supplemented with *ad libitum* concentrations of the food bacterium *Serratia marcescens* (Kaltz et al. 2003).

Selection protocol. For each selection line, we performed weekly dispersal events in 2-patch dispersal arenas built from 14 mL plastic tubes, interconnected by 5-cm silicon tubing (inner diameter = 0.6 cm). First, we filled the dispersal arena with ~6 mL of lettuce medium to establish the connection between the two tubes, and blocked the connection with a plastic clamp. We then added the infected *Paramecium* cultures into one of the two interconnected tubes (tube one), and filled the second patch (tube two) with lettuce medium, with final volumes in both tubes topped up to 13 mL. We then removed the clamp, allowing free active dispersal of infected (and uninfected) individuals from tube one to tube two, for three hours. After the dispersal event, we blocked the connection with the clamp and determined population density in both tubes by counting the number of individuals in 200-1000 µL samples under a dissecting microscope. Each line was then cultured for a further week in 20 mL of bacterised lettuce medium, before the next dispersal and selection event occurred (Fig. 1).

We performed 55 dispersal and propagation cycles. For the first 30 cycles we adjusted the number of individuals placed in tube one (~2000 individuals), and propagated after dispersal for both treatments to approximately match them between dispersal treatments. Due to contamination of

selected cultures, we extracted infectious forms from each selection line (for protocol, see Magalon et al. 2010), and inoculated a new batch of naïve, 63D hosts, and continued the selection experiment for another 25 cycles. During those last 25 cycles, we ceased correcting for density at each propagation event to allow for more natural range expansion growth dynamics to occur. The transition between the two selection regimes is indicated by the dashed vertical line in Figure 2.

Measurements. During the long-term experiment, we took routine measurements of dispersal rates, calculated as the number of dispersing individuals in tube two divided by the total number of individuals in tube one and two. Population density was taken at the end of each one-week growth cycle, and from those samples we likewise determined infection prevalence in a population by staining 20-30 individuals with 1% lacto-aceto orcein (Fokin and Görtz, 2009) on a microscope slide and determined their infection status under phase-contrast (1000x), as well as the fraction of hosts that were carrying 'infectious' forms (i.e., horizontal transmission stages, see Nidelet et al. 2007).

Parasite adaptation assays

At the end of the experiment, parasites from core and front selection treatments were extracted (following Magalon et al. 2010) and assayed for their impact on host facilitated dispersal, life-history traits and the demographic performance of an infected host population, using naïve hosts. Any observed difference between the two selection treatments is thus indicative of an evolutionary response of the parasite to selection acting on host dispersal. To assess the generality of trait expression, we tested the evolved parasites on the 63D genotype (same genotype as evolved with, but an unselected naïve culture), but also on genotypes C023 and C173, which were both highly susceptible to *H. undulata* (Zilio et al. 2019, in prep.).

Each of the three host genotypes was confronted with freshly prepared inocula of each of the evolved parasite selection line (core and front) as well as with a 'mock inoculum' obtained by

crushing uninfected 63D cultures. We established a total of 33 inoculation replicates (2 selection treatments x 5 evolved parasite selection lines x 3 host genotypes + [1 mock x 3 host genotypes]), which were divided into three technical replicates on day 4, by splitting each infected culture into three new replicates of one mL. To these 99 assay replicates, 3 mL bacterised medium was added on day 4, and then again 10 mL on day 9 and 13. We aimed at maximum infection success (important for all further measurements), and used all extracted parasite inocula from each selection line for our experimental assay. All inoculation doses were comparable to (and higher than) previous experimental inocula doses used in this system. Preliminary analyses showed no effect of inocula dose on infectivity (d.f. = 7, $\chi^2 = 10.812$, $p = 0.147$, see Suppl. material for further discussion).

Host-facilitated dispersal

Between day 14 and 19 post inoculation, we used the assay replicate tubes to measure host-facilitated dispersal, as described above. For this assay, we added a third tube to the previously described dispersal setup, allowing *Paramecium* to disperse from the middle tube to the two outer tubes (thereby increasing the number of dispersers).

For better resolution of dispersal estimates, we concentrated the *Paramecium* populations prior to the assay, by gentle centrifugation at 3500 RPM for 15 minutes and removing the *Paramecium*-free supernatant. Dispersal arenas were filled with ~2800 individuals and free dispersal allowed for three hours. Taking 0.5 mL-samples from the central tube (resident) and a total of 3 mL from the outer tubes (pooled dispersal tubes), we estimated *Paramecium* densities and the proportion of infected individuals in dispersal and resident patches. From these estimates we calculated the dispersal rate of infected hosts. In total, 99 dispersal assays were conducted (90 infected populations and 9 uninfected mock cultures across the three host genotypes), with at least one replicate of each treatment combination tested per day. For statistical analysis, we excluded 16 replicates with very

low population density and/or infection prevalence (<10%), which prevented accurate estimation of dispersal of infected individuals.

Parasite life-history traits

Infectivity. Four days post inoculation, we assessed infection prevalence in the 33 inoculated cultures, as described above. This measurement describes infectivity, as defined as the capacity to successfully establish infections (Fels, Vignon and Kaltz, 2008).

Infection persistence and population density. From day 6 to 19 post inoculation, we tracked population density and infection prevalence in the assay replicate tubes, using a blocked sliding window (day 6-8, 11-13 and 14-19), with each selection line measured three times in regular intervals. These data reflect demographic and epidemiological processes occurring after infections have established and therefore provide indirect information on parasite virulence and infection persistence.

Horizontal investment. We also tracked the production of horizontal transmission propagules over time, and analysed investment into horizontal transmission between day 11-15 DPI. This time window represents the end of the first round of infections, before development of the next round of early transmission propagules arise.

Infection latency. From our measures of production of horizontal transmission propagules, we obtain a time series of within-host parasite development. From these observations we estimated the delay in the onset of horizontal transmission (latency). This was estimated by fitting kernel smoothing splines to each time series (via JMP version 14, SAS Institute Inc, Cary, NC) and extrapolating the timepoint (days post inoculation) at which 20% of the infected individuals in a population were producing infectious forms. Using 10 or 30% infectious forms threshold provided qualitatively similar results (Suppl. material, Fig. S.2 and Table S.1).

Population level impacts of infection

To compare parasite effects on host fitness, we isolated single infected individuals at five days post infection into replicate tubes and allowed them to multiply for a total of nine days under common-garden conditions in two mL plastic tubes containing bacterised lettuce medium. After verifying infection status (LAO fixation, as described above) of these monoclonal cultures, we started the virulence assay by placing single individuals in PCR tubes filled with 200 μ L of bacterised medium. We checked tubes daily for survival for 20 days. In addition, cell density was determined on day two and four (by counting cells through the plastic tubes), on day 10 (from 50 μ L samples) and on day 20 (total volume) where *Paramecium* were still alive. This assay was performed for 12 infected singletons from each parasite selection line, giving a total of 120 replicates. Using this data, we calculated the risk of extinction (proportion of populations alive at day 20), the maximum population density reached, as well as “growth potential” calculated from the area under the curve (AUC, using the trapezoidal rule) of cell density for each replicate. The growth potential was used as a demographic growth metric to convey information about how infection with each of the evolved parasites impact on both growth rate, carrying capacity, and death rate of infected hosts.

Statistical analysis

All statistical analyses were performed in R (ver. 3.3.3; R Development Core Team, available at www.r-project.org). To analyse variation in parasite traits, we used generalised linear mixed-effect models, with parasite selection treatment, host genotype, and their interaction as fixed effects, and in our random error structure, selection line and an interaction between selection line and host genotype (via a random intercept and random slope approach) was incorporated. Models with binomial error structure (logit link) were used for analyses of host-facilitated dispersal (proportion infected dispersers), infection persistence (proportion infected individuals at day 14-19), horizontal transmission investment (proportion infectious individuals at day 11-15 post infection) and risk of

extinction (proportion of populations alive after 20 days). Standard linear mixed-effect models were employed for maximum population size and growth potential (estimated as area under the curve as explained above).

From the initial 33 inocula, we then analysed infectivity, by using a generalised mixed model with host genotype, parasite selection treatment (and their interaction) as fixed effect, and included selection line as our random effect. To assess latency, we used a linear mixed effect with same fixed, and random effects as above. The significance of fixed effects was tested using analysis of variance (ANOVA Type III, car package: Fox & Weisberg, 2018). Lastly, we performed post-hoc tests on each host genotype independently to test for parasite selection treatment effects.

Results

Demographic and epidemiological variation during the long-term selection experiment

Routine measurements taken during the long-term experiment indicate evolutionary effects of the high and low dispersal selection treatments (front and core, respectively) on dispersal behaviour, demography and epidemiologically relevant traits. Over the first 30 cycles, and then again after the reset of parasites onto new naïve hosts (cycle 31-55), infected populations in the front selection treatment developed up to three times higher dispersal rates than core populations (46 out of 53 treatment cycle means; Fig. 2A). Front populations also reached on average 1.5x higher population densities than core populations (45 out of 53 means; Fig. 2B). To separate parasite from host responses to the applied dispersal selection treatments, the following assays tested evolved parasites on three genotypes of naïve hosts after 55 cycles of experimental selection for high (front) and low (core) dispersal.

Increased dispersal at the invasion front

Overall, dispersal rates of infected hosts were consistently lower than those observed in uninfected mock cultures (Fig. 3, and see Suppl. material, section B), consistent with the observation that

infection often reduces the dispersal capacity of a host (Fellous et al. 2011; Nørgaard, B. L. Phillips and Hall, 2019). However, hosts infected with front parasites tended to disperse more than those infected with the core parasites (Fig. 3), suggesting that the front parasite had evolved a mechanism which induced less negative impact on host dispersal, ultimately increasing its own dispersal. This trend was observed on all three host genotypes (average 7 to 20% higher dispersal of front parasites relative to core), although formal analysis was restricted to host genotypes 63D and C173, due to low infection prevalence and hence missing data of the core parasites on host C023.

This restricted analysis revealed a significant effect of parasite selection treatment (d.f. = 1, $\chi^2 = 5.756$, $p = 0.016$) and host genotype (d.f. = 1, $\chi^2 = 13.178$, $p > 0.001$), but no evidence of an interaction (d.f. = 1, $\chi^2 = 0.073$, $p = 0.787$). Thus, despite variation between pathogen genotypes, the front parasites always dispersed at a higher rate than core parasites. The observed patterns were robust to variation in demographic or epidemiological conditions, as neither population density nor infection prevalence had significant effects on dispersal rates when added to our statistical model ($p > 0.25$; details not shown).

Evolutionary shift in parasite life-history traits

Initial infectivity. Inoculation resulted in considerable levels of infection in all three host genotypes (Fig. 4A). At day 4 (first point at which infection can be quantified), we found no significant difference in infectivity between the parasites from front and core selection treatments (core parasite mean 0.556 ± 0.041 & front parasite mean 0.510 ± 0.028 SE; $df = 1$, $\chi^2 = 0.719$, $p = 0.371$), nor did we observe any evidence of differences in infectivity between host genotypes, nor any interaction (see Suppl. material, section C). We detected no differences in population density among the core and front parasites (d.f. = 1, $\chi^2 = 1.718$, $p = 0.199$), although we found a significant effect of host genotype on population density (d.f. = 2, $\chi^2 = 11.004$, $p = 0.003$), but no interaction effect (Fig. 4C).

Infection persistence and population density. During the second week of infection, differences in infection prevalence built up among host genotypes and parasite treatments (Fig. 4B). Due to low infection prevalence in assay replicates for host genotype C023, formal analysis of differences in infection persistence was restricted to host genotypes 63D and C173, but estimates of C023 has been included in figure 4 for visual identification of trends. The restricted analysis revealed a much higher infection prevalence of front evolved parasites on all host genotypes (32-53% on average), whereas the mean prevalence of core parasites more than halved (13-27%; main effect of selection treatment: $df = 1$, $\chi^2 = 18.833$, $p = <0.001$; see Suppl. material, section C). This analysis also revealed a significant effect of host genotype (d.f. = 1, $\chi^2 = 1.718$, $p = 0.199$), but no evidence of an interaction (d.f. = 2, $\chi^2 = 0.994$, $p = 0.318$), suggesting that the front parasites maintained higher infection prevalence relative to core parasites, across all host genotypes (Fig. 4B).

Interestingly, differences in population density likewise accumulated as infection progressed over time (Fig. 4D). Again, formal analysis was restricted to genotypes 63D and C173, and revealed a significant interaction effect between parasite selection treatment and host genotype (d.f. = 2, $\chi^2 = 8.588$, $p = 0.003$), suggesting that the responses in density varied between genotypes and selection treatments. Post-hoc test showed that front parasites maintained higher population density in both host genotypes (63D: d.f. = 1, $\chi^2 = 9.104$, $p = 0.003$ & C173: d.f. = 1, $\chi^2 = 35.784$, $p > 0.001$), but the differences between the treatment was greatest for host genotype C173.

Latency and investment into horizontal transmission. Front and core evolved parasites differed in the rate of conversion from the reproductive to the infectious state (Fig. 5A). On two out of the three host genotypes (63D, C023), infections with front parasites had a 15% later onset of production of horizontal transmission stages than those with core parasites (sign. effect of selection treatment, d.f. = 1, $\chi^2 = 5.843$, $p = 0.016$), but likewise differed between the host genotypes (d.f. = 2, $\chi^2 = 11.643$, $p = 0.003$), and we found no evidence of a significant interaction (see Suppl.

material, section D). Furthermore, the front parasites also invested less in horizontal transmission, as analysed as proportion of infected individuals carrying infectious forms at the final phase before the second round of infections (analysed between day 11-15, see Fig. 5B). However, formal analysis revealed a significant effect of the interaction term (d.f. = 21, $\chi^2 = 8.708$, $p = 0.013$), and post-hoc analysis indicated that the pattern of reduced investment in horizontal infection in front parasites, was only statistically significant in host genotype C173 (Fig. 5B, d.f. = 1, $\chi^2 = 6.933$, $p = 0.008$).

Population level impact of infection

Having established that front and core evolved parasites vary in their dispersal capacity and in their infection persistence and transmission strategies, we tested how infection with the two evolved parasites impacted on their host population, in terms of the risk of infection, maximum population size and population growth potential. This assay was performed from singletons that were allowed to divide over a period of 20 days. Overall, the singleton assay revealed patterns of differentiation between front and core evolved parasites in their effect on host fitness, measured as the risk of population extinction (Fig. 6A), maximum population size (Fig. 6B) and growth potential (Fig. 6C); but only when encountering the host genotype that they had coevolved with during the dispersal selection (63D).

Analysis of risk of extinction revealed a significant interaction effect (parasite selection x host genotype: d.f. = 2, $\chi^2 = 6.524$, $p = 0.038$), and subsequent analysis revealed that the observed significant effect of parasite selection treatment was only present in host genotype 63D (Fig. 6A, d.f. = 1, $\chi^2 = 8.808$, $p = 0.003$, see Suppl. material, section E). Similar patterns were also observed for maximum population size and growth potential, where the main model showed a significant interaction term (d.f. = 2, $\chi^2 = 16.843$, $p > 0.001$ and d.f. = 1, $\chi^2 = 24.221$, $p > 0.001$), and subsequent analyses again revealed that the increased population size (d.f. = 1, $\chi^2 = 29.089$, $p >$

0.001) and growth potential (d.f. = 1, $\chi^2 = 28.262$, $p > 0.001$) in the front parasite was only significant in in host genotype 63D.

Summarised, for host genotype 63D, we see that the front evolved parasite generally caused lower risk of extinction, maintained higher population densities (2-fold increase), and maintained a higher growth potential (Fig. 6). In contrast, for the other host genotypes, there was little difference between the two pathogen treatments in the metric of population growth and persistence. Instead, for genotype C173 and C023, both parasites induced high risk of extinction, reduced cell division and therefore lower maximum population density, ultimately suggesting that both genotypes are particularly vulnerable to infection with *H. undulata*.

Discussion

In agreement with empirical examples and suggested by emerging theory (Osnas, Hurtado and Dobson, 2015), we experimentally show that parasites evolve correlated changes in a series of life-history traits in response to dispersal selection imposed on the host. Parasites at the front evolved towards imposing less negative impact on host dispersal, ultimately optimizing their own dispersal. Adaptations facilitating higher dispersal were associated with changes in transmission strategy and reduced negative impact of infection on host population growth potential and survival. Such rapidly evolved “invasion syndromes” have been identified in natural disease systems such as in the spread of avian malaria in Europe (Pérez-Tris and Bensch, 2005), or the spread of lungworm in invasive cane toads in Australia, where lungworm at the invasion front exhibit distinct life-history traits (reduced age at maturity, larger infective and free-living larvae and larger eggs, see Kelehear, Brown and Shine, 2012). Our results confirm that pathogens arriving at the leading edge of an invasion are likely to be more benign and that the optimal balance between a pathogens transmission and exploitation strategies will depend on dispersal dynamics of the host.

Most infections reduce (Fellous et al. 2011; Nørgaard, B. L. Phillips and Hall, 2019; Nørgaard, Ben L. Phillips and Hall, 2019), or alter host dispersal in one way or another (Thomas et al. 2002; Hawley et al. 2013; Wesolowska and Wesolowski, 2014). However, with strong selection for hosts to disperse (such as at an invasion front), parasites are under selection to either meet these increased dispersal needs and keep up with the front line of the host population, or be lost from these population altogether. We show how such dispersal adaptations in a parasite is related to shift in transmission strategies; parasites at the invasion front tended to invest less in horizontal transmission (Fig. 5). The ability of parasites to shift between transmission strategies is not new. Shift in transmission strategy in response to host population growth rate (Magalon et al. 2010) or lifespan (Nidelet, Koella and Kaltz, 2009), has been previously established, and Berngruber et al. (2015), for example, also show how a latent, less virulent, predominantly vertically transmitted phage wins the competition against a virulent mutant in spatially structured epidemics, but when spatial structure is eroded, the latent phage goes extinct (see also modelling approach by Su, Chen and Yang, 2019). Our results show that changes in host mobility are another important, and likely widespread, driver of evolutionary change in pathogen transmission strategies.

In this system, horizontal transmission is associated with higher virulence and larger infections reduce cell division of infected hosts more than small infections. Horizontal transmission also decrease the efficacy of vertical transmission, creating a trade-off between the two transmission strategies (Kaltz et al. 2003; Restif and Kaltz, 2006). We predicted that the core parasite should be selected mainly by their capacity to transmit, but, opposite to our predictions (Kamo and Boots, 2006; Kamo, Sasaki and Boots, 2007), the core parasite caused high reductions in host growth potential, transmitted mostly horizontally and imposed a high risk of population extinction, which are all traits associated with high parasite virulence (Day and Proulx, 2004). The front parasite, on the other hand, was indeed selected for its ability to reduce host dispersal the least, and evolved correlated shift in infection strategies; this parasite allowed for high growth of its host population by

investing more in vertical transmission (and started production of horizontal transmission stages later), and imposed reduced risk of extinction, which are all indicators of reduced virulence.

Overall, our data shows that parasites at the invasion front is selected for traits that cause reduced virulence. This finding is contrary to previous findings of increased virulence at the front line, such as the virulent rabbit haemorrhagic disease virus (Moss et al. 2002; Boots, Hudson and Sasaki, 2004). Rather, in our study, front parasites were less virulent and caused less reductions in host dispersal, supporting to the hypothesis that a trade-off between host-facilitated dispersal and virulence may exist (Osnas et al. 2015). Particularly, we show how such trade-off is associated with changes in parasite transmission strategy, where front parasites invested less in horizontal transmission. Importantly, since vertically transmitted parasites may have a large dispersal advantage, the evolutionary pressure for vertical transmission at the invasion front might have been strengthened over time (see also Su, Chen and Yang, 2019).

While the evolved responses in dispersal and transmission strategy appeared to be general, and expressed by both parasites when infecting all three host genotypes, responses in the impact of infection on host population dynamics appeared to be genotype specific, and only present in the host genotype that the parasites were initially evolved with (63D). Visualization of the multivariate response of all measured traits (Fig. 7), highlights that core and front parasites evolve predominately along an axis that contrast dispersal with investment in horizontal transfer, but for host genotype 63D there is a much clearer separation due to changes in the risk of extinction and population growth potential. This suggest that while corelated shifts in impact of infection and changes in transmission strategies might be universal, the trade-offs that manifests in terms of population level processes and growth, are specific to the host that a pathogen is most likely to encounter.

In summary, our findings suggest that during periods of no, or limited host spatial movement, evolution may select for increase parasite virulence, while during periods with high dispersal, evolution should favour reduced virulence at the invasion front. We show how host dispersal gives rise to changes in exploitation strategies, and such shift may be driven by the existence of a trade-off between host-facilitated dispersal and virulence. While the exact correlation and trade-off between dispersal and parasite life-history traits can be system-specific, our results reiterate how shifts between horizontal and vertical transmission strategies allow a pathogen to optimize transmission in response to dispersal dynamics of its host population. Our work highlight how invasion and range expansion processes can alter parasite virulence and infection strategies, and such evolutionary changes is important to account for in future predictions of disease outbreak in the wild.

Acknowledgements

This work was supported by the 2019 Gottfrey Hewitt mobility award granted to LN.

Chapter 5 - Figures & Tables

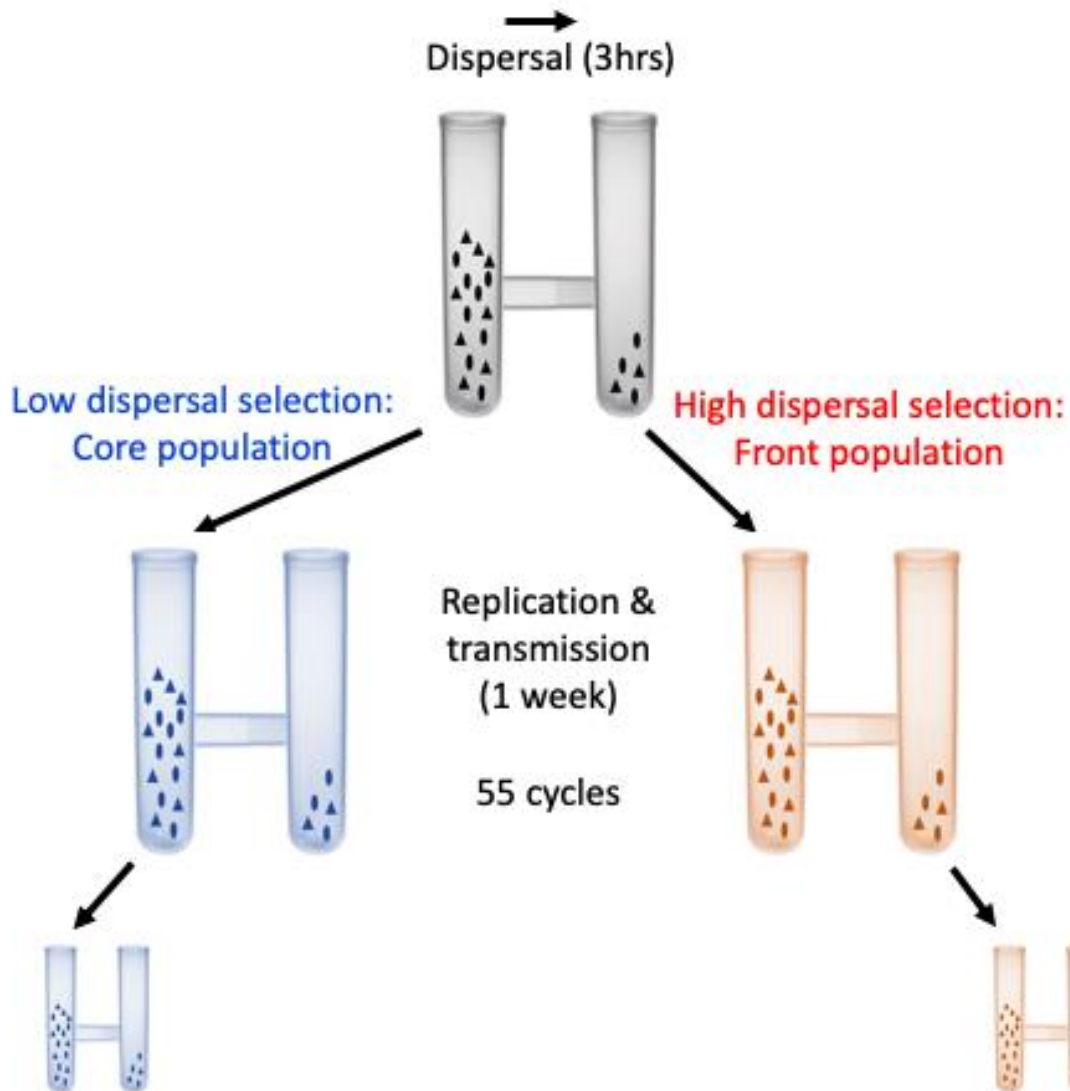


Figure 1. Experimental evolution setup. We selected for high (red) and low (blue) dispersal by weekly allowing for active dispersal of coevolving host and parasites in two-patch microcosms during a three-hour period. At each cycle, dispersing (infected and uninfected) individuals were transferred to a new tube, representing the high selection treatment, whereas residing individuals is transferred to another tube representing the low dispersal selection treatment. This procedure was repeated for 55 cycles after which we isolated the evolved parasites to test for evolutionary adaptations in response to high and low host-facilitated dispersal.

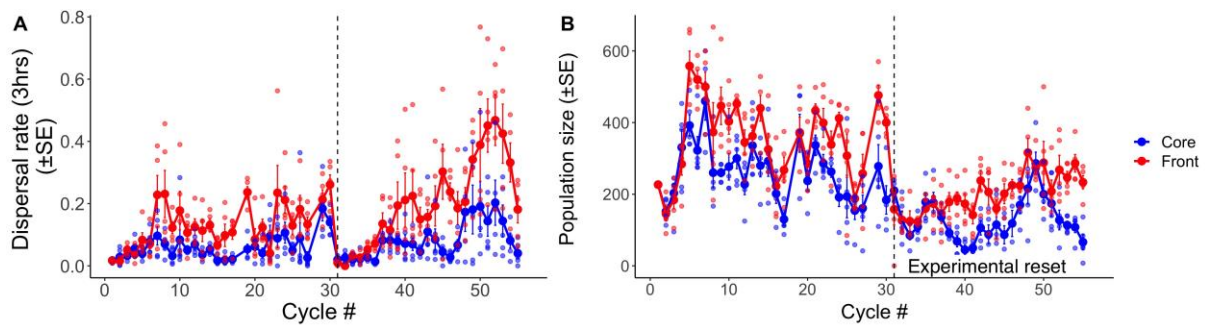


Figure 2. Long-term experimental selection data for A) dispersal rate and B) population size. Red dots represent populations (host and parasite) selected for high dispersal (front population), and blue represent populations selected for low dispersal (core population). Filled large dots and connecting lines are mean values across selection lines (\pm SE), and dull small points represent raw data from individual selection lines at each dispersal cycle. Black dashed line indicates the experimental reset at cycle 31 due to contamination.

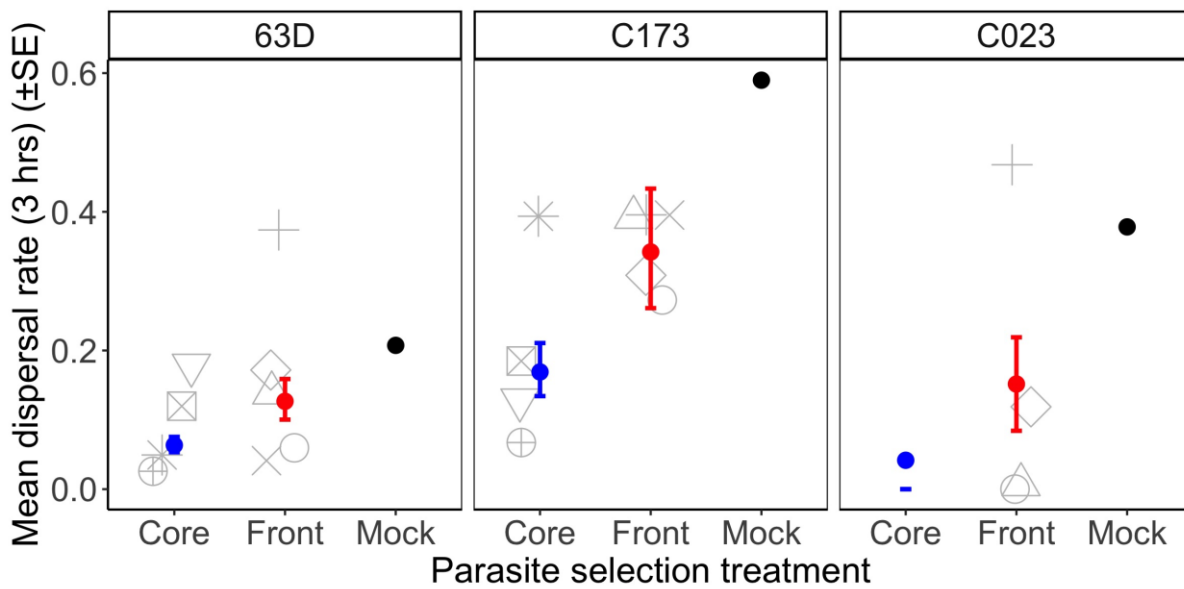


Figure 3. Mean dispersal rate (3 hr) of naïve unselected *Paramecia* infected with evolved core (blue) or front (red) parasites and the reference uninfected mock culture (black). Shown are fitted means for front and core parasites (\pm SE) from a generalised mixed-effect model for host genotypes 63D and C173. Grey differentially shaped points represent raw data for individual selection line means and panels represent the three naïve host genotypes. Due to low infection prevalence in host C023, this genotype has not been included in the model, and raw data means (\pm SE) is included only for visualization of dispersal trends.

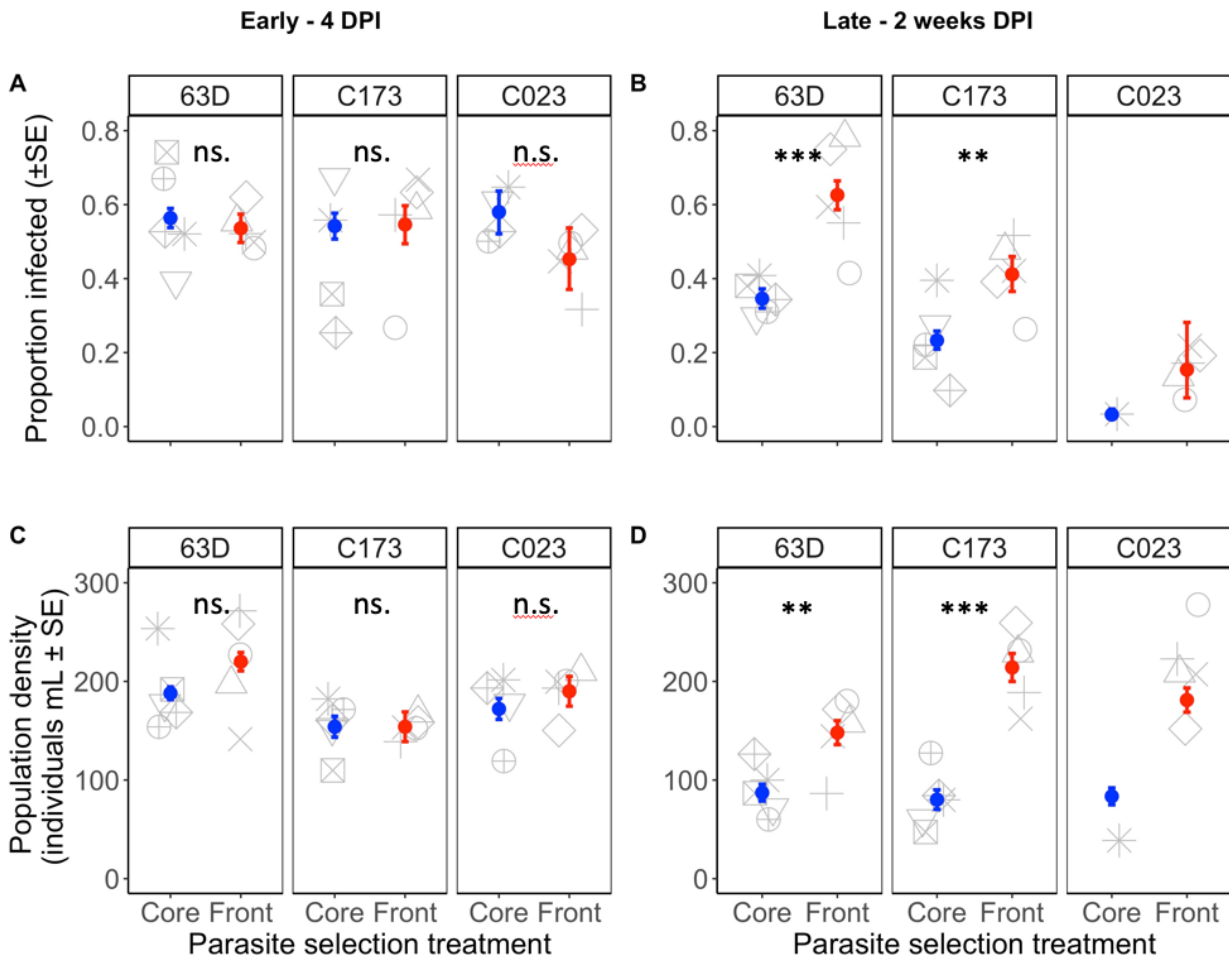


Figure 4. A, B) proportion of infected individuals in populations inoculated with evolved core (blue) or front (red) parasites and, C, D) population density (individuals mL⁻¹). Left panels (A, C) are early measures on day four post infection and right panels (B, D) are late measurements, two weeks post infection. Coloured dots are fitted means (±SE) using a generalised mixed effect model. Grey differentially shaped points represent individual selection line means and panels are different host genotypes. Due to low infection prevalence in host C023 in the measurement of population density and infection prevalence after two weeks of infection, this genotype has not been included in the models, and raw data means (±SE) is included only for visualization of infection and density trends. Post-hoc tests for difference between core and front in the analysed host genotype are indicated at the top of each panel. (ns. > 0.1, . p > 0.05, * p < 0.05, ** p < 0.01, *** p < 0.001).

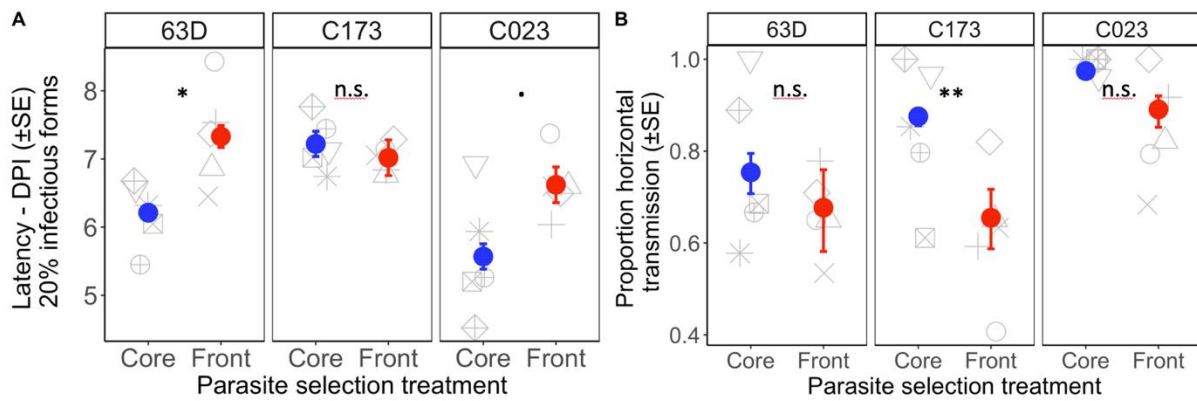


Figure 5. A) Investment into horizontal transmission, and B) latency defined as time (DPI) until 20% of infected hosts in a population has switched to producing horizontal transmission spores, for core (blue) and front (red) parasites. Coloured bars are predicted mean (\pm SE) and grey differentially shaped dots represent raw data for each individual selection line and panels are the different host genotypes. Post-hoc tests for difference between core and front in each host genotype are indicated at the top of each panel. (ns. > 0.1 , . $p > 0.05$, * $p < 0.05$, ** $p < 0.01$, *** $p < 0.001$).

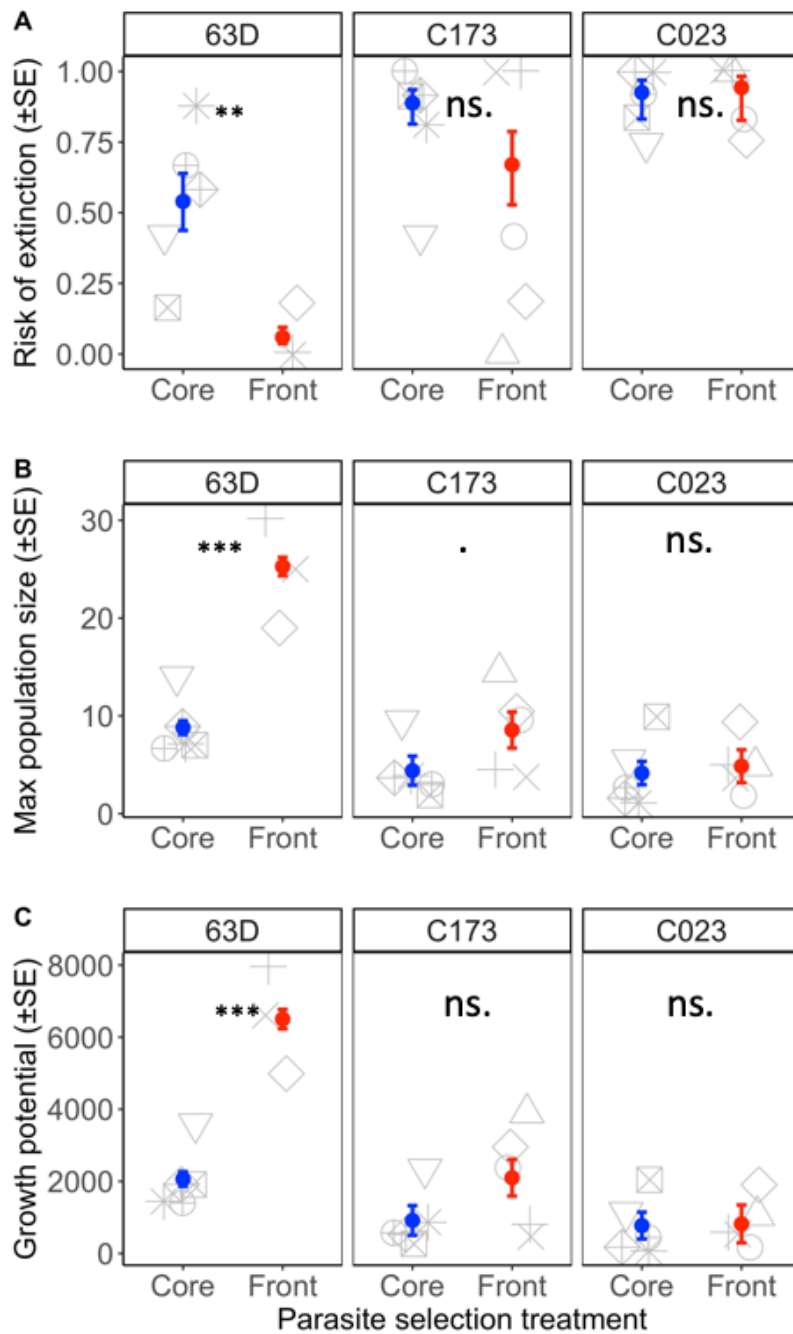


Figure 6. Population level impact of infection depicted as A) risk of extinction, B) maximum population size, and C) growth potential. Coloured dots are fitted means (\pm SE) using a generalised mixed effect model. Grey differentially shaped points represent individual selection line means and panels are different host genotypes. Post-hoc tests for difference between core and front in each host genotype are indicated at the top of each panel. (ns. > 0.1 , . $p > 0.05$, * $p < 0.05$, ** $p < 0.01$, *** $p < 0.001$).

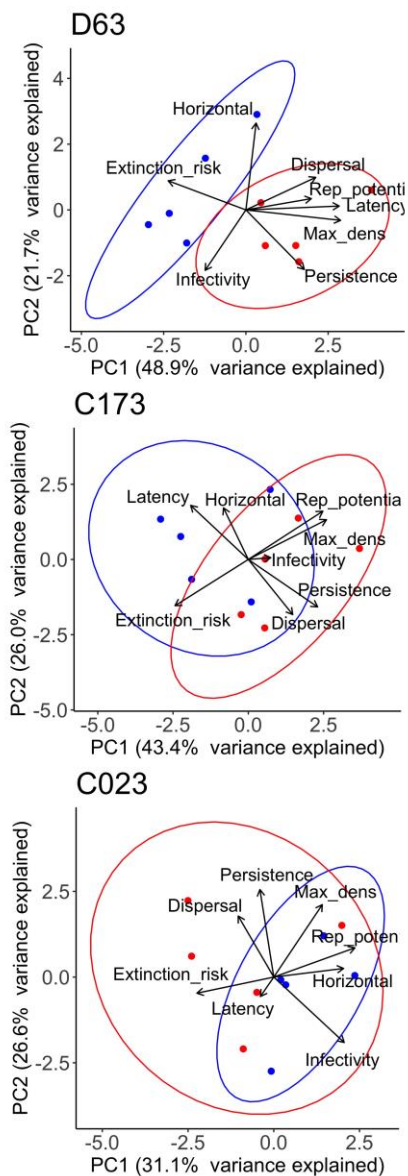


Figure 7. The multivariate responses of parasite traits to selection for high (front, red) and low (core, blue) dispersal. Each panel represent a principal component analysis for core and front parasite inoculated on different host genotypes (63D, C173 and C023). Loadings of each parasite trait (dispersal rate, infectivity, infection persistence, horizontal transmission, latency, maximum density, reproductive potential and risk of extinction) to the relevant multivariate axes are indicated by the direction and angle of each traits vector (arrows and associated labels). Ellipsoids indicate parasite selection treatment clustering based on a multivariate t-distribution and 90% confidence level.

Chapter 5 - Supplementary material

Section A: Inoculation procedure and test of inoculum size on infectious outcome

Unselected, naïve host populations of three genotypes: 63D, C023 and C173 were infected with the evolved parasites, selected for high or low dispersal (front and core, respectively). Parasite spores from front and core treatments were harvested by centrifugation for 20 minutes at 35000 rpm. We removed the supernatant and crushed the remaining culture using a Qiagen tissue lyser (1.45 minutes at 30 oscillation frequency).

The number of infectious forms obtained from individual selection lines varied up to one order of magnitude. Below a threshold of ~10-20 infective forms per μL , there is no evidence of dose dependency in this system, and our inoculation doses were all higher than previously applied infection doses in this system. Our inocula doses ranged from ~35 to ~1000 infective spores per μL and we would therefore expect maximum infection success for all selection lines. Preliminary logistic regression with binomial error structure (logit link) was used to screen for inocula dose effects on infection success, but revealed no significant effect (d.f. = 7, $\chi^2 = 10.812$, $p = 0.147$). Thus, we found no evidence for correcting infection success for inocula dose in this system, indicating that all inoculations had reached maximum infection capacity at the applied dose. Lastly, infections are usually confounded by one to three infectious forms that are up taken by filter feeding, and infection occur within 24 hrs post inoculation.

Section B: The influence of infection on dispersal behaviour

Table S.1. Mean dispersal rate \pm SE for infected individuals from each parasite selection treatment (core & front) and unexposed mock cultures, for each of the three host genotypes.

| Host genotype | Treatment | Dispersal rate \pm SE |
|----------------------|------------------|---|
| 63D | Core | 0.09 \pm 0.03 |
| | Front | 0.16 \pm 0.04 |
| | Mock | 0.21 \pm 0.17 |
| C173 | Core | 0.19 \pm 0.04 |
| | Front | 0.35 \pm 0.04 |
| | Mock | 0.59 \pm 0.09 |
| C023 | Core | 0.02 \pm 0.02 |
| | Front | 0.15 \pm 0.07 |
| | Mock | 0.38 \pm 0.11 |

Table S.2. ANOVA output from the generalised mixed effect models predicting for dispersal rate of infected individuals (host genotype 63C and C173 only) using host genotype (Hg) and parasite selection treatment (trt) (and their interaction) as fixed effects and the random error structure included selection line and an interaction between selection line and host genotype (via a random intercept and random slope approach).

| Trait | D.f. | χ^2 | p-value | Prob. sign. |
|------------------------------------|-------------|----------------------------|----------------|--------------------|
| Dispersal rate (excl. C023) | | | | |
| Selection treatment | 1 | 5.756 | 0.016 | * |
| Host genotype | 1 | 13.178 | > 0.001 | *** |
| Hg x trt | 1 | 0.073 | 0.787 | |

Section C: Infection prevalence and persistence

From day 6 to 19 post inoculation, we track infection prevalence in the assay replicate tubes, using a blocked sliding window (day 6-8, 11-13 and 14-19), with each treatment measured three times in regular intervals (three measurements per selection line).

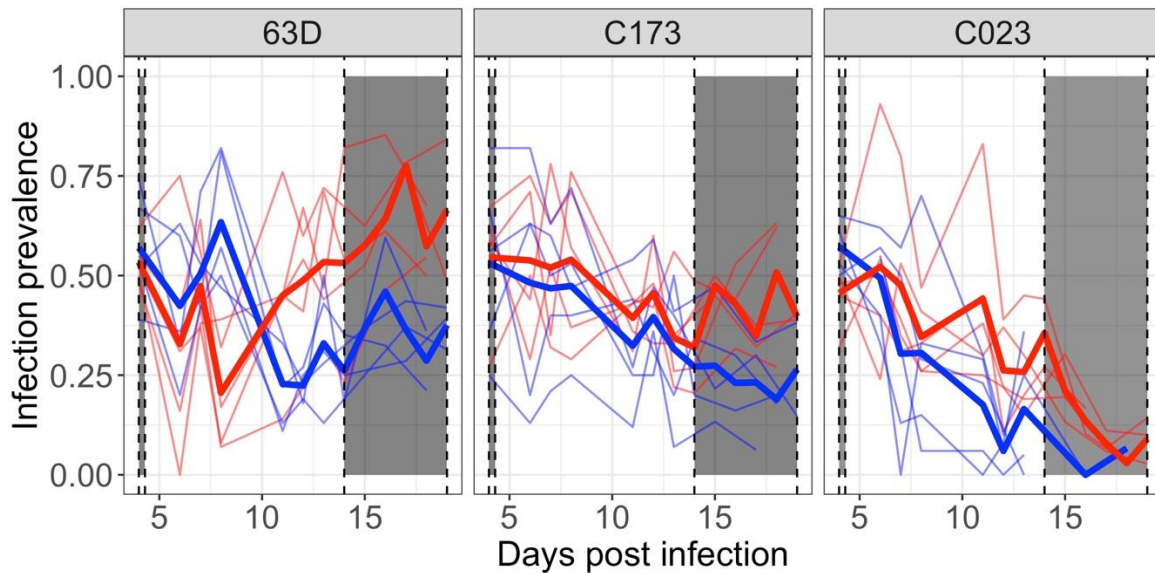


Figure S.1. Timeseries (in days post infection) of infection prevalence for core (blue) and front (red) parasites. Thin lines are mean values for replicates of each selection line and thick lines are mean for each treatment. In grey is the time interval at which we assessed infectiousness (day 4) and infection persistence (day 14-19).

Table S.3. ANOVA output from the generalised mixed effect model using host genotype (Hg), parasite selection treatment (trt) and their interaction as fixed effects and the random error structure included selection line and an interaction between selection line and host genotype (via a random intercept and random slope approach). Shown are results of a) infectiousness at day 4, b) infection persistence (model excluding host genotype C023), c) early population density at day 4, and d) late population density.

| Trait | D.f. | χ^2 | p-value | Prob. sign. |
|--|-------------|----------|----------------|--------------------|
| a) Infectiousness | | | | |
| Selection treatment | 1 | 0.719 | 0.371 | |
| Host genotype | 2 | 0.357 | 0.836 | |
| Hg x trt | 2 | 1.055 | 0.59 | |
| b) Infection persistence (excl. C023) | | | | |
| Selection treatment | 1 | 18.833 | >0.001 | *** |
| Host genotype | 1 | 20.709 | >0.001 | *** |
| Hg x trt | 1 | 0.994 | 0.318 | |
| c) Early population density | | | | |
| Selection treatment | 1 | 1.718 | 0.199 | |
| Host genotype | 2 | 11.004 | 0.003 | ** |
| Hg x trt | 2 | 1.127 | 0.569 | |
| d) Late population density | | | | |
| Selection treatment | 1 | 28.904 | >0.001 | *** |
| Host genotype | 1 | 5.992 | 0.014 | * |
| Hg x trt | 2 | 8.588 | 0.003 | ** |

Section D: Latency and investment into horizontal transmission

To determine latency, we identified the point at which 20% of the infected individuals in a population carried horizontally transmitted, infectious forms. To test the robustness of this measure, we likewise included models of the time at which 10% and 30% infectious forms were reached.

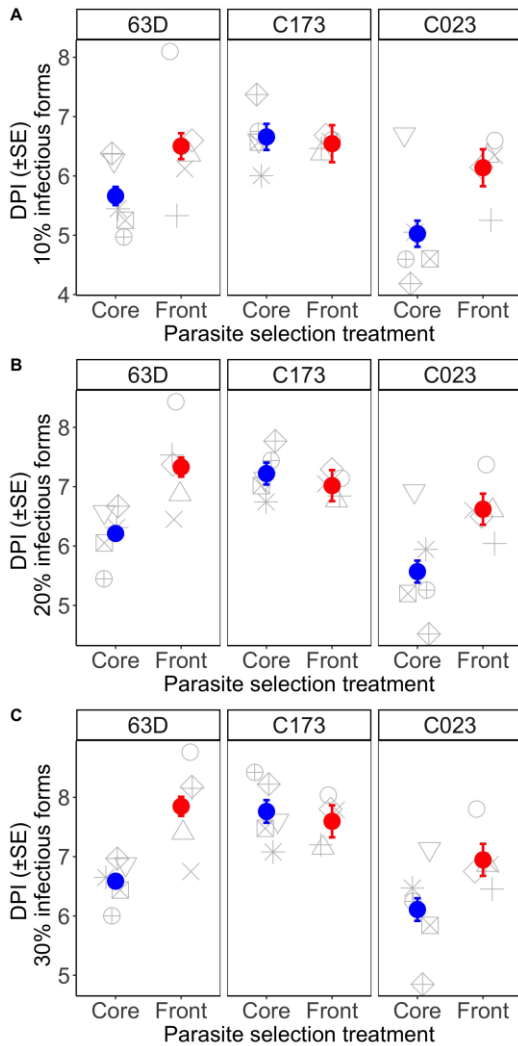


Figure S.2. Time (days post infection) until A) 10%, B) 20% and C) 30% of infected individuals in a population were carrying infectious forms. Blue dots represent fitted means (\pm SE) for core (blue) and front (red) parasites. Grey differentially shaped points are raw data for each selection line, and each panel represent different host genotypes.

Table S.4. ANOVA results from models using the timepoint at which 10, 20 and 30% of infected individuals in a population carries infectious forms. In all models we used parasite selection treatment (Gp), host genotype (Gh) and their interaction as fixed effects and selection line as our random effect.

| 10% infectious forms | D.f. | χ^2 | p-value | Prob. sign. |
|-----------------------------|-------------|----------------------------|----------------|--------------------|
| Parasite selection (Gp) | 1 | 3.956 | 0.047 | * |
| Host genotype (Gh) | 2 | 13.926 | <0.001 | *** |
| Gp * Gh | 2 | 5.558 | 0.062 | . |
| 20% infectious forms | | | | |
| Parasite selection (Gp) | 1 | 8.228 | 0.004 | ** |
| Host genotype (Gh) | 2 | 17.057 | <0.001 | *** |
| Gp * Gh | 2 | 8.708 | 0.013 | * |
| 30% infectious forms | | | | |
| Parasite selection (Gp) | 1 | 7.985 | 0.005 | ** |
| Host genotype (Gh) | 2 | 19.093 | <0.001 | *** |
| Gp * Gh | 2 | 7.638 | 0.022 | * |

Table S.5. ANOVA results from the generalised mixed effect model using host genotype (Hg), parasite selection treatment (trt) and their interaction as fixed effects and the random error structure included selection line and an interaction between selection line and host genotype (via a random intercept and random slope approach). Shown are results from analysis of horizontal transmission and latency.

| Trait | D.f. | χ^2 | p-value | Prob. sign. |
|--------------------------------|-------------|----------------------------|----------------|--------------------|
| Horizontal transmission | | | | |
| Selection treatment | 1 | 5.843 | 0.016 | * |
| Host genotype | 2 | 11.643 | 0.003 | ** |
| Hg x trt | 2 | 3.206 | 0.201 | |
| Latency | | | | |
| Selection treatment | 1 | 8.218 | 0.004 | ** |
| Host genotype | 2 | 17.157 | >0.001 | *** |
| Hg x trt | 2 | 8.708 | 0.013 | * |

Section E: Population level impact of infection

Table S.6. ANOVA output from the generalised mixed effect model using host genotype (Hg), parasite selection treatment (trt) and their interaction as fixed effects and the random error structure included selection line and an interaction between selection line and host genotype (via a random intercept and random slope approach). Shown are results from analysis of the risk of extinction, maximum population size and growth potential.

| Trait | D.f. | χ^2 | p-value | Prob. sign. |
|--------------------------------|-------------|----------------------------|----------------|--------------------|
| Risk of extinction | | | | |
| Selection treatment | 1 | 8.051 | 0.005 | . |
| Host genotype | 2 | 19.861 | >0.001 | *** |
| Hg x trt | 2 | 6.524 | 0.038 | * |
| Maximum population size | | | | |
| Selection treatment | 1 | 17.341 | >0.001 | *** |
| Host genotype | 2 | 36.831 | >0.001 | *** |
| Hg x trt | 2 | 16.843 | >0.001 | *** |
| Growth potential | | | | |
| Selection treatment | 1 | 1.058 | 0.304 | |
| Host genotype | 2 | 42.213 | >0.001 | *** |
| Hg x trt | 2 | 24.221 | >0.001 | *** |

Table S.7. ANOVA output from post-hoc models revealing the effect of parasite selection treatment on the risk of extinction, maximum population size and growth potential for each of the three host genotypes.

| Risk of extinction | D.f. | χ^2 | p-value | Prob. sign. |
|--------------------------------|-------------|----------------------------|----------------|--------------------|
| 63D | 1 | 8.808 | 0.003 | ** |
| C173 | 1 | 0.968 | 0.325 | |
| D023 | 1 | 0.134 | 0.714 | |
| Maximum population size | | | | |
| 63D | 1 | 29.089 | > 0.001 | *** |
| C173 | 1 | 2.538 | 0.111 | |
| D023 | 1 | 0.008 | 0.929 | |
| Growth potential | | | | |
| 63D | 1 | 28.262 | > 0.001 | *** |
| C173 | 1 | 3.034 | 0.0816 | |
| D023 | 1 | 0.111 | 0.741 | |

Risk of extinction

In addition to the above analysis on the risk extinction, we likewise performed a cox proportional hazards analysis, analysing the risk of population extinction of singleton populations over the duration of the assay.

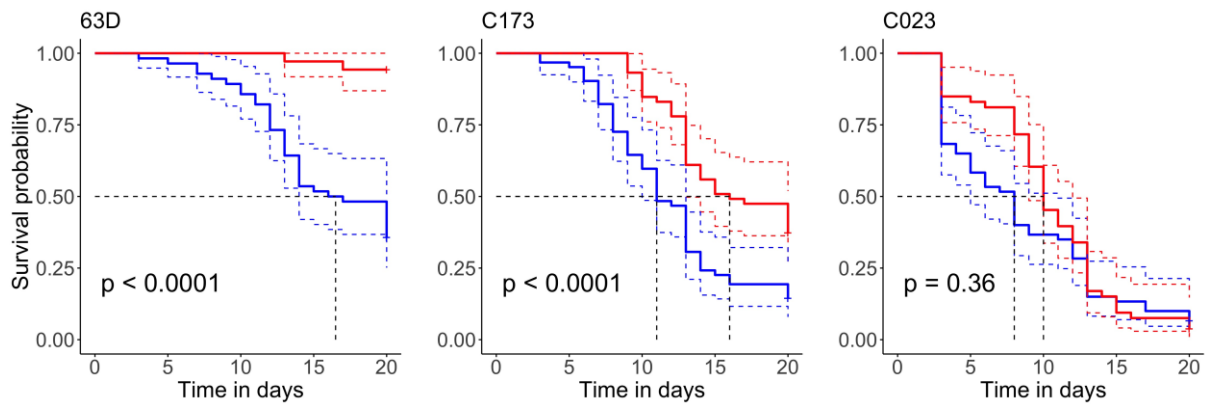


Figure S.3. Cox-proportional hazards model of the probability of survival (i.e., risk of extinction) for populations infected with front (red) and core (blue) parasites, in each of the three naive host genotypes (63D, C173 and C023). Dashed coloured lines represent 95% confidence intervals and black dashed line represent the time at which 50% of populations had gone extinct for each of the two parasite selection treatments.

Chapter 6: General discussion

In this thesis, I explored a variety of ways in which the demographic conditions met in invasive, range expanding, or colonizing host populations may influence the evolution, spread and severity of infectious disease. My work has highlighted that spatiotemporal variation and patch colonization processes may select for different pathogen invasion strategies, and a pathogen is generally faced with an important trade-off between host facilitated dispersal and its ability to proliferate within a host, and maximise transmission. Furthermore, I show how variation in patch quality and energy availability impacts on pathogen fitness, and that both hosts and its pathogens benefit from the increased energy available in low density populations. Another consistent finding throughout my thesis, is that spatial variation and range expansion processes may give rise to multiple layers of patch quality for a pathogen; hosts at the invasion front allow for optimization of within-host proliferation, whereas hosts in the established core provide less energy available for exploitation, but such high density populations facilitates better conditions for between-host secondary transmission.

The stepwise invasion process and the potential for diversifying selection

In my first experimental chapter, I centre on how dynamics in colonizing host populations may give rise to diversifying selection to act on a pathogen species. My data suggested that complex (rather than simple colonizer-competitor) relationships exist between within-population performance and dispersal, and indicated that for a pathogen to become successful, it must balance the trade-off between host-facilitated dispersal and transmission, as previously suggested by Osnas et al. (2015). I empirically showed that pathogens best at invading long-established host populations were generally poor dispersers, whereas pathogens that performed well in recently established, low density host populations also generally expressed high dispersal abilities. Thus, as a result of an ongoing host range expansion or metapopulation colonization, pathogens are likely to encounter

host populations with various demographic background, and pathogens will naturally be selected for different colonization and dispersal abilities with respect to the host population encountered. My results suggest that host population dynamics may be an important factor in the maintenance of pathogen genetic diversity and in the manifestation of different pathogen invasion- and colonization strategies across space and time.

In the literature, we find examples of how population demography can shape, for example, pathogen invasion thresholds (Dallas, Krkošek and Drake, 2018), or how foraging interference in some systems limits transmission when a pathogen encounter high host densities (Civitello et al. 2013). Yet another body of literature show how resource rich patches both attract and support greater host and pathogen densities, facilitating a constant supply of infected carriers across a landscape (e.g., Leach et al. 2016; Becker et al. 2018). This chapter stands out by linking the demographic or colonization history of a host population to the specific steps or challenges that any pathogen might face when invading a host population. By independently testing the performance of different pathogen genotypes in their invasion characteristics at the same time, my results reveal how diversifying selection may operate within a single pathogen species across a gradient of host colonization phases.

How energy scope and host life-history determine pathogen fitness

In chapter 3, I explored how organisms at various population densities differ in the rate at which they consume, transform and expend energy, and how energetic scaling in a host impact on pathogen fitness. I confirmed that hosts in low density maintained higher amount of discretionary energy, predominantly driven by an energetic advantage in terms of feeding, at low density. The next question was then how such differences in discretionary energy translates into pathogen fitness. I showed that increased discretionary energy translated into higher pathogen fitness, but that density-mediated increases in host body size explained a huge proportion of the fitness advantage

achieved by a pathogen in low density populations. As such, this finding highlights the evolutionary importance of density-mediated changes in life-history traits of a given host, and how energy and life-history jointly impact on pathogen fitness.

This piece of research builds on recent studies that explore how rates of energy intake and expenditure can vary with population density (Ghedini, White and Marshall, 2017), and I show that such universal link to how energy scope determine individual growth across population densities, applies both to the growth of hosts, as well as their pathogens. Taken together, these observations provide a mechanistic understanding of why conditions met in low density populations, such as in a recently colonized host population, or at the invasion front, often favour the production of infectious propagules (see Kelehear, Brown and Shine, 2012). On the other hand, low density conditions provide fewer opportunities for secondary transmission, where selection might favour parasite traits that enable longer environmental persistence (see also Fenton and Hudson, 2002) . Therefore, it appears that tension between the conditions that allow for optimization of within-host transmission, versus the conditions that optimize between-host transmission, gives rise to multiple layers of patch quality for a pathogen. On a spatial scale, however, whether the energetic advantage attained at the front of a range expanding host population will promote epidemic spread, depends on a series of other ecological and evolutionary factors, such as the ability of a pathogen to spread to new locations, as well as resources available in a given environment (as discussed above, but see Hess, 1996; Becker et al. 2018).

Sexual dimorphism as a lever for life-history optimization

Building from theory and my findings in chapter 2, it is likely that a pathogen faces a trade-off between the capacity to spread through a landscape via host-facilitated dispersal, and the ability to exploit host resources to optimize transmission. In the previous chapters, I have considered heterogeneities in a host population that arise as a consequence of changes in population density,

resource competition and growth rates. Sexual dimorphism, however, represents another important source of heterogeneity in many natural populations. How phenotypic and genetic differences between the two sexes impact on infectious disease outcomes, has been explored in a variety of ways (reviewed in Gipson and Hall, 2016). However, little attention had been allocated to exploring the idea that a pathogen might be able to mitigate any dispersal-colonization, or dispersal-transmission trade-off, by taking advantage of sexual dimorphism in the host population. Previous work has linked the spatial spread of pathogens to the male sex (Streicker et al. 2016), but had never explored whether transmission opportunities in such scenarios are then optimized in the opposite sex. By infecting male and female *Daphnia*, I showed how *P. ramosa* can optimize both within-host transmission and between-host dispersal by differentially infecting the two sexes.

These results suggest that the sexes might offer a mixed dispersal strategy, and a form of bet hedging for the pathogen (Fellous and Koella, 2009; Soghigian and Livdahl, 2017). Although whether this prediction holds in other systems, will be sensitive to the direction and strength of sexual dimorphism, as well as the relative density of the two sexes in a population. Given the large diversity of sexually dimorphic host populations in nature, however, it is likely, that the ability of a pathogen to tailor the infection strategy separately to males and females, could be widespread, and have important implications for disease dynamics in sexually dimorphic host population.

Dispersal and correlated changes in parasite life-history

By imposing directional selection on host dispersal, I show that pathogens at the invasion front evolve towards causing less negative impact on host dispersal, and that such adaptation came with correlated evolutionary changes in infection strategy. These findings provide support for the hypothesis that a trade-off between dispersal and transmission may exist (Osnas, Hurtado and Dobson, 2015). My results suggest that a pathogen responds to increased dispersal needs by increasing its investment in vertical (less virulent) transmission, and by causing less negative impact

on its host populations cell division and survival. Indeed, this work confirms the hypothesis that a pathogen might benefit from optimizing dispersal rate of its infected carrier (Kamo and Boots, 2006; Lion, Van Baalen and Wilson, 2006; Altizer, Bartel and Han, 2011), and that such evolutionary change in dispersal patterns comes at a cost of altered virulence and transmission strategies.

Previous research has explored the potential for pathogen evolution in response to local versus global interactions (Boots and Sasaki, 1999; Boots et al. 2009), or over short evolutionary time scales during an ongoing epidemic (see Griette et al. 2015; Osnas et al. 2015). Importantly, however, my study stands out from existing literature, in that I show how dispersal selection imposed on the host population itself causes correlated shifts in pathogen life-history traits. Furthermore, no other experimental studies (to the best of my knowledge) has explored the evolution of pathogens that spread with their host, creating a scenario of both host and parasite range expansion. It is my hope, however, that future studies will follow up on these findings, and test the spatial spread and competitive abilities of such evolved core and front parasites in a spatially organised common garden setup. By doing so, it would be possible to unravel whether the observed evolutionary changes in dispersal and transmission strategy actually translates into the predicted spatial diversification; the front parasite should keep up with the front of an expanding host population, whereas the core parasite should outcompete front parasites that fail to disperse. Taken together, this chapter provides new insight into how dispersal and associated population dynamics may drive evolutionary shift in pathogen infection strategy and thus in the virulence of an invading pathogen. These findings have large implications for disease predictions on a spatial scale (see Parratt, Numminen and Laine, 2016). Thus, if the spatial spread of a pathogen is restricted to host facilitated dispersal, we may expect evolution to favour different pathogen dispersal and virulence strategies across a landscape, and such evolutionary trajectories will be determined by the demographic and environmental conditions encountered.

Conclusions

My thesis emphasizes the pivotal importance of incorporating information about host population dynamics into predictions of the evolution of infectious disease on a spatial scale. In the wild, pathogens are always encountering host populations that vary in their time since colonization, in their patch to patch connectivity and in the dispersal opportunities. Overall, I show that pathogens may vary greatly in their ability to invade, reproduce, cause secondary infection, and spread to new locations, ultimately causing diversification between the pathogen genotypes that are likely to persist at the invasion front, versus the pathogen genotypes that is likely to persist in an established core population.

A reoccurring theme throughout my work is the importance of host dispersal and the ability of a pathogen to evolve in response to dynamics encountered in the host population. In particular, conditions in spatiotemporally dynamic host populations that favour within-host proliferation are unlikely to also favour between-host secondary transmission. This tension might cause changes in the selective pressures experienced by a pathogen as it spreads through a landscape of host populations at various stages of colonization or along an invasion gradient.

Future directions

The recognition that evolutionary adaptations in a pathogen occur at an ecologically relevant scale certainly highlights the need for understanding the evolutionary dynamics of infectious disease on a spatial scale. My work demonstrates that a greater focus on the impact of host population dynamics, will lead to new insights into disease evolution and epidemic spread across a landscape. It is my hope that this research, and the recent work by other researchers in this field, will inspire a greater appreciation of how host population dynamics can fundamentally change the current disease predictions.

There are still a multitude of ecological and evolutionary questions to raise within the fields of ecology, epidemiology and invasion biology. Emerging evidence, for example, demonstrate the potential for differential immune investment in host individuals across an invasion gradient, which represents an important avenue of research to incorporate into evolutionary epidemiology. It would be interesting to test whether the energetic advantage achieved in low density, applies to other species (including vertebrates), and whether such differences in energy scope contributes to differences in energy allocation into life-history traits, including immune investment. Furthermore, experimental studies are needed to test whether the presence of infectious disease will increase, or even hinder the rate of host population expansion or invasion (Dunn and Hatcher, 2015; Flory, et al. 2017). Thus, developing a better understanding of the dual-directional host-pathogen interactions on a spatial scale, could improve the reliability of future predictions of the evolution of infectious disease in dynamic host population, as well as the impact of infectious disease on host invasion processes (Flory et al. 2017) and population stability (Frickel, Sieber and Becks, 2016).

Cited literature

- Altermatt, F. & Ebert, D. (2010). Populations in small, ephemeral habitat patches may drive dynamics in a *Daphnia magna* metapopulation. *Ecology*, 91, 2975–2982.
- Altizer, S., Bartel, R. & Han, B.A. (2011). Animal migration and infectious disease risk. *Science*, 331, 296–302.
- Alton, L.A., White, C.R., & Seymour, R.S. (2007). Effect of aeral O₂ partial pressure on bimodal gas exchange and air-breathing behaviour in *Trichogaster leeri*. *Jour. Exp. Biol.*, 219, 451–519.
- Anderson, R.M. & May, R.M. (1981). The population dynamics of microparasites and their invertebrate hosts. *R. Soc. London Ser. B*, 291, 451–519.
- Anderson, R.M. & May, R.M. (1991). *Infectious diseases of humans: dynamics and control*. Oxford University Press, Oxford.
- Andre, J.-B. & Hochberg, M.E. (2005). Virulence evolution in emerging infectious diseases. *Evolution*, 59, 1406–1412.
- Becker, D.J., Hall, R.J., Forbes, K.M., Plowright, R.K. & Altizer, S. (2018a). Anthropogenic resource subsidies and host–parasite dynamics in wildlife. *Philos. Trans. R. Soc. B*, 373, 20170086.
- Becker, D.J., Snedden, C.E., Altizer, S. & Hall, R.J. (2018b). Host dispersal responses to resource supplementation determine pathogen spread in wildlife metapopulations. *Am. Nat.*, 192, 503–517.
- Bedhomme, S., Agnew, P., Vital, Y., Sidobre, C. & Michalakis, Y. (2005). Prevalence-dependent costs of parasite virulence. *PLOS Biol.*, 3, e262.
- Ben-Ami, F., Regoes, R.R. & Ebert, D. (2008). A quantitative test of the relationship between parasite dose and infection probability across different host-parasite combinations. *Proc. R. Soc. B*, 275, 853–859.
- Berngruber, T.W., Froissart, R., Choisy, M. & Gandon, S. (2013). Evolution of virulence in emerging epidemics. *PLoS Pathog.*, 9, e1003209.
- Berngruber, T.W., Lion, S. & Gandon, S. (2015). Spatial structure, transmission modes and the evolution of viral exploitation strategies. *PLoS Pathog.*, 11, e1004810.
- Bieger, A. & Ebert, D. (2009). Expression of parasite virulence at different host population densities under natural conditions. *Oecologia*, 160, 247–255.
- Binning, S.A., Shaw, A.K. & Roche, D.G. (2017). Parasites and host performance: Incorporating infection into our understanding of animal movement. *Integr. Comp. Biol.*, 57, 267–280.
- Blackburn, T.M., Pyšek, P., Bacher, S., Carlton, J.T., Duncan, R.P., Jarošík, V., *et al.* (2011). A proposed unified framework for biological invasions. *Trends Ecol. Evol.*, 26, 333–339.
- Bonte, D. & Doherty, M. (2016). Dispersal: a central and independent trait in life history. *Oikos*, 126, 472–479.
- Boots, M., Childs, D., Reuman, D.C. & Meador, M. (2009). Local interactions lead to pathogen-driven change to host population dynamics. *Curr. Biol.*, 19, 1660–1664.
- Boots, M., Hudson, P.J. & Sasaki, A. (2004). Large shifts in pathogen virulence relate to host population structure. *Science*, 303, 842–844.

- Boots, M. & Meador, M. (2007). Local interactions select for lower pathogen infectivity. *Science*, 315, 1284–1286.
- Boots, M. & Sasaki, A. (1999). “Small worlds” and the evolution of virulence: infection occurs locally and at a distance. *Proc. R. Soc. B*, 266, 1933–1938.
- Boots, M. & Sasaki, A. (2000). The evolutionary dynamics of local infection and global reproduction in host-parasite interactions. *Ecol. Lett.*, 3, 181–185.
- Bradley, C.A. & Altizer, S. (2005). Parasites hinder monarch butterfly flight: Implications for disease spread in migratory hosts. *Ecol. Lett.*, 8, 290–300.
- Breheny, P. & Burchett, W. (2017). Visualization of regression models using visreg. *R J.*, 9, 56–71.
- Brockhurst, M.A. & Koskella, B. (2013). Experimental coevolution of species interactions. *Trends Ecol. Evol.*, 28, 367–375.
- Brown, M.J.F., Loosli, R. & Schmid-Hempel, P. (2000). Condition-dependent expression of virulence in a trypanosome infecting bumblebees. *Oikos*, 91, 421–427.
- Buckley, L.B., Nufio, C.R. & Kingsolver, J.G. (2014). Phenotypic clines, energy balances and ecological responses to climate change. *J. Anim. Ecol.*, 83, 41–50.
- Bull, J.J. (1994). Virulence. *Evolution*, 48, 1423–1437.
- Burns, C.W. (2000). Crowding-induced changes in growth, reproduction and morphology of *Daphnia*. *Freshw. Biol.*, 43, 19–29.
- Burton, O.J., Phillips, B.L. & Travis, J.M.J. (2010). Trade-offs and the evolution of life-histories during range expansion. *Ecol. Lett.*, 13, 1210–1220.
- Calcagno, V., Mouquet, N., Jarne, P. & David, P. (2006). Coexistence in a metacommunity: the competition-colonization trade-off is not dead. *Ecol. Lett.*, 9, 897–907.
- Cameron, J.N. (1986). Appendix 2 - Solubility of O₂ and CO₂ at different temperatures and salinities. In: *Principles of Physiological Measurement*. Academic Press, London, p. 255.
- Carvalho, G.R. & Crisp, D.J. (1987). The clonal ecology of *Daphnia magna* (Crustacea: Cladocera): I. Temporal changes in the clonal structure of a natural population. *J. Anim. Ecol.*, 56, 453–468.
- Civitello, D.J., Pearsall, S., Duffy, M.A. & Hall, S.R. (2013). Parasite consumption and host interference can inhibit disease spread in dense populations. *Ecol. Lett.*, 16, 626–634.
- Civitello, D.J., Penczykowski, R.M., Smith, A.N., Shocket, M.S., Duffy, M. a. & Hall, S.R. (2015). Resources, key traits and the size of fungal epidemics in *Daphnia* populations. *J. Anim. Ecol.*, 84, 1010–1017.
- Clerc, M., Ebert, D. & Hall, M.D. (2015). Expression of parasite genetic variation changes over the course of infection: implications of within-host dynamics for the evolution of virulence. *Proc. R. Soc. B*, 282, 20142820.
- Connallon, T. & Hall, M.D. (2018). Genetic constraints on adaptation: a theoretical primer for the genomics era. *Ann. N. Y. Acad. Sci.*, 1422, 65–87.
- Coombs, D., Gilchrist, M.A. & Ball, C.L. (2007). Evaluating the importance of within- and between-host selection pressures on the evolution of chronic pathogens. *Theor. Popul. Biol.*, 72, 576–591.
- Cousineau, S. V. & Alizon, S. (2014). Parasite evolution in response to sex-based host

- heterogeneity in resistance and tolerance. *J. Evol. Biol.*, 27, 2753–2766.
- Cressler, C.E., Nelson, W.A., Day, T. & Mccauley, E. (2014). Disentangling the interaction among host resources, the immune system and pathogens. *Ecol. Lett.*, 17, 284–293.
- Cwynar, L.C. & MacDonald, G.M. (1987). Geographical variation of lodgepole pine in relation to population history. *Am. Nat.*, 129, 463–469.
- Dallas, T.A., Krkošek, M. & Drake, J.M. (2018). Experimental evidence of a pathogen invasion threshold. *R. Soc. Open Sci.*, 5, 171975.
- Daversa, D.R., Fenton, A., Dell, A.I., Garner, T.W.J. & Manica, A. (2017). Infections on the move: how transient phases of host movement influence disease spread. *Proc. R. Soc. B*, 284, 20171807.
- Day, T. & Gandon, S. (2007). Applying population-genetic models in theoretical evolutionary epidemiology. *Ecol. Lett.*, 10, 876–888.
- Day, T. & Proulx, S.R. (2004). A general theory for the evolutionary dynamics of virulence. *Am. Nat.*, 163, E40–E63.
- DeLong, J.P., Hanley, T.C. & Vasseur, D.A. (2014). Competition and the density dependence of metabolic rates. *J. Anim. Ecol.*, 83, 51–58.
- DeLong, J.P. & Hanson, D.T. (2009). Density-dependent individual and population-level metabolic rates in a suite of single-celled Eukaryotes. *Open Biol. J.*, 2, 32–37.
- Drake, J.M. & Griffen, B.D. (2009). Speed of expansion and extinction in experimental populations. *Ecol. Lett.*, 12, 772–778.
- Duneau, D. & Ebert, D. (2012). Host sexual dimorphism and parasite adaptation. *PLoS Biol.*, 10.
- Dunn, A.M. & Hatcher, M.J. (2015). Parasites and biological invasions: Parallels, interactions, and control. *Trends Parasitol.*, 31, 189–199.
- Dwyer, G. & Morris, W.F. (2006). Resource-dependent dispersal and the speed of biological invasions. *Am. Nat.*, 167, 165–176.
- Dybdahl, M.F. & Lively, C.M. (1996). The Geography of coevolution: comparative population structures for a snail and its trematode parasite. *Evolution*, 50, 2264–2275.
- Ebenhard, T. (1991). Colonisation in metapopulations: a review of theory and observations. *Biol. J. Linn. Soc.*, 42, 105–121.
- Ebert, D. (2005). *Ecology, epidemiology and evolution of parasitism in Daphnia*. Natl. Libr. Med. (US), Natl. Cent. Biotechnol.
- Ebert, D., Carius, H.J., Little, T.J. & Decaestecker, E. (2004). The evolution of virulence when parasites cause host castration and gigantism. *Am. Nat.*, 164, S19–S32.
- Ebert, D., Duneau, D., Hall, M.D., Luijckx, P., Andras, J.P., Du Pasquier, L., *et al.* (2016). A population biology perspective on the stepwise infection process of the bacterial pathogen *Pasteuria ramosa* in *Daphnia*. *Adv. Parasitol.*, 91, 265–310.
- Ebert, D., Zschokke-Rohringer, C.D. & Carius, H.J. (1998). Within–and between–population variation for resistance of *Daphnia magna* to the bacterial endoparasite *Pasteuria ramosa*. *Proc. R. Soc. London. Ser. B Biol. Sci.*, 265, 2127–2134.
- Ebert, D., Zschokke-Rohringer, C.D. & Carius, H.J. (2000). Dose effects and density-dependent regulation of two microparasites of *Daphnia magna*. *Oecologia*, 122, 200–209.

- Epstein, P.R. (2000). Is global warming harmful to health? *Science*, 283, 50–57.
- Erm, P., Hall, M.D. & Phillips, B.L. (2019). Anywhere but here: local conditions alone drive dispersal in *Daphnia*. *PeerJ Press*, 7, e6599.
- Eshelman, C.M., Vouk, R., Stewart, J.L., Halsne, E., Lindsey, H. a, Schneider, S., *et al.* (2010). Unrestricted migration favours virulent pathogens in experimental metapopulations: evolutionary genetics of a rapacious life history. *Phil. Trans. R. Soc. B*, 365, 2503–2513.
- Ewald, P.W. (1995). The evolution of virulence: A unifying link between parasitology and ecology. *J. Parasitol.*, 81, 659–669.
- Fairbairn, D.J. (1997). Allometry for sexual size dimorphism: pattern and process in the coevolution of body size in males and females. *Annu. Rev. Ecol. Syst.*, 28, 659–687.
- Fellous, S., Duncan, A.B., Quillery, E., Vale, P.F. & Kaltz, O. (2012). Genetic influence on disease spread following arrival of infected carriers. *Ecol. Lett.*, 15, 186–192.
- Fellous, S. & Koella, J.C. (2009). Different transmission strategies of a parasite in male and female hosts. *J. Evol. Biol.*, 22, 582–588.
- Fellous, S., Quillery, E., Duncan, A.B. & Kaltz, O. (2011). Parasitic infection reduces dispersal of ciliate host. *Biol. Lett.*, 7, 327–329.
- Fels, D., Vignon, M. & Kaltz, O. (2008). Ecological and genetic determinants of multiple infection and aggregation in a microbial host-parasite system. *Parasitology*, 135, 1373–1383.
- Fenton, A.A. & Hudson, P.J. (2002). Optimal infection strategies : should macroparasites hedge their bets ? *Oikos*, 96, 92–101.
- Flory, S.L., Alba, C., Clay, K., Holt, R.D. & Goss, E.M. (2018). Emerging pathogens can suppress invaders and promote native species recovery. *Biol. Invasions*, 20, 5-8.
- Fokin, S.I. & Görtz, H.-D. (2009). Diversity of *Holospora* bacteria in *Paramecium* and their characterization. In: *Endosymbionts in Paramecium*. pp. 162–194.
- Fox, J., & Weisberg, S. (2018). *An R companion to applied regression* (3rd ed.). Thousand Oaks, CA, Sage.
- Frickel, J., Sieber, M. & Becks, L. (2016). Eco-evolutionary dynamics in a coevolving host-virus system. *Ecol. Lett.*, 19, 450–459.
- Fronhofer, E.A. & Altermatt, F. (2015). Eco-evolutionary feedbacks during experimental range expansions. *Nat. Commun.*, 6, 6844.
- Fronhofer, E.A., Gut, S. & Altermatt, F. (2017). Evolution of density-dependent movement during experimental range expansions. *J. Evol. Biol.*, 30, 2165–2176.
- Gandon, S. (2002). Local adaptation and the geometry of host – parasite coevolution. *Ecol. Lett.*, 5, 246–256.
- Gandon, S. (2004). Evolution of multihost parasites. *Evolution*, 58, 455–469.
- Gandon, S., Capowiez, Y., Dubois, Y., Michalakis, Y. & Olivieri, I. (1996). Local adaptation and gene-for-gene coevolution in a metapopulation model. *Proc. R. Soc. B*, 263, 1003–1009.
- Gandon, S., Mackinnon, M.J., Nee, S. & Read, A.F. (2001). Imperfect vaccines and the evolution of pathogen virulence. *Nature*, 414, 751–755.

- Gandon, S. & Michalakis, Y. (2002). Local adaptation, evolutionary potential and host-parasite coevolution: Interactions between migration, mutation, population size and generation time. *J. Evol. Biol.*, 15, 451–462.
- Ghedini, G., White, C.R. & Marshall, D.J. (2017). Does energy flux predict density-dependence? An empirical field test. *Ecology*, 98, 3116–3126.
- Gilpin, M.E. & Ayala, F.J. (1973). Global models of growth and competition. *Proc. Natl. Acad. Sci.*, 70, 3590–3593.
- Giometto, A., Rinaldo, A., Carrara, F. & Altermatt, F. (2014). Emerging predictable features of replicated biological invasion fronts. *Proc. Natl. Acad. Sci.*, 111, 297–301.
- Gipson, S.A.Y. & Hall, M.D. (2016). The evolution of sexual dimorphism and its potential impact on host-pathogen coevolution. *Evolution*, 70, 959–968.
- Gipson, S.A.Y. & Hall, M.D. (2018). Interactions between host sex and age of exposure modify the virulence-transmission trade-off. *J. Evol. Biol.*, 31, 428–437.
- Görtz, H.D. & Dieckmann, J. (1980). Life cycle and infectivity of *Holospora elegans* Haffkine, a micronucleus-specific symbiont of *Paramecium caudatum* (Ehrenberg). *Protistologia*, 16, 591–603.
- Grenfell, B. & Harwood, J. (1997). (Meta)population dynamics of infectious diseases. *Trends Ecol. Evol.*, 12, 395–399.
- Griette, Q., Raoul, G. & Gandon, S. (2015). Virulence evolution at the front line of spreading epidemics. *Evolution*, 69, 2810–2819.
- Haag, C.R., Riek, M., Hottinger, J.W., Pajunen, V.I. & Ebert, D. (2006). Founder events as determinants of within-island and among-island genetic structure of *Daphnia* metapopulations. *Heredity*, 96, 150–158.
- Hajek, A.E. & Tobin, P.C. (2011). Introduced pathogens follow the invasion front of a spreading alien host. *J. Anim. Ecol.*, 80, 1217–1226.
- Hall, M.D., Bento, G. & Ebert, D. (2017). The evolutionary consequences of stepwise infection processes. *Trends Ecol. Evol.*, 32, 612–623.
- Hall, M.D. & Ebert, D. (2012). Disentangling the influence of parasite genotype, host genotype and maternal environment on different stages of bacterial infection in *Daphnia magna*. *Proc. R. Soc. B Biol. Sci.*, 279, 3176–3183.
- Hall, M.D. & Mideo, N. (2018). Linking sex differences to the evolution of infectious disease life-histories. *Philos. Trans. R. Soc. B Biol. Sci.*, 373, 20170431.
- Hall, M.D., Routtu, J. & Ebert, D. (2019). Dissecting the genetic architecture of a stepwise infection process. *Mol. Ecol.*, 28, 3942–3957.
- Hall, S.R., Knight, C.J., Becker, C.R., Duffy, M.A., Tessier, A.J. & Cáceres, C.E. (2009a). Quality matters: Resource quality for hosts and the timing of epidemics. *Ecol. Lett.*, 12, 118–128.
- Hall, S.R., Simonis, J.L., Nisbet, R.M., Tessier, A.J. & Cáceres, C.E. (2009b). Resource ecology of virulence in a planktonic host-parasite system: An explanation using dynamic energy budgets. *Am. Nat.*, 174, 149–162.
- Hall, S.R., Sivars-Becker, L., Becker, C., Duffy, M.A., Tessier, A.J. & Cáceres, C.E. (2007). Eating yourself sick: Transmission of disease as a function of foraging ecology. *Ecol. Lett.*, 10, 207–218.

- Hanski, I. (1991). Single-species metapopulation dynamics: Concepts, models and observations. *Biol. J. Linn. Soc.*, 42, 17–38.
- Hanski, I. & Gilpin, M. (1991). Metapopulation dynamics - brief history and conceptual domain. *Biol. J. Linn. Soc.*, 42, 3–16.
- Haraguchi, Y. & Sasaki, A. (2000). The evolution of parasite virulence and transmission rate in a spatially structured population. *J. Theor. Biol.*, 203, 85–96.
- Hawley, D.M., Osnas, E.E., Dobson, A.P., Hochachka, W.M. & Ley, D.H. (2013). Parallel patterns of increased virulence in a recently emerged wildlife pathogen. *PLoS Biol.*, 11, e1001570.
- Heffernan, J.M., Smith, R.J. & Wahl, L.M. (2005). Perspectives on the basic reproductive ratio. *J. R. Soc. Interface*, 2, 281–293.
- Hess, G. (1996). Disease in metapopulation models: Implications for conservation. *Ecology*, 77, 1617–1632.
- Hill, A.J.K., Thomas, C.D. & Blakeley, D.S. (1999). Evolution of flight morphology in a butterfly that has recently expanded its geographic range. *Oecologia*, 121, 165–170.
- Hite, J.L. & Cressler, C.E. (2018). Resource-driven changes to host population stability alter the evolution of virulence and transmission. *Philos. Trans. R. Soc. Lond. B*, 373, 20170087.
- Hutchinson, G.E. (1951). Copepodology for the ornithologist. *Ecology*, 32, 571–577.
- Kaltz, O., Koella, J.C., Evolutive, L.D.P., Pierre, U. & Bernard, S. (2003). Host growth conditions regulate the plasticity of horizontal and vertical transmission in *Holospora undulata*, a bacterial parasite of the protozoan *Paramecium caudatum*. *Evolution*, 57, 1535–1542.
- Kamo, M. & Boots, M. (2006). The evolution of parasite dispersal, transmission, and virulence in spatial host populations. *Evol. Ecol. Res.*, 8, 1333–1347.
- Kamo, M., Sasaki, A. & Boots, M. (2007). The role of trade-off shapes in the evolution of parasites in spatial host populations: An approximate analytical approach. *J. Theor. Biol.*, 244, 588–596.
- Kelehear, C., Brown, G.P. & Shine, R. (2012). Rapid evolution of parasite life history traits on an expanding range-edge. *Ecol. Lett.*, 15, 329–337.
- Kerr, B., Neuhauser, C., Bohannan, B.J.M. & Dean, A.M. (2006). Local migration promotes competitive restraint in a host-pathogen “tragedy of the commons”. *Nature*, 442, 75–78.
- Kluttgen, B., Dulmer, U., Engels, M., Ratte, H., Klüttgen, B., Dülmer, U., *et al.* (1994). ADaM, an artificial freshwater for the culture of zooplankton. *Water Res.*, 28, 743–746.
- Kvam, O.V., and Kleiven, O.T. (1995). Diel horizontal migration and swarm formation in *Daphnia* in response to *Chaoborus*. *Hydrobiologia*, 207:177–184.
- Lenski, R.E. & May, R.M. (1994). The evolution of virulence in parasites and pathogens: reconciliation between two competing hypotheses. *J. Theor. Biol.*, 169, 253–265.
- Li, X.-Y. & Kokko, H. (2018). Sex-biased dispersal: a review of the theory. *Biol. Rev.*, 94, 721–736.
- Lighton, J.R.B. (2008). *Measuring metabolic rates: a manual for scientists*. Oxford University Press, Oxford.
- Lion, S., Van Baalen, M. & Wilson, W.G. (2006). The evolution of parasite manipulation of host dispersal. *Proc. R. Soc. B*, 273, 1063–1071.
- Lion, S. & Boots, M. (2010). Are parasites “prudent” in space? *Ecol. Lett.*, 13, 1245–1255.

- Lion, S. & Gandon, S. (2015). Evolution of spatially structured host-parasite interactions. *J. Evol. Biol.*, 28, 10–28.
- Lipsitch, M., Nowak, M.A., Ebert, D. & May, R.M. (1995). The population dynamics of vertically and horizontally transmitted parasites. *Proc. Biol. Sci.*, 260, 321–327.
- Lochmiller, R.L. & Deerenberg, C. (2000). Trade-offs in evolutionary immunology: just what is the cost of immunity? *Oikos*, 88, 87–98.
- Luijckx, P., Ben-Ami, F., Mouton, L., Du Pasquier, L. & Ebert, D. (2011). Cloning of the unculturable parasite *Pasteuria ramosa* and its *Daphnia* host reveals extreme genotype-genotype interactions. *Ecol. Lett.*, 14, 125–131.
- Lürling, M., Roozen, F., Van Donk, E. & Goser, B. (2003). Response of *Daphnia* to substances released from crowded congeners and conspecifics. *J. Plankton Res.*, 25, 967–978.
- Magalon, H., Nidelet, T., Martin, G. & Kaltz, O. (2010). Host growth conditions influence experimental evolution of life history and virulence of a parasite with vertical and horizontal transmission. *Evolution*, 64, 2126–2138.
- Malerba, M.E., White, C.R. & Marshall, D.J. (2017). Phytoplankton size-scaling of net energy flux across light and biomass gradients. *Ecology*, 98, 3106–3115.
- May, R.M. & Anderson, R.M. (1983). Epidemiology and genetics in the coevolution of parasites and hosts. *Proc. R. Soc. London B*, 219, 281–313.
- Michel, J., Ebert, D. & Hall, M.D. (2016). The trans-generational impact of population density on host-parasite interactions. *BMC Evol. Biol.*, 16, 1–12.
- Mideo, N., Alizon, S. & Day, T. (2008). Linking within- and between-host dynamics in the evolutionary epidemiology of infectious diseases. *Trends Ecol. Evol.*, 23, 511–517.
- Mondet, F., de Miranda, J.R., Kretzschmar, A., Le Conte, Y. & Mercer, A.R. (2014). On the front line: Quantitative virus dynamics in honeybee (*Apis mellifera* L.) colonies along a new expansion front of the parasite *Varroa destructor*. *PLoS Pathog.*, 10, e1004323.
- Moore, J. (2002). *Parasites and the behaviour of animals*. Oxford Ser. Ecol. Evol. Oxford University Press.
- Moss, S.R., Turner, S.L., Trout, R.C., White, P.J., Hudson, P.J., Desai, A., *et al.* (2002). Molecular epidemiology of rabbit haemorrhagic disease virus. *J. Gen. Virol.*, 83, 2461–2467.
- Nidelet, T. & Kaltz, O. (2007). Direct and correlated responses to selection in a host-parasite system: Testing for the emergence of genotype specificity. *Evolution*, 61, 1803–1811.
- Nidelet, T., Koella, J.C. & Kaltz, O. (2009). Effects of shortened host life span on the evolution of parasite life history and virulence in a microbial host-parasite system. *BMC Evol. Biol.*, 9, 1–10.
- Nielsen, M. V. & Olsen, Y. (1989). The dependence of the assimilation efficiency in *Daphnia magna* on the ¹⁴C-labeling period of the food alga *Scenedesmus acutus*. *Limnol. Oceanogr.*, 34, 1311–1315.
- Nørgaard, L.S., Phillips, B.L. & Hall, M.D. (2019a). Can pathogens optimize both transmission and dispersal by exploiting sexual dimorphism in their hosts? *Biol. Lett.*, 15, 20190180.
- Nørgaard, L.S., Phillips, B.L. & Hall, M.D. (2019b). Infection in patchy populations: Contrasting pathogen invasion success and dispersal at varying times since host colonization. *Evol. Lett.*, 3, 555–566.

- Nowak, M.A. & May, R.M. (1994). Superinfection and the evolution of parasite virulence. *Proc. R. Soc. B*, 255, 81–89.
- Olito, C., White, C.R., Marshall, D.J. & Barneche, D.R. (2017). Estimating monotonic rates from biological data using local linear regression. *J. Exp. Biol.*, 220, 759–764.
- Osnas, E.E. & Dobson, A.P. (2011). Evolution of virulence in heterogeneous host communities under multiple trade-offs. *Evolution*, 66, 391–401.
- Osnas, E.E., Hurtado, P.J. & Dobson, A.P. (2015). Evolution of pathogen virulence across space during an epidemic. *Am. Nat.*, 185, 332–342.
- Pajunen, V.I. & Pajunen, I. (2003). Long-term dynamics in rock pool *Daphnia* metapopulations. *Ecography (Cop.)*, 26, 731–738.
- Parratt, S.R., Numminen, E. & Laine, A.-L. (2016). Infectious disease dynamics in heterogeneous landscapes. *Annu. Rev. Ecol. Evol. Syst.*, 47, 283–306.
- Penczykowski, R.M., Laine, A.L. & Koskella, B. (2016). Understanding the ecology and evolution of host-parasite interactions across scales. *Evol. Appl.*, 9, 37–52.
- Penczykowski, R.M., Lemanski, B.C.P., Sieg, R.D., Hall, S.R., Ochs, J.H., Kubanek, J., *et al.* (2014). Poor resource quality lowers transmission potential by changing foraging behaviour. *Funct. Ecol.*, 28, 1245–1255.
- Pérez-Tris, J. & Bensch, S. (2005). Dispersal increases local transmission of avian malarial parasites. *Ecol. Lett.*, 8, 838–845.
- Perkins, A.A., Phillips, B.L., Baskett, M.L. & Hastings, A. (2013). Evolution of dispersal and life history interact to drive accelerating spread of an invasive species. *Ecol. Lett.*, 16, 1079–1087.
- Perkins, S.E., Altizer, S., Bjornstad, O., Burdon, J.J., Clay, K., Gómez-aporicio, L., *et al.* (2008). Invasion Biology and Parasitic Infections. In: *Infectious Disease Ecology*.
- Perkins, T.A., Boettiger, C. & Phillips, B.L. (2016). After the games are over: life-history trade-offs drive dispersal attenuation following range expansion. *Ecol. Evol.*, 6, 6425–6434.
- Phillips, B.L. (2009). The evolution of growth rates on an expanding range edge. *Biol. Lett.*, 5, 802–804.
- Phillips, B.L. (2015). Evolutionary processes make invasion speed difficult to predict. *Biol. Invasions*, 17, 1949–1960.
- Phillips, B.L., Brown, G.P. & Shine, R. (2010a). Evolutionarily accelerated invasions: The rate of dispersal evolves upwards during the range advance of cane toads. *J. Evol. Biol.*, 23, 2595–2601.
- Phillips, B.L., Brown, G.P., Shine, R., Benjamin, R.P., Gregory P., B., Shine, *et al.* (2010b). Life-history evolution in range-shifting populations. *Ecology*, 91, 1617–1627.
- Phillips, B.L., Kelehear, C., Pizzatto, L., Brown, G.P., Barton, D. & Shine, R. (2010c). Parasites and pathogens lag behind their host during periods of host range advance. *Ecology*, 91, 872–881.
- Phillips, B.L. & Puschendorf, R. (2013). Do pathogens become more virulent as they spread? Evidence from the amphibian declines in Central America. *Proc. Biol. Sci.*, 280, 20131290.
- Phillips, B.L., Puschendorf, R., VanDerWal, J. & Alford, R.A. (2012). There is no evidence for a temporal link between pathogen arrival and frog extinctions in North-Eastern Australia. *PLoS One*, 7, e52502.

- Platt, T. & Irwin, B. (1973). Caloric content of phytoplankton. *Limnol. Oceanogr.*, 18, 306–310.
- Plowright, R.K., Parrish, C.R., McCallum, H., Hudson, P.J., Ko, A.I., Graham, A.L., *et al.* (2017). Pathways to zoonotic spillover. *Nat. Rev Microbiol.*, 15, 502–510.
- Poulin, R. (1996). Sexual inequalities in helminth infections: a cost of being male? *Am. Nat.*, 147, 287–295.
- Pulkkinen, K. & Ebert, D. (2004). Host starvation decreases parasite load and mean host size in experimental populations. *Ecology*, 85, 823–833.
- Pulliam, H.R. (2016). Sources, sinks, and population regulation. *Am. Nat.*, 132, 652–661.
- Regoes, R.R., Nowak, M.A. & Bonhoeffer, S. (2000). Evolution of virulence in a heterogeneous host population. *Evolution*, 54, 64–71.
- Restif, O. & Kaltz, O. (2006). Condition-dependent virulence in a horizontally and vertically transmitted bacterial parasite. *Oikos*, 114, 148–158.
- Ritz, C., Baty, F., Streibig, J.C. & Gerhard, D. (2015). Dose-response analysis using R. *PLoS One*, 10, e0146021.
- de Roode, J.C., Yates, A.J. & Altizer, S. (2008). Virulence-transmission trade-offs and population divergence in virulence in a naturally occurring butterfly parasite. *Proc. Natl. Acad. Sci.*, 105, 7489–7494.
- Roulin, A.C., Routtu, J., Hall, M.D., Janicke, T., Colson, I., Haag, C.R., *et al.* (2013). Local adaptation of sex induction in a facultative sexual crustacean: insights from QTL mapping and natural populations of *Daphnia magna*. *Mol. Ecol.*, 22, 3567–3579.
- Sakai, A.K., Allendorf, F.W., Holt, J.S., Lodge, D.M., Molofsky, J., With, K.A., *et al.* (2001). The population biology of invasive species. *Annu. Rev. Ecol. Syst.*, 32, 305–332.
- Schalk, G. & Forbes, M.R. (1997). Male biases in parasitism of mammals: effects of study type, host age, and parasite taxon. *Nord. Soc. Oikos*, 78, 67–74.
- Schinazi, R.B. (2000). Horizontal versus vertical transmission of parasites in a stochastic spatial model. *Math. Biosci.*, 168, 1–8.
- Schmid-Hempel, P. (2009). Immune defence, parasite evasion strategies and their relevance for “macroscopic phenomena” such as virulence. *Philos. Trans. R. Soc. B*, 364, 85–98.
- Schmid-Hempel, P. (2011). *Evolutionary parasitology - The integrated study of infections, immunology, ecology, and genetics*.
- Seppala, O., Liljeroos, K., Karvonen, A. & Jokela, J. (2008). Host condition as a constraint for parasite reproduction. *Oikos*, 117, 749–753.
- Sheldon, B.C. & Verhulst, S. (1996). Ecological immunology - costly parasite defenses and trade-offs in evolutionary ecology. *Trends Ecol. Evol.*, 11, 317–321.
- Sheridan, L.A.D., Poulin, R., Ward, D.F. & Zuk, M. (2000). Sex differences in parasitic infections among arthropod hosts: is there a male bias? *Nord. Soc. Oikos*, 88, 327–334.
- Soghigian, J. & Livdahl, T. (2017). Differential response to mosquito host sex and parasite dosage suggest mixed dispersal strategies in the parasite *Ascogregarina taiwanensis*. *PLoS One*, 12, e0184573.
- Simmons, A.D. & Thomas, C.D. (2004). Changes in dispersal during species’ range expansions. *Am. Nat.*, 164, 378–395.

- Soubeyrand, S. & Laine, A.-L. (2017). When group dispersal and allee effect shape metapopulation dynamics. *Ann. Zool. Fennici*, 54, 123–138.
- Strauss, A.T., Civitello, D.J., Caceres, C.E. & Hall, S.R. (2015). Success, failure and ambiguity of the dilution effect among competitors. *Ecol. Lett.*, 18, 916–926.
- Streicker, D.G., Winternitz, J.C., Satterfield, D.A., Condori-Condori, R.E., Broos, A., Tello, C., *et al.* (2016). Host–pathogen evolutionary signatures reveal dynamics and future invasions of vampire bat rabies. *Proc. Natl. Acad. Sci.*, 113, 10926–10931.
- Su, M., Chen, G. & Yang, Y. (2019). Dynamics of host-parasite interactions with horizontal and vertical transmissions in spatially heterogeneous environment. *Phys. A Stat. Mech. its Appl.*, 517, 452–458.
- Su, M., Li, W., Li, Z., Zhang, F. & Hui, C. (2009). The effect of landscape heterogeneity on host-parasite dynamics. *Ecol. Res.*, 24, 889–896.
- Sullivan, L.L., Li, B., Miller, T.E.X., Neubert, M.G. & Shaw, A.K. (2017). Density dependence in demography and dispersal generates fluctuating invasion speeds. *Proc. Natl. Acad. Sci.*, 114, 5053–5058.
- Thomas, C.D. (2000). Dispersal and extinction in fragmented landscapes. *Proc. Biol. Sci.*, 267, 139–145.
- Thomas, F., Adamo, S. & Moore, J. (2005). Parasitic manipulation: Where are we and where should we go? *Behav. Processes*, 68, 185–199.
- Thomas, F., Schmidt-Rhaesa, A., Martin, G., Manu, C., Durand, P. & Renaud, F. (2002). Do hairworms (*Nematomorpha*) manipulate the water seeking behaviour of their terrestrial hosts? *J. Evol. Biol.*, 15, 356–361.
- Thompson, O., Gipson, S.A.Y. & Hall, M.D. (2017). The impact of host sex on the outcome of co-infection. *Sci. Rep.*, 7, doi:10.1038/s41598-017-00835-z.
- Tilman, D. (1994). Competition and biodiversity in spatially structured habitats. *Ecology*, 75, 2–16.
- Torchin, M.E., Lafferty, K.D., Dobson, A.P., McKenzie, V.J. & Kuris, A.M. (2003). Introduced species and their missing parasites. *Nature*, 421, 628–630.
- Wei, W. & Krone, M.S. (2005). Spatial invasion by a mutant pathogen. *J Theor Biol.*, 236, 335–348.
- Wesołowska, W. & Wesołowski, T. (2014). Do *Leucochloridium* sporocysts manipulate the behaviour of their snail hosts? *J. Zool.*, 292, 151–155.
- White, C.R. (2011). Allometric estimation of metabolic rates in animals. *Comp. Biochem. Physiol. Part A*, 158, 346–357.
- Wichterman, R. (1986). *The biology of Paramecium*. Plenum Press, New York.
- Winsor, G.L. & Innes, D.J. (2002). Sexual reproduction in *Daphnia pulex* (Crustacea:Cladocera): observations on male mating behavior and avoidance of inbreeding. *Freshw. Biol.*, 47, 441–450.
- Yashchenko, V., Fossen, E.I., Kielland, Ø.N. & Einum, S. (2016). Negative relationships between population density and metabolic rates are not general. *J. Anim. Ecol.*, 85, 1070–1077.
- Zuk, M. (2009). The sicker sex. *PLoS Pathog.*, 5, e1000267.